

EUROPEAN ORGANISATION FOR NUCLEAR RESEARCH (CERN)



JHEP 10 (2023) 079
DOI: [10.1007/JHEP10\(2023\)079](https://doi.org/10.1007/JHEP10(2023)079)



CERN-EP-2023-073
1st December 2023

Search for periodic signals in the dielectron and diphoton invariant mass spectra using 139 fb^{-1} of $p p$ collisions at $\sqrt{s} = 13 \text{ TeV}$ with the ATLAS detector

The ATLAS Collaboration

A search for physics beyond the Standard Model inducing periodic signals in the dielectron and diphoton invariant mass spectra is presented using 139 fb^{-1} of $\sqrt{s} = 13 \text{ TeV}$ $p p$ collision data collected by the ATLAS experiment at the LHC. Novel search techniques based on continuous wavelet transforms are used to infer the frequency of periodic signals from the invariant mass spectra and neural network classifiers are used to enhance the sensitivity to periodic resonances. In the absence of a signal, exclusion limits are placed at the 95% confidence level in the two-dimensional parameter space of the clockwork gravity model. Model-independent searches for deviations from the background-only hypothesis are also performed.

1 Introduction

Typical experimental searches for physics beyond the Standard Model (SM) at the Large Hadron Collider (LHC) search for new resonant peaks or non-resonant deviations in kinematic distributions, such as the invariant mass of two-particle systems. However, more complicated signatures are possible and have received little attention in experimental searches so far. One such possibility, which appears in several theoretical extensions to the SM, is a signal that gives rise to periodic structures. This type of signal is predicted by models with small mass splittings among many resonances.

Extensions to the SM with these features include the continuum clockwork gravity model [1, 2], which has an identical five-dimensional spacetime metric to the linear dilaton scenario [3, 4]. This spacetime metric also approximates the dual of Little String Theory [5, 6]. As the same theory can be interpreted as either a linear dilaton model or as the continuum version of a clockwork model, this theory is referred to as the Clockwork/Linear Dilaton (CW/LD) model. These models are well motivated, as the continuum spacetime version of the clockwork gravity model can address the Higgs boson mass naturalness problem [1]. The CW/LD model is also related to previous proposed solutions to the hierarchy problem, including theories with large extra dimensions [7, 8] and Randall–Sundrum (RS) models where the extra dimension is warped [9].

The CW/LD model predicts a narrowly-spaced spectrum of resonances in mass. The mass spectrum and couplings of this tower of Kaluza–Klein (KK) gravitons are described by two parameters, k and M_5 . The parameter k is a mass parameter that determines the onset of the KK graviton spectrum and M_5 is the five-dimensional (5D) reduced Planck mass, the fundamental scale of the theory. As the cross-section for the CW/LD model approximately scales inversely with M_5 , $\sigma \propto 1/M_5^3$, a limit on the signal strength in this search can be directly translated to a limit on M_5 for a given value of k .

The mass splittings predicted by the CW/LD model are generally on the order of a few percent near the onset of the graviton spectrum and eventually decrease, falling below 1% for high graviton mode numbers [2]. Therefore, when looking at the invariant mass of the decay products of these resonances in experiments, the narrowly-spaced spectrum of resonances predicted by the model may appear as a long-range semi-periodic structure. The narrow spacing of the mass spectrum requires an excellent detector resolution in order to resolve these resonances which can be satisfied by relying on two electrons or two photons in the final state. This paper presents a search for periodic contributions to the diphoton and dielectron invariant mass spectra using 139 fb^{-1} of $\sqrt{s} = 13\text{ TeV}$ proton–proton (pp) collision data recorded by the ATLAS detector from 2015 to 2018 at the LHC. Previous searches for physics beyond the SM in high-mass diphoton final states and dielectron final states during Run 2 of the LHC using pp collisions at $\sqrt{s} = 13\text{ TeV}$ were conducted by the ATLAS and CMS experiments [10–14]. The CMS experiment performed a search for the same CW/LD signal using only diphoton events in a search for a non-resonant excess at high invariant masses. The CMS result excludes values of M_5 in the range of 10 TeV to 1 TeV for values of k in the range of 0.1 GeV to 5 TeV [13].

2 Analysis strategy

This analysis is based on two previous ATLAS resonance searches performed in the dilepton [10] and diphoton [12] channels in the mass range of 225 – 6000 GeV and 150 – 5000 GeV , respectively. The same data samples and background estimation methods were used, in both cases, relying on data-driven

techniques. The two previous analyses also estimated the background from simulation and found excellent compatibility with the estimations from data. Therefore, this analysis takes advantage of the precise data-driven background estimates while also benefitting from the availability of a simulation-based background estimates. The background estimates from simulation include a complete set of systematic uncertainties in both of the analysis channels, which is important for this analysis because the “spurious-signal” uncertainty derived in Refs. [10, 12] is applicable only to searches which consider a single narrow resonance. The simulation-based uncertainties from previous searches are used instead and their effect on the background estimation is incorporated using the methodology developed in a previous ATLAS search for non-resonant signatures in the dilepton channel [11]. Finally, this analysis also relies on transformational and statistical methods developed in Ref. [15] in order to deal with data featuring periodic structures.

A brief description of the ATLAS detector is given in Section 3. The data and simulated event samples are discussed in Section 4 and an overview of the event selection in each analysis channel is described in Section 5. The signal modelling is presented in Section 6 and the background estimation methods are discussed briefly in Section 7. The sources of systematic uncertainties are discussed in Section 8, while the uncertainty estimation process is described in Section 9.

This analysis performs a search for generic periodic features in the dielectron and diphoton invariant mass spectra, in the same mass ranges considered in Refs. [10, 12]. The dielectron and diphoton channels are analysed separately due to potential overlaps in their event selections. This search uses a continuous wavelet transform (CWT) to analyse these mass spectra in the frequency domain.¹ The output of the CWT is a two-dimensional image of the wavelet amplitude in the frequency versus mass space, referred to as a “scalogram.” The potential periodicity of a signal can be revealed in the image, for example as a local “blob” around a small range of frequencies or masses. While conventional resonant and non-resonant searches may be suboptimal, particularly in the case of small CW/LD-like signals, the CWT may still provide an enhancement of a new signal’s semi-periodic nature. This enhancement provides a clear separation of a signal from the background and suggests that the search should be conducted in the CWT space rather than in the mass space alone. The CWT method is described briefly in Section 10.

In the limit of infinite statistical precision, the local features of a potential signal in the CWT images can be clearly visible and separable from the background-only case. When accounting for realistic statistical fluctuations due to the finite-size distributions in the mass space, the signal features wash out partially in the CWT images and the separation power becomes significantly smaller. Therefore, machine-learning techniques are applied to distinguish periodic contributions to the diphoton and dielectron CWT images made using the invariant mass spectra. Model-independent results are provided using an autoencoder-based anomaly detection procedure to search for generic periodic deviations in the scalograms. The CW/LD model is used as a benchmark model for a model-specific search using the CWT images. A neural network binary classifier is trained on the CWT images made from background-only and signal-plus background mass distributions to provide a test statistic for discovery of potential periodic resonances with specific k and M_5 values. In both the model-independent and model-specific searches, the test-statistic used during the statistical inference portion of the analysis is based on the machine-learning outputs themselves. As the CW/LD signal may introduce a non-resonant enhancement above the SM background in the mass space, the statistical inference in the two searches can be dominated by the non-resonant signal features instead of the semi-periodic contribution. Therefore, the two searches are performed with and without specific thresholds imposed to reduce potential non-resonant contributions and focus the sensitivity on the periodic features. The statistical analysis of the two methods and the related thresholds are discussed in

¹ In this analysis, the transformed variable is the invariant mass rather than time.

Section 11. The model-independent results and the model-specific exclusion limits set in the k - M_5 plane of the CW/LD model are given in Section 12.

The previous dilepton analysis [10] also included a dimuon analysis channel that could be sensitive to a potential CW/LD signal. However, the mass resolution becomes much worse for high-mass dimuon events compared with the dielectron channel. These resolution effects cause the individual modes in the KK tower to merge and the signal periodicity cannot be resolved. For this reason, the dimuon channel is not used in this search.

3 ATLAS detector

The ATLAS experiment [16–18] is a multipurpose particle detector with a forward-backward symmetric cylindrical geometry and nearly 4π coverage in solid angle.² It consists of an inner tracking detector surrounded by a thin superconducting solenoid providing a 2T axial magnetic field, electromagnetic and hadronic calorimeters, and a muon spectrometer. The inner detector (ID) covers the pseudorapidity range $|\eta| < 2.5$ and consists of silicon pixel, silicon microstrip, and transition radiation tracking detectors. Lead/liquid-argon (LAr) sampling calorimeters provide electromagnetic (EM) energy measurements with high granularity. A steel/scintillating-tile hadron sampling calorimeter covers the central pseudorapidity range ($|\eta| < 1.7$). The endcap and forward regions are instrumented with LAr calorimeters for both the EM and hadronic energy measurements up to $|\eta| = 4.9$. The muon spectrometer surrounds the calorimeters, covering the region $|\eta| < 2.7$ and is based on three large superconducting air-core toroidal magnets with eight coils each. The field integral of the toroids ranges between 2.0 and 6.0 Tm across most of the detector acceptance. A two-level trigger system is used to select events. The first-level trigger is implemented in custom hardware and uses a subset of the detector information to accept events at a rate below 100 kHz. A software-based trigger then reduces the accepted event rate to an average of 1 kHz for offline storage [19]. An extensive software suite [20] is used in the reconstruction and analysis of real and simulated data, in detector operations, and in the trigger and data acquisition systems of the experiment.

4 Data and simulated event samples

The data used for the search consists of the pp collision data recorded by the ATLAS experiment at $\sqrt{s} = 13$ TeV during the 2015 to 2018 LHC data-taking period. After requiring stable beam conditions and data quality selections with all ATLAS subsystems operational [21], the data sample corresponds to an integrated luminosity of $139.0 \pm 2.4 \text{ fb}^{-1}$ [22]. The LUCID-2 detector [23] was used for the primary luminosity measurements.

The events used in this analysis were recorded using a set of diphoton and dielectron triggers. Events in the diphoton channel were recorded using a diphoton trigger that required at least two energy clusters in the EM calorimeter with transverse energies (E_T) greater than 35 and 25 GeV for the E_T -ordered leading and subleading photon candidates, respectively. Both of the clusters were required to satisfy photon identification criteria based on the shower shapes in the EM calorimeters. The triggers used in 2015 and

² ATLAS uses a right-handed coordinate system with its origin at the nominal interaction point (IP) in the centre of the detector and the z -axis along the beam pipe. The x -axis points from the IP to the centre of the LHC ring, and the y -axis points upward. Cylindrical coordinates (r, ϕ) are used in the transverse plane, ϕ being the azimuthal angle around the z -axis. The pseudorapidity is defined in terms of the polar angle θ as $\eta = -\ln \tan(\theta/2)$.

2016 required both of the photons to satisfy the *loose* identification requirement [24]. In 2017 and 2018, due to the greater instantaneous luminosity, the diphoton trigger requirements were tightened and both of the photons were required to satisfy the *medium* identification requirement. The efficiency of the diphoton trigger relative to the event selection given in Section 5 is over 99% for the 2015–2016 data and above 98% for the 2017–2018 data [25].

Events in the dielectron channel were collected using several dielectron triggers. The trigger used in 2015 required both of the electrons to satisfy the *loose* identification criteria and E_T thresholds of 12 GeV. In 2016, the E_T thresholds were increased to 17 GeV for both electrons and the electrons were required to satisfy the *very loose* identification criteria [24]. In 2017 and 2018, the identification criteria were left unchanged and the E_T thresholds were increased to 24 GeV for both of the electrons [25].

Although the background in this analysis is estimated by using data-driven methods, simulated Monte Carlo (MC) events are used to optimise the analysis selections, determine appropriate fit functions for the data, estimate background compositions, and evaluate signal acceptances and efficiencies. As the KK modes in the CW/LD model are on-shell, the interference effects between the resonant signals and all background processes are neglected in both the diphoton and dielectron channels.

For the diphoton channel, the largest background comes from the production of two prompt photons which represents the irreducible background in this search channel. Smaller background contributions come from events containing a photon and a jet and events with two jets, where the jets are misidentified as photons. These smaller backgrounds are estimated by using a data-driven technique, the two-dimensional sideband method, described in Ref. [26].

Events with two prompt photons were simulated using the SHERPA 2.2.4 [27, 28] event generator. Matrix elements were calculated with up to one additional parton at next-to-leading-order (NLO) and including two or three additional partons at leading-order (LO) in perturbative QCD (pQCD). These matrix elements were merged with the SHERPA parton-shower simulation using the ME+PS@NLO prescription [29–32]. The NNPDF3.0NNLO parton distribution function (PDF) set [33] was used and paired with a dedicated parton-shower tune in the SHERPA generator.

For the dielectron channel, the main prompt backgrounds arise from Drell–Yan (DY), top-quark pair ($t\bar{t}$), single-top-quark, and diboson production. The background contribution from non-prompt electrons from multijet and $W +$ jets processes is estimated by using a data-driven technique, the matrix method, as described in Ref. [34].

The DY [35] sample was generated using the PowHEG Box v1 [36–39] event generator with the CT10 PDF set [40] and interfaced with the PYTHIA 8.186 [41] parton shower program. Next-to-next-to-leading-order (NNLO) corrections in pQCD and NLO corrections in electroweak (EW) theory were calculated and applied to the simulated DY events. The pQCD corrections were computed with VRAP v0.9 [42] and the CT14 NNLO PDF set [43]. The EW corrections were computed with MCSANC [44] which accounts for quantum electrodynamic effects due to initial-state radiation, interference between initial and final-state radiation, and Sudakov logarithm single-loop corrections.

The diboson [45] processes with fully leptonic and semileptonic final states were simulated using SHERPA 2.2.1 with the CT10 PDF set. Matrix elements were calculated at NLO accuracy in QCD for up to one additional parton and at LO accuracy for up to three additional parton emissions. The matrix element calculations were matched and merged with the SHERPA parton shower based on Catani–Seymour dipole factorisation [46, 47] using the ME+PS@NLO prescription. The diboson and DY backgrounds

were generated in slices of dilepton mass in order to enhance the MC statistical precision in the high-mass region.

The $t\bar{t}$ and single-top-quark samples were generated with PowHEG Box v2 [36–38, 48–51] at NLO using the NNPDF3.0NLO PDF [33] in the matrix element and interfaced to PYTHIA 8.230 [52] in order to model the parton shower, hadronisation, and underlying event, with parameters set according to the A14 tune [53] and using the NNPDF2.3LO set of PDFs [54]. These samples were normalised to the theoretical cross-sections calculated at NNLO in pQCD and include resummation of the next-to-next-to-leading logarithmic soft gluon terms as provided by Top++ 2.0 [55].

Resonant single-graviton MC samples were simulated using a Randall–Sundrum model [9]. These MC samples were generated at LO in pQCD using PYTHIA 8 with the NNPDF2.3LO PDF set and the A14 tune. In these samples, only the lightest KK graviton excitation was generated. For the diphoton decay channel, the samples were generated with a KK graviton mass m_{G^*} in the range of 150–5000 GeV. A fixed coupling value of $k/\bar{M}_{\text{Pl}} = 0.01$, where $\bar{M}_{\text{Pl}} = M_{\text{Pl}}/\sqrt{8\pi}$ is the reduced Planck scale, was used to ensure a sufficiently narrow-width signal. For the dielectron decay channel, samples were generated with masses in the range of 200–6000 GeV and with a fixed coupling value of $k/\bar{M}_{\text{Pl}} = 0.1$. These samples are used to determine the acceptance and efficiency of selecting the CW/LD signal.

Additional MC samples incorporating a series of RS graviton resonances were generated at LO in pQCD using PYTHIA 8.244 with the NNPDF2.3LO PDF set and the A14 tune. In these samples, only the direct graviton decays into dielectron and diphoton final-states were simulated. Samples were generated for k values of 300 GeV, 500 GeV, 1 TeV, and 2 TeV with M_5 fixed to a value of 6 TeV. These samples are used to validate the analytic signal templates of the CW/LD signals, which are discussed in detail in Section 6.

The effects of multiple $p\bar{p}$ interactions in the same bunch crossing as that of the hard scatter plus those from adjacent bunch crossings (pile-up) are included in all simulated samples. Pile-up collisions were generated with PYTHIA 8.186 using the NNPDF2.3LO PDF set and the ATLAS A3 set of tuned parameters [56]. Simulated event samples were weighted to reproduce the distribution of the average number of interactions per bunch crossing observed in the data [57].

The spin-2 diphoton simulated signal events, and DY, $t\bar{t}$, single-top-quark, and diboson background events were processed using a detailed simulation of the ATLAS detector [58] based on GEANT4 [59]. The irreducible prompt $\gamma\gamma$ background and spin-2 dielectron signals were processed using a fast simulation of the ATLAS detector [60], where the full simulation of the calorimeter is replaced with a fast parameterisation of the calorimeter response. All simulated events were reconstructed with the same reconstruction algorithms as those used for data.

Generator-level-only MC samples of the NLO DY background are used for the modelling studies described in Section 7. These samples could not be produced with the ATLAS detector simulation due to the large number of events required [10].

5 Object and event selection

Complete descriptions of the object definitions and event selections are given in Ref. [10] for the dielectron channel and Ref. [12] for the diphoton channel. The criteria are identical to the ones applied in this analysis and a brief description is given here.

The event selection in the diphoton channel requires at least two reconstructed photon candidates with $E_T > 25$ GeV and $|\eta| < 2.37$, excluding candidates in the transition region $1.37 < |\eta| < 1.52$ between the barrel and endcap EM calorimeters. The two highest- E_T photons are used to form the diphoton candidate and are used with additional information from the tracking detectors to identify the diphoton primary vertex [61]. After the diphoton primary vertex is identified, the leading and subleading photons are required to have $E_T/m_{\gamma\gamma} > 0.35$ and 0.25, respectively. The diphoton invariant mass, $m_{\gamma\gamma}$, is required to be greater than 150 GeV. To reduce the background from jets, photon candidates must satisfy the *tight* identification criteria based on shower shapes in the EM calorimeter [24].

Events in the dielectron channel are selected by requiring at least one pair of reconstructed electron candidates. Each event is required to contain at least one reconstructed pp interaction vertex, where the primary vertex is defined as the vertex with the highest sum of track transverse momenta squared. Electron candidates are reconstructed from ID tracks matched to energy clusters deposited in the EM calorimeter [24, 62]. All selected electrons are required to have $E_T > 30$ GeV and $|\eta| < 2.47$. As in the diphoton channel, electron candidates in the transition region ($1.37 < |\eta| < 1.52$) are not considered. The final selection requires that the electrons satisfy the *medium* identification working point.

Electron candidate tracks are required to satisfy $|d_0/\sigma(d_0)| < 5$ and $|z_0 \sin \theta| < 0.5$ mm, where d_0 and z_0 are the transverse and longitudinal impact parameters defined relative to the primary vertex position and $\sigma(d_0)$ is the uncertainty on d_0 . This selection ensures that the electron candidate track is consistent with the primary vertex of the event.

If there are more than two electrons in the same event, the two electrons with the highest E_T are selected to form the dielectron pair. An opposite-sign electron charge requirement is not applied due to a high probability of charge misidentification for high- E_T electrons. The reconstructed invariant mass of the dielectron pair, m_{ee} , is required to be above 225 GeV to avoid the region dominated by decays of the Z boson which cannot be described using the same background parameterisation as the high-mass region.

To suppress the backgrounds from misidentified jets, the photon and electron candidates are required to satisfy calorimeter- and track-based isolation criteria. The photons are required to satisfy the *tight* isolation which is 90–95% efficient for the analysis selection [24]. Electrons are required to satisfy the *gradient* isolation which is 99% efficient for the analysis selection [24].

6 Signal modelling

The CW/LD signals are modelled using analytic invariant mass templates constructed from a range of inputs including PDF information, branching ratio, and detector resolution modelling derived from the previous ATLAS diphoton and dielectron analyses.

For each reconstructed mass bin, the expected number of signal events is determined by computing the contribution from the entire KK graviton tower. The estimate of the expected number of signal events for a given reconstructed mass bin i is given by

$$N_i^{\text{reco}} = L_{\text{int}} \cdot \sum_G \sigma_G \cdot \mathcal{B}_G(G \rightarrow XX) \cdot P(M_i|M_G) \cdot (A \times \epsilon)_G \quad (1)$$

where the index G runs over the KK graviton modes whose masses are within the search range. In Eq. (1), L_{int} is the integrated luminosity, σ_G is the production cross-section, \mathcal{B}_G denotes the branching ratio, and $(A \times \epsilon)_G$ is the acceptance times efficiency for a given mass, M_G , of the KK graviton. The $P(M_i|M_G)$

term represents the probability to reconstruct an event in invariant mass bin i for events with an input true mass of M_G that satisfy the selection requirements and is referred to as the transfer function (TF). The TF provides a smooth transformation between the true and reconstructed invariant mass spectrum by modelling the detector effects. The convolution becomes a product as the true masses M_G are discrete and the natural widths can be neglected as the resonances are described by the narrow-width-approximation (NWA) over the range of true masses considered in this analysis.

The cross-sections and branching ratios for the gravitons in the CW/LD signal are taken from Ref. [2], where the effects of heavy graviton cascade decays into lighter graviton pairs are included in the total width when calculating the diphoton and dielectron branching ratios. The additional contributions to the signal from these cascade decays into diphoton and dielectron final states are not considered.

The TF and acceptance times efficiency terms are derived following the methodologies of the previous ATLAS dielectron and diphoton resonance searches [10, 12] and are briefly outlined below. These terms are derived using the DY MC samples and the resonant single-graviton MC samples for the dielectron and diphoton channels, respectively.

For the dielectron channel, the detector response is defined in the TF with respect to the relative dilepton mass resolution $(m_{\ell\ell} - m_{\ell\ell}^{\text{true}})/m_{\ell\ell}^{\text{true}}$, where $m_{\ell\ell}^{\text{true}}$ is the generated dilepton mass at Born level before final-state radiation. The mass resolution is parameterised as the sum of a Gaussian distribution and a Crystal Ball function [63, 64]. The Gaussian component in this function describes the central peak of the detector response and the Crystal Ball component is used to model the effects of bremsstrahlung in the dielectron system. The parameterisation of the relative dilepton mass resolution is determined using a simultaneous fit to the resolution function to the DY MC events. The DY MC sample is separated into 200 bins of equal size in $m_{\ell\ell}^{\text{true}}$ based on a logarithmic scale in the dielectron mass range from 130 GeV to 6000 GeV. The mass resolution fit is repeated to evaluate the uncertainty in the fit parameters by shifting individually the lepton energy and momentum scale and resolutions by their uncertainties. Although the resolution function is derived on spin-1 events, the results are found to be compatible with the true response coming from the spin-2 gravitons.

For the diphoton channel, the TF describes the detector resolution of the invariant mass using a double-sided Crystal Ball (DSCB) function [63, 65] with the parameters expressed as a function of the resonance mass, m_X . The DSCB parameters are extended to lower masses relative to Ref. [12] as the CW/LD signals considered in this analysis can contain graviton masses below 500 GeV, which were not considered in the previous analysis.

Analytic templates allow for signal shapes to be created for any choice of k and M_5 . These templates are confirmed to agree with the MC samples generated at the specific points in the k – M_5 plane discussed in Section 4. Examples of the expected signal shapes in each analysis channel are shown in Figure 1 for $k = 1200$ GeV, $M_5 = 3000$ GeV and for $k = 2000$ GeV, $M_5 = 8500$ GeV.

7 Background modelling

The diphoton and dielectron search channels in this analysis use the same data-driven background estimation technique based on a functional form fit to the data. Each analysis channel uses a single functional form to model the background across the full invariant mass spectrum. The analytic form for the background in each channel is determined from a fit to the background expectation derived from MC simulation and control-region data.

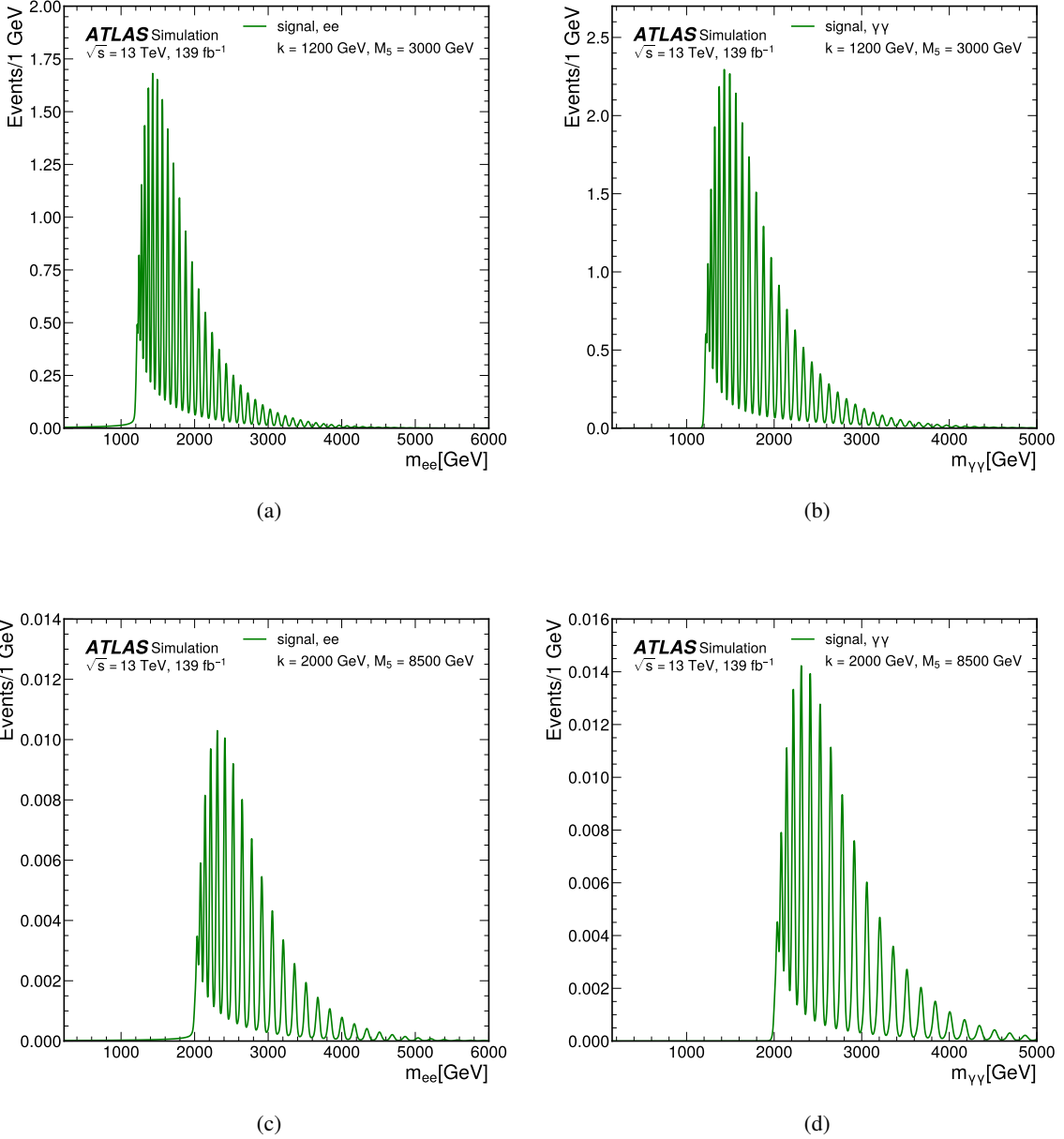


Figure 1: The expected signal invariant mass shape in the (a) ee and (b) $\gamma\gamma$ channels, where the CW/LD parameter values $k = 1200 \text{ GeV}$ and $M_5 = 3000 \text{ GeV}$ are used to generate the analytic signal template shapes. The expected signal invariant mass shape for CW/LD parameter values $k = 2000 \text{ GeV}$ and $M_5 = 8500 \text{ GeV}$ are shown in the (c) ee and (d) $\gamma\gamma$ channels. From these two different signal points, it can be seen that the parameter k determines the onset of the KK graviton spectrum.

For the dielectron channel, the functional form is taken from the analysis in Ref. [10], where the fit was performed on a background template with contributions from the MC estimate of the DY, $t\bar{t}$, diboson, and single-top processes and the data-driven estimate of the reducible backgrounds arising from the multijet

and W +jet processes. The function is parameterised as a function of $m_{\ell\ell}$ and is given by:

$$f_{ee}(m_{\ell\ell}) = f_{BW,Z}(m_{\ell\ell}) \cdot (1-x)^b \cdot x^{\sum_{i=0}^3 p_i \log(x)^i} \quad (2)$$

where $x = m_{\ell\ell}/\sqrt{s}$ and $f_{BW,Z}(m_{\ell\ell})$ is a non-relativistic Breit–Wigner function with $M_Z = 91.1876$ GeV and $\Gamma_Z = 2.4952$ GeV [66]. The b and p_i parameters are fixed to the values from the fit to data in Ref. [10] and the $(1-x)^b$ term ensures that the background fit tends to zero as $x \rightarrow 1$, consistent with the expectation from the collision energy of the LHC. The background function is normalised such that its integral corresponds to the total number of events in the signal region.

For the diphoton channel, the largest background component arises from the non-resonant production of photon pairs ($\gamma\gamma$ events). Smaller contributions to the total background come from events containing a photon and a jet misidentified as a photon (γj events) and from events with two jets where both of the jets are misidentified as photons (jj events). The relative contribution from each of these processes is determined using a two-dimensional sideband method described in Ref. [26]; the overall $\gamma\gamma$ purity increases as a function of $m_{\gamma\gamma}$ from around 89% at 150–200 GeV to around 97% above 400 GeV. The relative uncertainty in the purity ranges from 0.5%–3% and the remainder of the background is dominated by γj events.

The analytic form for the diphoton channel is chosen from the family of functions used in previous analyses to describe the diphoton invariant mass spectrum [67], following the procedure described in Ref. [12]. The background function is described by the following form

$$f(x; b, a_0, a_1) = (1 - x^{1/3})^b x^{a_0 + a_1 \log(x)} \quad (3)$$

where b, a_0, a_1 are free parameters and $x = m_{\gamma\gamma}/\sqrt{s}$.

The dielectron and diphoton invariant mass distributions passing all selections are shown in Figure 2 along with the background-only fits, example clockwork signals for each channel, and the corresponding signal-plus-background fits.

8 Uncertainties

The previous dilepton [10] and diphoton [12] data-driven analyses extracted full MC-based uncertainties, which are used in this search to construct systematically-varied distributions as discussed in Section 9. The variations considered in both the dielectron and diphoton channels come from theoretical and experimental uncertainties in the simulated backgrounds, uncertainties in the detector response and signal yield, and uncertainties induced by the data-driven background estimates.

The following theoretical uncertainties are considered for variations in the DY and $\gamma\gamma$ components: the variations of the nominal PDF set, variations of the factorisation and renormalisation scales, and the effect of choosing different PDF sets. The variations in the nominal PDF set for the DY background are determined using 90% CL CT14NNLO PDF error set, while the PDF variations for the $\gamma\gamma$ background are constructed from all of the replicas within the NNPDF3.0 NNLO set. The factorisation and renormalisation scales are varied independently by a factor of two to estimate the perturbative uncertainties for these background MC samples. Theoretical uncertainties in the DY component from the variation of the strong coupling, electroweak corrections, and photon-induced corrections [68] are also considered. An additional

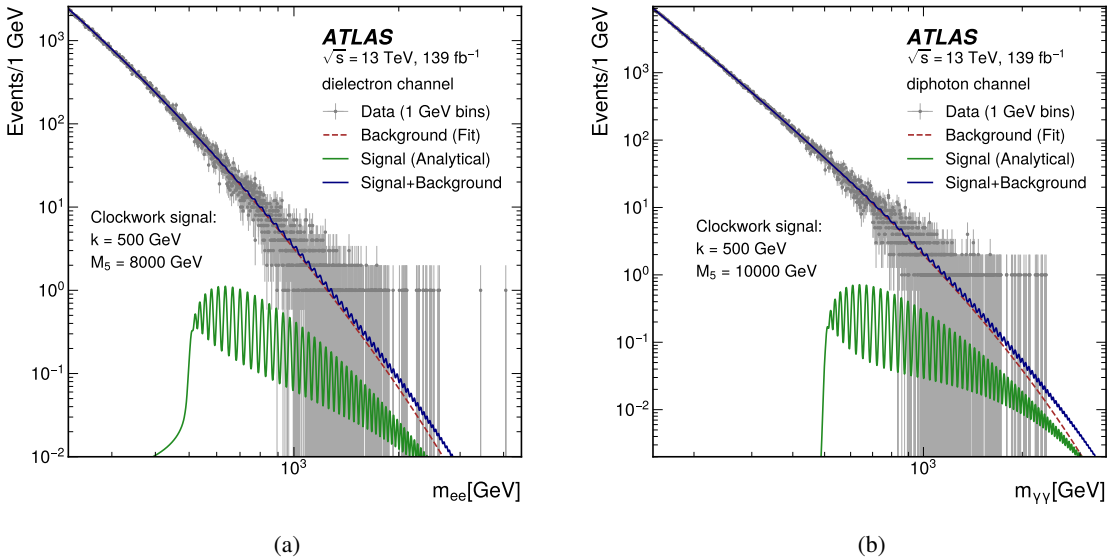


Figure 2: (a) The dielectron and (b) diphoton invariant mass distributions for events passing the full event selection, with the respective background-only fit parameterisation, an analytical clockwork signal, and the signal-plus-background parametrisation. The clockwork signal parameters are selected close to the sensitivity limit of this analysis. For the dielectron channel in (a) the clockwork signal is given for $k = 500$ GeV and $M_5 = 8000$ GeV, while the diphoton channel in (b) shows a signal with $k = 500$ GeV and $M_5 = 10000$ GeV.

uncertainty is applied in the dielectron channel to account for the theoretical cross-section uncertainties of the $t\bar{t}$ process.

The experimental uncertainties considered in the diphoton (dielectron) analysis channel include uncertainties on the luminosity determination, pile-up profile, trigger efficiency, photon (electron) energy scale and resolution, and the efficiency of photon (electron) identification and isolation requirements. More details of the determination of the experimental systematic uncertainties can be found in Refs. [10, 12].

The systematic uncertainties in the detector response are determined by varying the energy scale and energy resolution of the electrons and photons [24]. The effect of the experimental uncertainties in the signal yield, based on the variations in the acceptance times efficiency, are also considered. An additional uncertainty is also derived for the signal based on the internal variations of the PDF set.

The largest data-driven uncertainty in the diphoton channel is a shape uncertainty that corresponds to the uncertainty in the relative contribution of the reducible γj background component. This uncertainty is estimated by varying the measured fraction of the $\gamma\gamma$ background according to its uncertainty from the two-dimensional sideband method mentioned in Section 7. A data-driven uncertainty in the normalisation of the reducible background component (referred to as the “fake” background) in the dielectron channel is also derived, following the methodology of Ref. [34].

In this analysis, each systematic uncertainty is either naturally two-sided or is symmetrised to provide a two-sided systematic uncertainty. The variations from systematic uncertainties in both analysis channels are smoothed using a sliding window method [10] with a width of 300 GeV. The value of the variation at each invariant mass is taken as the average of all points in the range $[m - 150 \text{ GeV}, m + 150 \text{ GeV}]$. For

invariant masses near the edge of the distribution, the input is extended by replicating the value of the variation at the edge.

The impact of the systematic uncertainties in the final result is quantified by changes in the test statistic values. The largest impact on the test statistic values comes from the theoretical uncertainties in the DY and diphoton continuum backgrounds due to the variations of the underlying PDF. The experimental uncertainties are sub-dominant to the theoretical uncertainties across the full mass range considered in each analysis channel.

9 Generation of pseudo-experiments

The analysis uses pseudo-datasets as inputs for the CWT, where one scalogram is generated for each pseudo-dataset. These scalograms are the basic ingredient for the statistical procedures used in this analysis and are also used for estimating the systematic uncertainties. The pseudo-datasets (or “toys”) are generated with background-only models based on the functional forms from Section 7 and with signal-plus-background models using the signal models discussed in Section 6 and the background-only models from Section 7. These toys are produced with finely-binned (1 GeV) mass spectra separately for the diphoton and dielectron final states. For the toys containing a signal, a specific choice of CW/LD model parameters is used. The generated pseudo-datasets are hereafter called statistical-only toys (stat-toys) or systematic toys (syst-toys) depending on whether systematic variations are considered when constructing the toy.

To make the stat-toys, the analytic shapes are constructed containing either a background-only shape or a signal-plus-background shape. The background component is given a normalisation corresponding to the data normalisation in the signal region of each analysis channel. Next, a Poisson-fluctuated toy distribution is generated from the analytic shape chosen. Each of these toys is then treated as a proxy for the real data in the subsequent statistical analysis discussed in Section 11.

To make the syst-toys, a similar procedure is followed as with the stat-toys, but starting from an alternative description of the background-only and signal-plus-background shapes. This analysis follows the procedure introduced in Ref. [11], which is described briefly below.

To make one syst-toy for the background-only case, the alternative background shape (called hereafter an uncertainty template) is built from the systematic variations that arise from the sources of both experimental and theoretical uncertainties as discussed in Section 8. In the background-only case, these systematic variations are given in the invariant mass space as shape variations around the background description from simulation, as obtained in Refs. [10, 12]. A relative variation is defined as the relative difference between the up or down variation and the background description from simulation. To obtain the absolute systematic difference for the nominal background description from data defined in Sections 6 and 7, the relative variation is multiplied by the nominal background description from data. Each uncertainty template is constructed from the nominal background description from data, summed with the weighted absolute systematic differences. The weights are randomly sampled from a Gaussian distribution, with a mean of zero and standard deviation of one. The number of such weights in each uncertainty template is equal to the number of systematic variations considered.

To replicate the procedures given in Refs. [10, 12], the resulting uncertainty template is Poisson-fluctuated to generate one uncertainty pseudo-dataset. This uncertainty pseudo-dataset is then fit with the background model from either Eq. (2) or Eq. (3), depending on the analysis channel. This procedure results in one smooth

alternative background description, replacing the fits done in Refs. [10, 12]. This alternative background description is then used to generate one respective background-only uncertainty pseudo-dataset.

To make one syst-toy in the signal-plus-background case, a similar procedure is followed with minor modifications. The procedure starts from the signal systematic variations discussed in Section 8. The nominal signal shape is described by Eq. (1). The absolute systematic difference for each variation is calculated directly for the nominal signal shape. The signal uncertainty template is constructed from the nominal signal shape, summed with the Gaussian-weighted absolute systematic differences. Each signal-plus-background uncertainty template is constructed as the sum of one smooth alternative background description, as discussed above, and one signal uncertainty template. The result is Poisson-fluctuated to generate one respective signal-plus-background uncertainty pseudo-dataset.

These procedures are repeated to generate background-only and signal-plus-background syst-toys ensembles, where each toy in these ensembles reflects a different (random) combination of all uncertainties. The syst-toys ensembles are used in the subsequent statistical analysis discussed in Section 11.

10 Continuous wavelet transforms

Continuous wavelet transforms are used in this search to convert the diphoton and dielectron invariant mass spectra into mass versus frequency information in the form of scalograms before applying the machine learning techniques discussed in Section 11. An overview of the CWT method used in this search is detailed below.

The CWT is a measure of similarity between a chosen wavelet and a signal. The wavelet is used to scan the signal for different frequencies of the wavelet throughout the invariant mass spectrum.

The wavelet $\psi(x)$ is a basis function localised in both the mass and frequency space and the CWT of a signal $f(m)$ at a scale³ α and translational parameter β is given by a projection on $\psi(x)$ for different α and β values [15]:

$$W(\alpha, \beta) = \frac{1}{\sqrt{\alpha}} \int_{-\infty}^{+\infty} f(m) \psi^* \left(\frac{m - \beta}{\alpha} \right) dm \quad (4)$$

A scalogram can be produced by taking the norm of the coefficient $W(\alpha, \beta)$ for all values of α and β . Therefore, the CWT in this analysis defines how much of a certain frequency is in the signal at a given invariant mass bin.

The *Morlet wavelet* [69] is used in this analysis as the choice of $\psi(x)$ in Eq. (4). The Morlet wavelet is chosen because it is Gaussian-shaped in the frequency domain, which minimises possible edge effects that could be interpreted as signal, as opposed to wavelets with sharp boundaries that can introduce edge effects [70]. It consists of a localised wave packet and is given by:

$$\psi(x) \equiv \frac{1}{\sqrt{B\pi}} e^{-x^2/B} \left(e^{i2\pi Cx} - e^{-\pi^2 BC^2} \right), \quad (5)$$

where B and C are constants which are chosen to be 2 and 1 respectively. This choice of C ensures that the CWT of a signal reaches a maximum when the signal wavelength approximately equals the scale α . The Morlet Wavelet is shown in Figure 3.

³ The scale α is inversely proportional to frequency, where higher scales represent the low frequency component and vice versa.

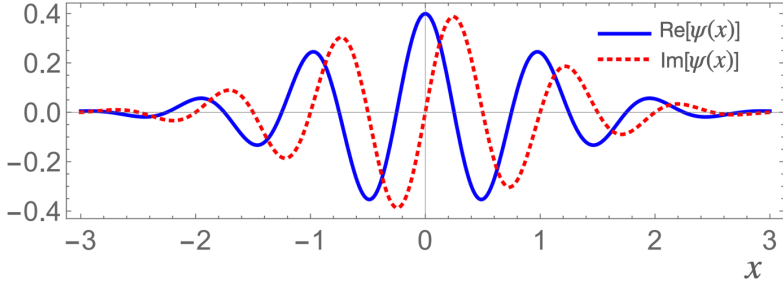


Figure 3: An illustration of the complex Morlet Wavelet used in the continuous wavelet transform in this analysis, split into real and imaginary components.

Example scalograms for the dielectron and diphoton channels can be seen in Figures 4 (without statistical fluctuation) and 5 (with statistical fluctuation). These scalograms are created after applying the CWT on a background-only distribution (Figures 4(a), 4(b), 5(a) and 5(b)) and on a signal-plus-background distribution (Figures 4(c), 4(d), 5(c) and 5(d)). The saturated area in the high-scale region occurs because the background distribution is not flat. Therefore, the background may still appear as periodic for very large scales, that is, those scales with small frequencies. The sharp transition seen between low $|W(\alpha, \beta)|$ and high $|W(\alpha, \beta)|$ values occurs because the $|W(\alpha, \beta)|$ values change quickly relative to the scale chosen for the z -axis.

The signal contribution in Figures 5(c) and 5(d) is clearly seen as a local small “island,” discernible from the continuum of the background shown in Figures 5(a) and 5(b), even when realistic statistical fluctuations are included. This signal-island represents the locality of the signal in both the mass and the scale (or frequency) spaces. Fixing M_5 and increasing the value of k shifts the signal-island in two ways. The signal-island is shifted horizontally to higher masses because the signal turn-on point in mass is roughly equal to the value of k . The signal-island is also shifted vertically towards higher scales because the spacing in the KK tower increases with k . Fixing k and changing M_5 only determines the prominence of the island, that is, it becomes more distinct with decreasing M_5 because of the inverse relationship between M_5 and the signal cross-section. Changing the mass resolution due to detector effects (within the uncertainties) only affects the $|W(\alpha, \beta)|$ values of the signal-island and this change is effectively equivalent to changing M_5 .

11 Data analysis

The diphoton and dielectron invariant mass distributions from the toys detailed in Section 9 are transformed into images using the CWT method described in Section 10 before being used to train a neural network (NN). The diphoton and dielectron images are treated as independent channels and are trained separately. Two types of convolutional NNs are used in this search, a classifier NN and an autoencoder (AE), which are discussed in Section 11.1 and Section 11.2, respectively. In both of the cases, the training is done using stat-toys, while the prediction is performed using syst-toys to evaluate the impact of the systematic uncertainties in the NN responses. As discussed in Section 9, the syst-toys already include a proper statistical representation of the data.

The classifier NN is used to probe for the periodic signals of the CW/LD model specifically (denoted here as model-dependent). On the other hand, the AE NN is used to search for more general anomalies in the

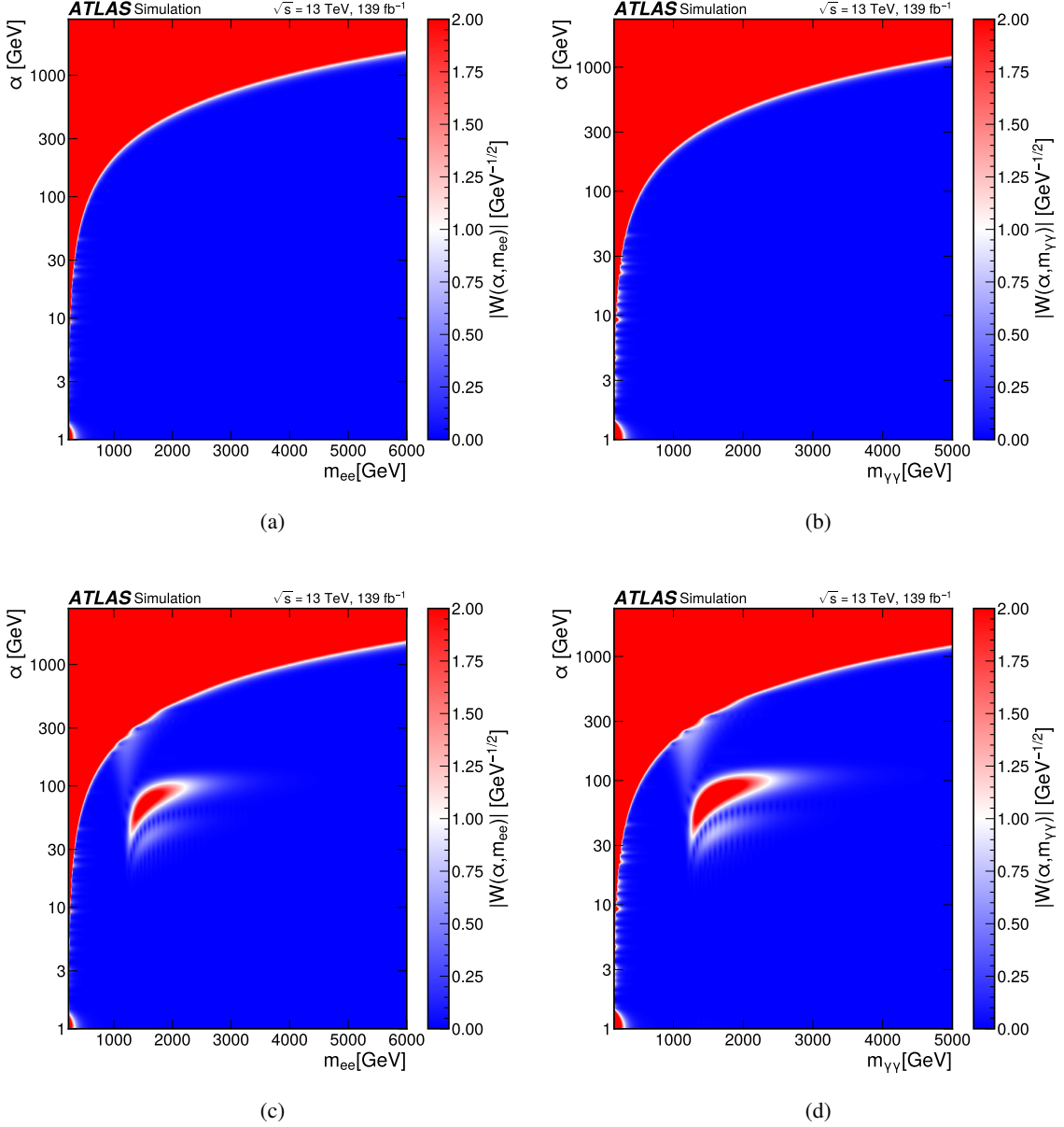


Figure 4: Scalogram output of the CWT of (a) dielectron and (b) diphoton background-only toy experiments and (c) dielectron and (d) diphoton signal-plus-background toy experiments with $k = 1200$ GeV and $M_5 = 3000$ GeV. These toys are produced without Poisson fluctuations. The signal contribution in (c) and (d) manifests as a localised ‘island’ in mass and scale, discernible from the continuum of the background shown in (a) and (b). The scalograms are provided here with a mass binning of 1 GeV. Here α is the CWT scale parameter and $W(\alpha, \beta)$ are the wavelet coefficients defined in Eq. (4), where the invariant mass of each channel takes the role of β .

data (denoted here as model-independent). Both of the neural networks used in this analysis are based on the setups given in Ref. [15]. The neural networks are implemented in Keras [71] using the TensorFlow backend [72]. The ADAM [73] optimiser is used to minimise the loss functions in each NN setup. The search is performed using a general form of a test statistic derived from the NN output itself.

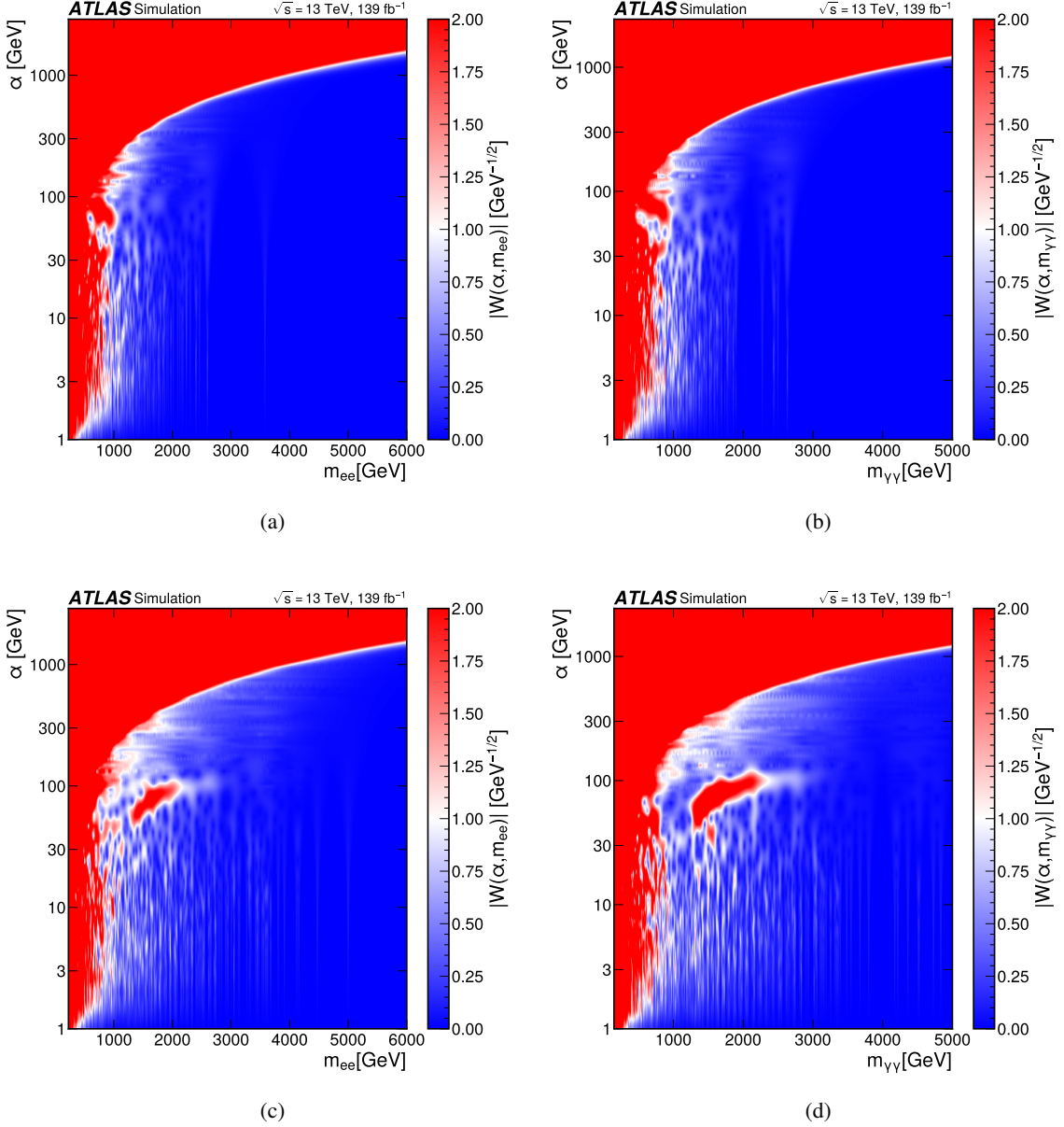


Figure 5: Scalogram output of the CWT of (a) dielectron and (b) diphoton background-only toy experiments and (c) dielectron and (d) diphoton signal-plus-background toy experiments with $k = 1200$ GeV and $M_5 = 3000$ GeV. These toys are produced with Poisson fluctuations arising from the statistical uncertainty of the data sample. These fluctuations are shown to dilute the presence of a signal. The signal contribution in (c) and (d) manifests as a localised “island” in mass and scale, discernible from the continuum of the background shown in (a) and (b). The scalograms are provided here with a mass binning of 1 GeV. Here α is the CWT scale parameter and $W(\alpha, \beta)$ are the wavelet coefficients defined in Eq. (4), where the invariant mass of each channel takes the role of β .

The loss functions associated with each of the NNs play the role of the likelihood function in a typical analysis. The loss function used in the classifier NN is the Binary Cross-Entropy (BCE) [74], while the AE NN uses the Mean Squared Error (MSE) loss function. The MSE loss function is further discussed in

Section 11.2. The training and validation loss are recorded as a function of the number of epochs and are inspected to verify that each NN gives good agreement in the output of the loss function when comparing the training and validation datasets.

In this analysis, the NN output in the classifier setup and the value of the loss function in the AE setup are used as test statistics. To set the exclusion limits on the model-dependent parameter space, the modified frequentist method, commonly known as the CL_s method [75–77], is used. This choice results in more conservative limits than those obtained by the standard p -value procedure [75, 76]. The dielectron and diphoton channels are analysed separately due to potential overlaps in their event selections.

11.1 Classifier NN

One possible way to discover a specific signal in a scalogram is with a classifier NN. In this analysis, the convolutional NN classifier setup from Ref. [15] is implemented for the model-dependent search. The CWT scalogram of the mass spectrum for each stat-toy, syst-toy, and the signal region data is produced and rebinned to ensure the inputs to the NN remain manageable. The mass for the NN inputs is rebinned into 40 GeV wide bins, while the scale is binned logarithmically. The stat-toy scalograms for the background-only and signal-plus-background cases are used for training the binary classifier convolutional NN, where the output of the network is between 0 (background-like) and 1 (signal-plus-background like).

In addition to the signal periodicity of the CW/LD model, these models can introduce a non-resonant tail above the SM background at high dielectron or diphoton invariant masses. For these high-mass ranges, the periodicity may no longer be as apparent due to the widening of the resonances with mass. This signal widening occurs because the experimental mass resolution worsens, which causes the merging of the signal mass peaks. This analysis focuses on the periodic features of the signal by adjusting the procedure such that the subsequent inference does not consider the effects of the non-resonant tail.

To achieve this adjustment, a cutoff is applied to the dielectron or diphoton mass distribution to remove events above a certain point in mass prior to training the classifier. This mass threshold is determined by calculating a signal’s local significance, S/σ_B , where S is the signal yield and σ_B is the local per-bin uncertainty. This uncertainty includes the statistical uncertainty and the systematic uncertainties described in Section 8, added in quadrature, of the background. The bin in the invariant mass distribution on a local signal peak where the per-bin-significance falls below 50% of its maximal value is chosen as the threshold. While the cutoff is independent of M_5 by construction, it does rise monotonically with k . Therefore, the cutoff values are calculated for a few points in k and are then fit with a second-order polynomial to allow for interpolation between the k points. As the long-range signal shape falls rapidly after reaching its maximum, alternative choices close to the nominal choice of 50% of the maximum local significance have little impact on the result. A lower significance choice, for example $S/\sigma_B \approx 10\%$ of the maximal value, effectively introduces no cutoff and the subsequent inference remains affected by the presence of the non-resonant tail feature. A higher significance choice, e.g., $S/\sigma_B \approx 90\%$ of the maximum value, removes the non-resonant tail effectively but also removes a large mass range where the periodicity is still apparent and reduces the search sensitivity to the intended feature. For the dielectron channel, the 50% threshold mass value ranges from 1400 to 6000 GeV for k in the range of 200 GeV to 5850 GeV. For the diphoton channel, the mass threshold ranges from 2000 to 5000 GeV for k in the range of 150 GeV to 4900 GeV.

For completeness, the classifier search without mass thresholds is also performed. In this case, the non-resonant feature of the signal may be present, while the periodicity may be unresolvable in the high mass region. The CWT and NN procedure can still provide some discrimination power between the

signal-plus-background and background-only distributions due to the non-resonant feature and additional oscillations available to describe the signal. Therefore, the sensitivity for low- k ($k \lesssim 1000$ GeV) signals is expected to be higher than for the case with mass thresholds. For high- k values, ($k \gtrsim 1000$ GeV), the sensitivities of the two methods are expected to be almost identical.

11.2 Autoencoder NN

A model-independent approach searching for anomalies in scalograms is performed using AEs. This technique has previously been applied to jet images in Refs. [78, 79] and was implemented and suggested for this type of search in Ref. [15]. The AE compresses a scalogram to a smaller set of parameters, which are then used to reconstruct the input scalogram. Instead of using the original background-only scalograms, they are standardised such that each bin in the scalogram is remapped to a local p-value in the range 0 to 1. The remapping per bin is done using the distribution of the original values in the specific bin from multiple scalograms. Further, to regularise the output, the negative logarithm of the remapped bin value (local p-value) is used to build a new two-dimensional input. This procedure is identical to the procedure in Ref. [15] and ensures that the loss function is not dominated by the region with high statistical precision. The AE is trained on background-only, stat-toy remapped scalograms to reproduce the original remapped scalograms (\mathbf{y}) by minimising the MSE loss function [79], L_{MSE} , as defined below:

$$L_{\text{MSE}}(\mathbf{y}, \hat{\mathbf{y}}) = \frac{1}{n} \sum_{i=1}^n |\mathbf{y}_i - \hat{\mathbf{y}}_i|^2, \quad (6)$$

where n is the number of bins used in the scalogram and $\hat{\mathbf{y}}$ is the output remapped scalogram from the AE.

After the AE model is trained, the AE should be able to approximately reproduce the original remapped scalogram if applied to a typical background-only syst-toy scalogram. Conversely, the AE may fail to reproduce the scalogram if applied to a data scalogram that contains a signal. This metric, L_{MSE} , is used as a test statistic. In this analysis, the AE is particularly sensitive to signals with periodic structures.

The L_{MSE} is also calculated per scalogram bin. For each bin, an ensemble of the L_{MSE} values for the background predictions is generated. From these ensembles, a local p -value is calculated for every scalogram bin. The statistically significant bins are then visible with p -values close to 0.

As discussed in Section 11.1, to focus the search on the periodicity features and avoid possible inference that is based only on non-resonant signals, two sets of selections are introduced. Unlike in Section 11.1, these selections cannot be based on a specific signal and should be characterised only based on information pertaining to the SM backgrounds. In the first method, the non-resonant features are removed by using the statistical error at the tail of the background template shape, $R = 1/\sqrt{B(m_{\min})}$, where $B(m_{\min})$ is the integral of the background template shape above some minimum invariant mass m_{\min} . Different m_{\min} thresholds are derived for different R values, where for each, the tail of the distribution above the threshold is removed before calculating the CWT. The thresholds and the respective invariant mass ranges for each channel are found in Table 1.

This procedure also prevents large statistical fluctuations in the high-mass tail of the background distribution from affecting the L_{MSE} of the AE predictions.

In the second approach, the scale range of the scalograms is instead modified and the mass range remains unrestricted. This approach, referred to as scale thresholding, avoids the large-scale region of the scalogram

Table 1: Different precision-driven thresholds considered for each analysis channel and the corresponding mass ranges probed in the model-independent analysis. For the no threshold scenario, the upper limit in mass is chosen such that the range goes 300 GeV beyond the last observed data point in the dielectron and diphoton mass spectra.

Threshold	Dielectron Mass Range [GeV]	Diphoton Mass Range [GeV]
$R < 10\%$	225–1520	150–1380
$R < 50\%$	225–2700	150–2400
No threshold	225–4400	150–2700

that may include continuum contributions from a signal. In this method, the bin content in the scalogram is replaced with zero if the scale α in that bin satisfies $\alpha > m/4$, where m denotes the mass value of that bin. In a similar way, to exclude the scales that are short and cannot be resolved experimentally, the bin content in the scalogram is replaced with zero if the bin satisfies $\alpha < m/100$. The results from both methods are given in Section 12.

Possible deviations in the data, arising from SM or beyond the SM effects, from the smoothly falling background model assumed in each analysis channel could be captured in the AE analysis. However, the sensitivity to any new signal is lessened as this approach is designed to be most sensitive for deviations which appear periodic.

12 Results

The scalograms for the data events passing all selections for the diphoton and dielectron channels are shown in Figure 6.

The model-independent results from the AE-based search with $R < 50\%$ are presented as the negative logarithm of the local p -values corresponding to these data scalograms and are shown in Figure 7.

To obtain the significance for the model-independent results, the L_{MSE} is calculated for each original and predicted scalogram pair, with the sum in Eq. (6) running over all of the scalogram bins. An ensemble of L_{MSE} values for the background prediction is then generated from many pairs of original and predicted scalograms. From this ensemble, the significance is calculated for the data scalogram.

The significances for the model-independent results in each analysis channel are given in Table 2. No significant deviations from the background-only hypothesis are observed. The largest deviation from the background-only (SM) hypothesis is found in the dielectron channel with the 50% threshold and the scale threshold, with an excess corresponding to a significance of 1.5σ .

For the AE-based model-independent result, an alternative approach is also tested where the training is performed using syst-toys rather than stat-toys. In this approach, all steps of the AE-based search after the training match the procedure described in Section 11.2. The significance values in this alternative approach are found to be comparable to the results given in Table 2.

The model-dependent results are also presented for each analysis channel. No significant deviation from the background-only hypothesis is seen in either of the analysis channels. Test statistic distributions assuming

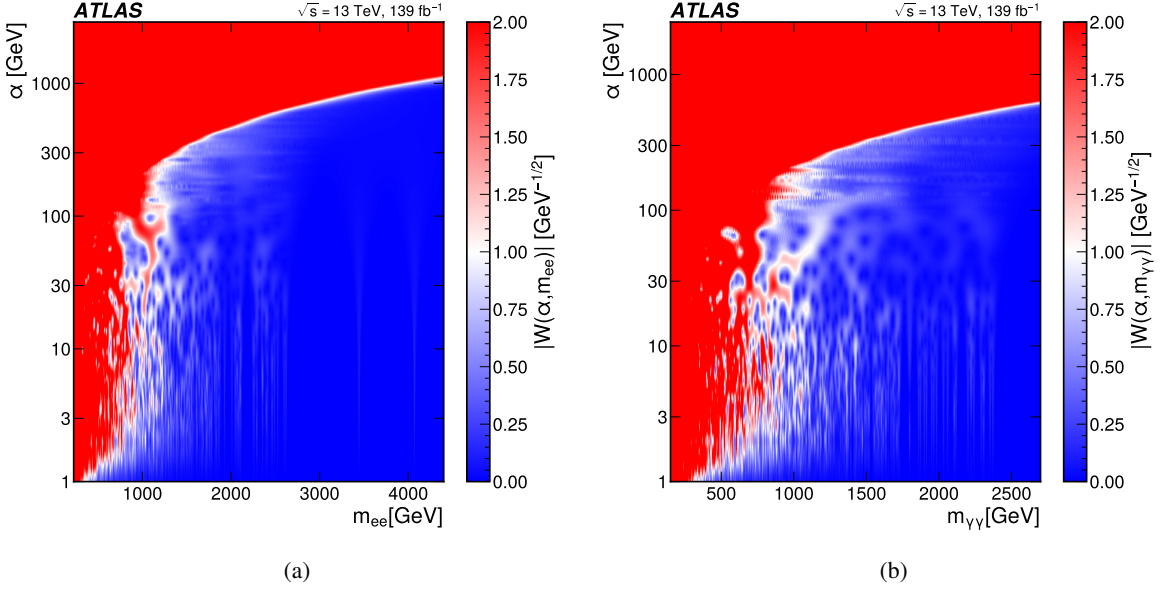


Figure 6: The scalogram output of the CWT for the (a) dielectron and (b) diphoton search channels for the observed signal region data. The scalograms are shown here with a mass binning of 1 GeV and are rebinned to a coarser binning before running the neural networks. Here α is the CWT scale parameter and $W(\alpha, \beta)$ are the wavelet coefficients defined in Eq. (4), where the invariant mass of each channel takes the role of β . The range of m_{ee} and $m_{\gamma\gamma}$ is chosen such that the plots cover approximately 300 GeV after the last observed data point.

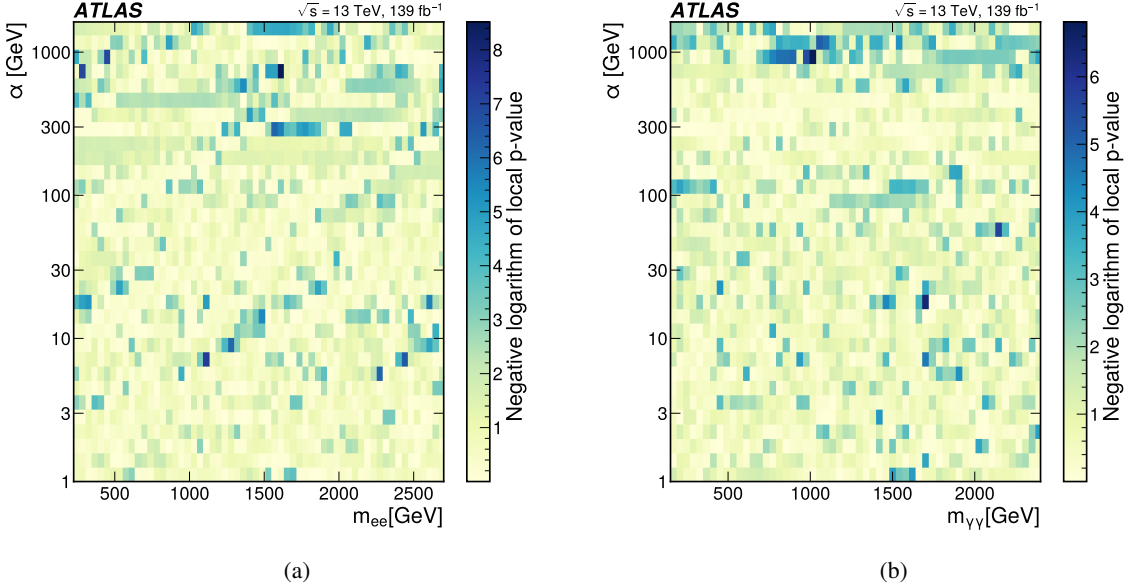


Figure 7: The negative logarithm of the local p -values calculated for the observed data mass distributions in the (a) dielectron and (b) diphoton search channels for the $R < 50\%$ scenario. Here α is the CWT scale parameter.

Table 2: The observed significance in each analysis channel for the different thresholds considered in the model-independent analysis. Each significance is signed with positive (negative) values indicating the loss from data is higher (lower) than the median loss from the expected background.

Threshold	Dielectron Significance	Diphoton Significance
$R < 10\%$	0.4	-1.8
$R < 50\%$	1.5	-0.2
No threshold	0.7	-0.7
Scale threshold	1.5	-0.6

both a signal model, with $k = 1033$ GeV and $M_5 = 9000$ GeV, and the Standard Model are shown in Figure 8 and they are compared with the test statistic from the observed data.

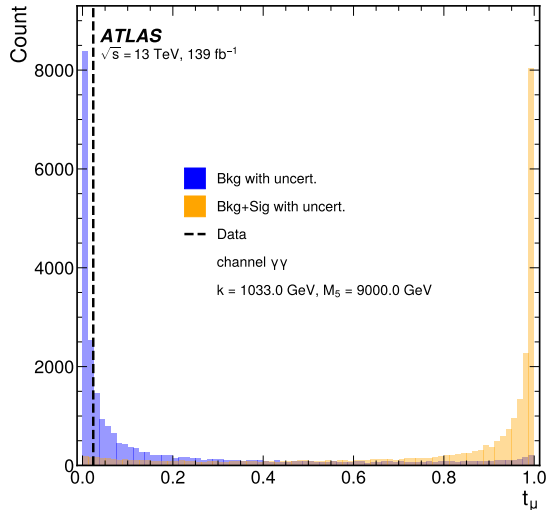


Figure 8: The distribution of the test statistic t_μ assuming a signal model μ with $k = 1033$ GeV and $M_5 = 9000$ GeV and assuming the Standard Model in the diphoton channel for the case where mass thresholds are applied. The pseudo-experiments used to generate the test statistic include the effects from the statistical uncertainty and all systematic uncertainties. The test statistic from observed data is shown as a dotted line.

In the absence of a clear signal, limits at 95% CL are set on the CW/LD model in the $k - M_5$ plane. The limits for the case with mass thresholding, as discussed in Section 11.1, are shown in Figure 9. Additional exclusions are shown for the case without mass thresholds in Figure 10. As expected, the sensitivity and corresponding limits are stronger for the case without mass thresholds in the region of $k \lesssim 1000$ GeV.

For the case with mass thresholds, the maximum excluded M_5 value in the diphoton channel is approximately 10 TeV for values of $k \approx 600$ GeV, while the maximum excluded M_5 value in the dielectron channel is approximately 8.4 TeV for values of $k \approx 900$ GeV. For the case without mass thresholds, the maximum excluded M_5 value in the diphoton channel is approximately 11 TeV for values of $k \approx 200 - 1000$ GeV, while the maximum excluded M_5 value in the dielectron channel is approximately 8.8 TeV for values of

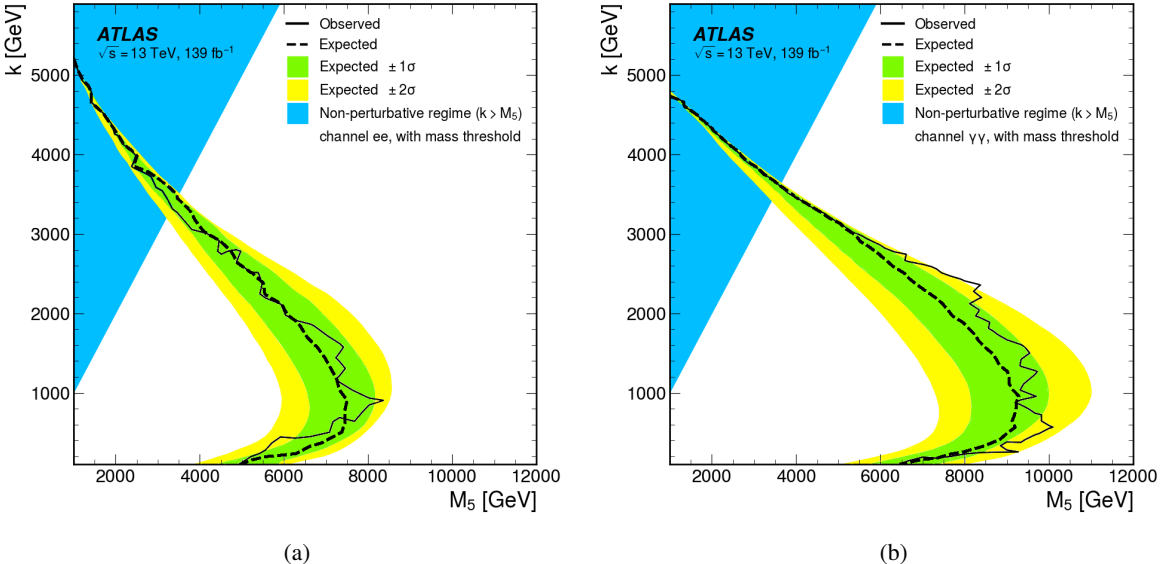


Figure 9: The expected and observed exclusion limits at 95% CL for the clockwork gravity model projected in the k - M_5 parameter space for the (a) ee and (b) $\gamma\gamma$ channels, both for the case with mass thresholds. The surrounding shaded bands represent the $\pm 1\sigma$ and $\pm 2\sigma$ uncertainties on the expected limit. The shaded area with $k > M_5$ illustrates the region of parameter space where the CW/LD theory becomes non-perturbative.

$k \approx 400$ GeV. The areas in k - M_5 where the observed limits are stronger than the expected limits indicate that the data is effectively smoother than the expected fluctuations arising from the statistical and systematic uncertainties.

The systematic uncertainties mainly impact the classifier result in the range of $500 < k < 1500$ GeV for both of the analysis channels. The statistical uncertainties dominate in the higher k ranges. The sensitivity of the classifier with systematic uncertainties is at most ~ 1 TeV weaker in M_5 exclusion than the limits evaluated without including the systematic uncertainties. The most dominant uncertainty contribution in both of the channels is due to the theoretical uncertainties in the background modelling.

It is worthwhile to mention that the NNs are initially trained on a lattice of points in the k - M_5 plane, where a dedicated training is performed for each lattice point. The results are verified to be similarly effective for the models in-between those lattice points.

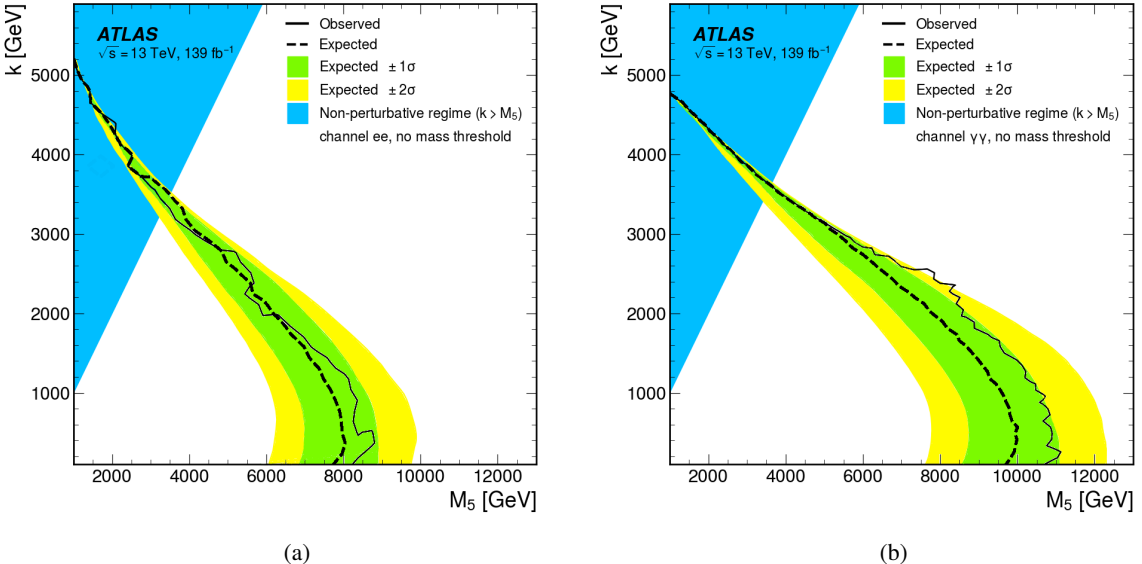


Figure 10: The expected and observed exclusion limits at 95% CL for the clockwork gravity model projected in the k - M_5 parameter space for the (a) ee and (b) $\gamma\gamma$ channels, both for the case without mass thresholds. The surrounding shaded bands represent the $\pm 1\sigma$ and $\pm 2\sigma$ uncertainties on the expected limit. The shaded area with $k > M_5$ illustrates the region of phase space where the CW/LD theory becomes non-perturbative.

13 Conclusion

Searches for periodic new phenomena in the dielectron and diphoton invariant mass spectra with the ATLAS experiment at the LHC are presented. The searches are conducted with 139 fb^{-1} of pp collision data at $\sqrt{s} = 13 \text{ TeV}$. The model-dependent result is optimised for spin-2 periodic resonances (KK gravitons) in the clockwork/linear-dilaton model. Model-independent results sensitive to more general periodic contributions are also presented.

The data observed in the ee and $\gamma\gamma$ invariant mass spectra are found to be consistent with the SM expectations. Without a significant excess, the 95% CL exclusion limits are set in the parameter space of the CW/LD model. This result excludes values of M_5 in the range 11 TeV to 1 TeV for values of k in the range 100 GeV to 5 TeV.

Acknowledgements

We thank CERN for the very successful operation of the LHC, as well as the support staff from our institutions without whom ATLAS could not be operated efficiently.

We acknowledge the support of ANPCyT, Argentina; YerPhI, Armenia; ARC, Australia; BMWFW and FWF, Austria; ANAS, Azerbaijan; CNPq and FAPESP, Brazil; NSERC, NRC and CFI, Canada; CERN; ANID, Chile; CAS, MOST and NSFC, China; Minciencias, Colombia; MEYS CR, Czech Republic; DNRF and DNSRC, Denmark; IN2P3-CNRS and CEA-DRF/IRFU, France; SRNSFG, Georgia; BMBF, HGF and

MPG, Germany; GSRI, Greece; RGC and Hong Kong SAR, China; ISF and Benoziyo Center, Israel; INFN, Italy; MEXT and JSPS, Japan; CNRST, Morocco; NWO, Netherlands; RCN, Norway; MEiN, Poland; FCT, Portugal; MNE/IFA, Romania; MESTD, Serbia; MSSR, Slovakia; ARRS and MIZŠ, Slovenia; DS/ NRF, South Africa; MICINN, Spain; SRC and Wallenberg Foundation, Sweden; SERI, SNSF and Cantons of Bern and Geneva, Switzerland; MOST, Taiwan; TENMAK, Türkiye; STFC, United Kingdom; DOE and NSF, United States of America. In addition, individual groups and members have received support from BCKDF, CANARIE, Compute Canada and CRC, Canada; PRIMUS 21/SCI/017 and UNCE SCI/013, Czech Republic; COST, ERC, ERDF, Horizon 2020 and Marie Skłodowska-Curie Actions, European Union; Investissements d’Avenir Labex, Investissements d’Avenir Idex and ANR, France; DFG and AvH Foundation, Germany; Herakleitos, Thales and Aristeia programmes co-financed by EU-ESF and the Greek NSRF, Greece; BSF-NSF and MINERVA, Israel; Norwegian Financial Mechanism 2014-2021, Norway; NCN and NAWA, Poland; La Caixa Banking Foundation, CERCA Programme Generalitat de Catalunya and PROMETEO and GenT Programmes Generalitat Valenciana, Spain; Göran Gustafssons Stiftelse, Sweden; The Royal Society and Leverhulme Trust, United Kingdom.

The crucial computing support from all WLCG partners is acknowledged gratefully, in particular from CERN, the ATLAS Tier-1 facilities at TRIUMF (Canada), NDGF (Denmark, Norway, Sweden), CC-IN2P3 (France), KIT/GridKA (Germany), INFN-CNAF (Italy), NL-T1 (Netherlands), PIC (Spain), ASGC (Taiwan), RAL (UK) and BNL (USA), the Tier-2 facilities worldwide and large non-WLCG resource providers. Major contributors of computing resources are listed in Ref. [80].

References

- [1] G. F. Giudice and M. McCullough, *A Clockwork Theory*, **JHEP** **02** (2017) 036, arXiv: [1610.07962 \[hep-ph\]](#).
- [2] G. F. Giudice, Y. Kats, M. McCullough, R. Torre and A. Urbano, *Clockwork/linear dilaton: structure and phenomenology*, **JHEP** **06** (2018) 009, arXiv: [1711.08437 \[hep-ph\]](#).
- [3] I. Antoniadis, S. Dimopoulos and A. Giveon, *Little string theory at a TeV*, **JHEP** **05** (2001) 055, arXiv: [hep-th/0103033](#).
- [4] I. Antoniadis, A. Arvanitaki, S. Dimopoulos and A. Giveon, *Phenomenology of TeV Little String Theory from Holography*, **Phys. Rev. Lett.** **108** (2012) 081602, arXiv: [1102.4043 \[hep-ph\]](#).
- [5] M. Berkooz, M. Rozali and N. Seiberg, *Matrix description of M-theory on T^4 and T^5* , **Phys. Lett.** **B408** (1997) 105, arXiv: [hep-th/9704089](#).
- [6] N. Seiberg, *New theories in six-dimensions and matrix description of M-theory on T^5 and T^5/Z_2* , **Phys. Lett.** **B408** (1997) 98, arXiv: [hep-th/9705221](#).
- [7] N. Arkani-Hamed, S. Dimopoulos and G. Dvali, *The Hierarchy problem and new dimensions at a millimeter*, **Phys. Lett. B** **429** (1998) 263, arXiv: [hep-ph/9803315](#).
- [8] I. Antoniadis, N. Arkani-Hamed, S. Dimopoulos and G. R. Dvali, *New dimensions at a millimeter to a Fermi and superstrings at a TeV*, **Phys. Lett. B** **436** (1998) 257, arXiv: [hep-ph/9804398](#).

- [9] L. Randall and R. Sundrum, *Large mass hierarchy from a small extra dimension*, Phys. Rev. Lett. **83** (1999) 3370, arXiv: [hep-ph/9905221](#).
- [10] ATLAS Collaboration, *Search for high-mass dilepton resonances using 139fb^{-1} of pp collision data collected at $\sqrt{s} = 13\text{ TeV}$ with the ATLAS detector*, Phys. Lett. B **796** (2019) 68, arXiv: [1903.06248 \[hep-ex\]](#).
- [11] ATLAS Collaboration, *Search for new non-resonant phenomena in high-mass dilepton final states with the ATLAS detector*, JHEP **11** (2020) 005, arXiv: [2006.12946 \[hep-ex\]](#), Erratum: JHEP **04** (2021) 142.
- [12] ATLAS Collaboration, *Search for resonances decaying into photon pairs in 139fb^{-1} of pp collisions at $\sqrt{s} = 13\text{ TeV}$ with the ATLAS detector*, Phys. Lett. B **822** (2021) 136651, arXiv: [2102.13405 \[hep-ex\]](#).
- [13] CMS Collaboration, *Search for physics beyond the standard model in high-mass diphoton events from proton–proton collisions at $\sqrt{s} = 13\text{ TeV}$* , Phys. Rev. D **98** (2018) 092001, arXiv: [1809.00327 \[hep-ex\]](#).
- [14] CMS Collaboration, *Search for resonant and nonresonant new phenomena in high-mass dilepton final states at $\sqrt{s} = 13\text{ TeV}$* , JHEP **07** (2021) 208, arXiv: [2103.02708 \[hep-ex\]](#).
- [15] H. Beauchesne and Y. Kats, *Searching for periodic signals in kinematic distributions using continuous wavelet transforms*, Eur. Phys. J. C **80** (2020) 192, arXiv: [1907.03676 \[hep-ph\]](#).
- [16] ATLAS Collaboration, *The ATLAS Experiment at the CERN Large Hadron Collider*, JINST **3** (2008) S08003.
- [17] ATLAS Collaboration, *ATLAS Insertable B-Layer Technical Design Report*, ATLAS-TDR-19; CERN-LHCC-2010-013, 2010, URL: <https://cds.cern.ch/record/1291633>, Addendum: ATLAS-TDR-19-ADD-1; CERN-LHCC-2012-009, 2012, URL: <https://cds.cern.ch/record/1451888>.
- [18] B. Abbott et al., *Production and integration of the ATLAS Insertable B-Layer*, JINST **13** (2018) T05008, arXiv: [1803.00844 \[physics.ins-det\]](#).
- [19] ATLAS Collaboration, *Performance of the ATLAS trigger system in 2015*, Eur. Phys. J. C **77** (2017) 317, arXiv: [1611.09661 \[hep-ex\]](#).
- [20] ATLAS Collaboration, *The ATLAS Collaboration Software and Firmware*, ATL-SOFT-PUB-2021-001, 2021, URL: <https://cds.cern.ch/record/2767187>.
- [21] ATLAS Collaboration, *ATLAS data quality operations and performance for 2015–2018 data-taking*, JINST **15** (2020) P04003, arXiv: [1911.04632 \[physics.ins-det\]](#).
- [22] ATLAS Collaboration, *Luminosity determination in pp collisions at $\sqrt{s} = 13\text{ TeV}$ using the ATLAS detector at the LHC*, ATLAS-CONF-2019-021, 2019, URL: <https://cds.cern.ch/record/2677054>.
- [23] G. Avoni et al., *The new LUCID-2 detector for luminosity measurement and monitoring in ATLAS*, JINST **13** (2018) P07017.
- [24] ATLAS Collaboration, *Electron and photon performance measurements with the ATLAS detector using the 2015–2017 LHC proton–proton collision data*, JINST **14** (2019) P12006, arXiv: [1908.00005 \[hep-ex\]](#).

- [25] ATLAS Collaboration, *Performance of electron and photon triggers in ATLAS during LHC Run 2*, Eur. Phys. J. C **80** (2020) 47, arXiv: [1909.00761 \[hep-ex\]](#).
- [26] ATLAS Collaboration, *Measurement of isolated-photon pair production in pp collisions at $\sqrt{s} = 7\text{ TeV}$ with the ATLAS detector*, JHEP **01** (2013) 086, arXiv: [1211.1913 \[hep-ex\]](#).
- [27] T. Gleisberg et al., *Event generation with SHERPA 1.1*, JHEP **02** (2009) 007, arXiv: [0811.4622 \[hep-ph\]](#).
- [28] E. Bothmann et al., *Event generation with Sherpa 2.2*, SciPost Phys. **7** (2019) 034, arXiv: [1905.09127 \[hep-ph\]](#).
- [29] S. Höche, F. Krauss, M. Schönherr and F. Siegert, *A critical appraisal of NLO+PS matching methods*, JHEP **09** (2012) 049, arXiv: [1111.1220 \[hep-ph\]](#).
- [30] S. Höche, F. Krauss, M. Schönherr and F. Siegert, *QCD matrix elements + parton showers. The NLO case*, JHEP **04** (2013) 027, arXiv: [1207.5030 \[hep-ph\]](#).
- [31] S. Catani, F. Krauss, B. R. Webber and R. Kuhn, *QCD Matrix Elements + Parton Showers*, JHEP **11** (2001) 063, arXiv: [hep-ph/0109231](#).
- [32] S. Höche, F. Krauss, S. Schumann and F. Siegert, *QCD matrix elements and truncated showers*, JHEP **05** (2009) 053, arXiv: [0903.1219 \[hep-ph\]](#).
- [33] The NNPDF Collaboration, R. D. Ball et al., *Parton distributions for the LHC run II*, JHEP **04** (2015) 040, arXiv: [1410.8849 \[hep-ph\]](#).
- [34] ATLAS Collaboration, *Search for new high-mass phenomena in the dilepton final state using 36 fb^{-1} of proton–proton collision data at $\sqrt{s} = 13\text{ TeV}$ with the ATLAS detector*, JHEP **10** (2017) 182, arXiv: [1707.02424 \[hep-ex\]](#).
- [35] ATLAS Collaboration, *Monte Carlo Generators for the Production of a W or Z/ γ^* Boson in Association with Jets at ATLAS in Run 2*, ATL-PHYS-PUB-2016-003, 2016, URL: <https://cds.cern.ch/record/2120133>.
- [36] P. Nason, *A new method for combining NLO QCD with shower Monte Carlo algorithms*, JHEP **11** (2004) 040, arXiv: [hep-ph/0409146](#).
- [37] S. Frixione, P. Nason and C. Oleari, *Matching NLO QCD computations with parton shower simulations: the POWHEG method*, JHEP **11** (2007) 070, arXiv: [0709.2092 \[hep-ph\]](#).
- [38] S. Alioli, P. Nason, C. Oleari and E. Re, *A general framework for implementing NLO calculations in shower Monte Carlo programs: the POWHEG BOX*, JHEP **06** (2010) 043, arXiv: [1002.2581 \[hep-ph\]](#).
- [39] S. Alioli, P. Nason, C. Oleari and E. Re, *NLO vector-boson production matched with shower in POWHEG*, JHEP **07** (2008) 060, arXiv: [0805.4802 \[hep-ph\]](#).
- [40] H.-L. Lai et al., *New parton distributions for collider physics*, Phys. Rev. D **82** (2010) 074024, arXiv: [1007.2241 \[hep-ph\]](#).
- [41] T. Sjöstrand, S. Mrenna and P. Skands, *A brief introduction to PYTHIA 8.1*, Comput. Phys. Commun. **178** (2008) 852, arXiv: [0710.3820 \[hep-ph\]](#).

- [42] C. Anastasiou, L. Dixon, K. Melnikov and F. Petriello, *High-precision QCD at hadron colliders: Electroweak gauge boson rapidity distributions at next-to-next-to leading order*, *Phys. Rev. D* **69** (2004) 094008, arXiv: [hep-ph/0312266](#).
- [43] S. Dulat et al.,
New parton distribution functions from a global analysis of quantum chromodynamics, *Phys. Rev. D* **93** (2016) 033006, arXiv: [1506.07443 \[hep-ph\]](#).
- [44] A. Arbuzov et al., *Update of the MCSANC Monte Carlo integrator, v. 1.20*, *JETP Lett.* **103** (2016) 131, arXiv: [1509.03052 \[hep-ph\]](#).
- [45] ATLAS Collaboration, *Multi-boson simulation for 13 TeV ATLAS analyses*, ATL-PHYS-PUB-2016-002, 2016, URL: <https://cds.cern.ch/record/2119986>.
- [46] T. Gleisberg and S. Höche, *Comix, a new matrix element generator*, *JHEP* **12** (2008) 039, arXiv: [0808.3674 \[hep-ph\]](#).
- [47] S. Schumann and F. Krauss,
A parton shower algorithm based on Catani–Seymour dipole factorisation, *JHEP* **03** (2008) 038, arXiv: [0709.1027 \[hep-ph\]](#).
- [48] S. Frixione, G. Ridolfi and P. Nason,
A positive-weight next-to-leading-order Monte Carlo for heavy flavour hadroproduction, *JHEP* **09** (2007) 126, arXiv: [0707.3088 \[hep-ph\]](#).
- [49] S. Alioli, P. Nason, C. Oleari and E. Re,
NLO single-top production matched with shower in POWHEG: s- and t-channel contributions, *JHEP* **09** (2009) 111, arXiv: [0907.4076 \[hep-ph\]](#), Erratum: *JHEP* **02** (2010) 011.
- [50] R. Frederix, E. Re and P. Torrielli,
Single-top t-channel hadroproduction in the four-flavour scheme with POWHEG and aMC@NLO, *JHEP* **09** (2012) 130, arXiv: [1207.5391 \[hep-ph\]](#).
- [51] E. Re, *Single-top Wt-channel production matched with parton showers using the POWHEG method*, *Eur. Phys. J. C* **71** (2011) 1547, arXiv: [1009.2450 \[hep-ph\]](#).
- [52] T. Sjöstrand et al., *An introduction to PYTHIA 8.2*, *Comput. Phys. Commun.* **191** (2015) 159, arXiv: [1410.3012 \[hep-ph\]](#).
- [53] ATLAS Collaboration, *ATLAS Pythia 8 tunes to 7 TeV data*, ATL-PHYS-PUB-2014-021, 2014, URL: <https://cds.cern.ch/record/1966419>.
- [54] NNPDF Collaboration, R. D. Ball et al., *Parton distributions with LHC data*, *Nucl. Phys. B* **867** (2013) 244, arXiv: [1207.1303 \[hep-ph\]](#).
- [55] M. Czakon and A. Mitov,
Top++: A program for the calculation of the top-pair cross-section at hadron colliders, *Comput. Phys. Commun.* **185** (2014) 2930, arXiv: [1112.5675 \[hep-ph\]](#).
- [56] ATLAS Collaboration, *The Pythia 8 A3 tune description of ATLAS minimum bias and inelastic measurements incorporating the Donnachie–Landshoff diffractive model*, ATL-PHYS-PUB-2016-017, 2016, URL: <https://cds.cern.ch/record/2206965>.
- [57] ATLAS Collaboration, *Measurement of the Inelastic Proton–Proton Cross Section at $\sqrt{s} = 13$ TeV with the ATLAS Detector at the LHC*, *Phys. Rev. Lett.* **117** (2016) 182002, arXiv: [1606.02625 \[hep-ex\]](#).

- [58] ATLAS Collaboration, *The ATLAS Simulation Infrastructure*, *Eur. Phys. J. C* **70** (2010) 823, arXiv: [1005.4568 \[physics.ins-det\]](#).
- [59] S. Agostinelli et al., *GEANT4 – a simulation toolkit*, *Nucl. Instrum. Meth. A* **506** (2003) 250.
- [60] ATLAS Collaboration, *The simulation principle and performance of the ATLAS fast calorimeter simulation FastCaloSim*, ATL-PHYS-PUB-2010-013, 2010, URL: <https://cds.cern.ch/record/1300517>.
- [61] ATLAS Collaboration, *Measurement of Higgs boson production in the diphoton decay channel in pp collisions at center-of-mass energies of 7 and 8 TeV with the ATLAS detector*, *Phys. Rev. D* **90** (2014) 112015, arXiv: [1408.7084 \[hep-ex\]](#).
- [62] ATLAS Collaboration, *Electron and photon reconstruction and performance in ATLAS using a dynamical, topological cell clustering-based approach*, ATL-PHYS-PUB-2017-022, 2017, URL: <https://cds.cern.ch/record/2298955>.
- [63] M. Oreglia, *A Study of the Reactions $\psi' \rightarrow \gamma\gamma\psi$* , SLAC-236, PhD thesis: Stanford University, 1980.
- [64] T. Skwarnicki, *A study of the radiative CASCADE transitions between the Upsilon-Prime and Upsilon resonances*, DESY-F31-86-02, PhD thesis: Cracow Institut of Nuclear Physics, 1986.
- [65] M. Oreglia et al., *Study of the reaction $\psi' \rightarrow \gamma\gamma\frac{J}{\psi}$* , *Phys. Rev. D* **25** (9 1982) 2259, URL: <https://link.aps.org/doi/10.1103/PhysRevD.25.2259>.
- [66] Particle Data Group, M. Tanabashi et al., *Review of Particle Physics*, *Phys. Rev. D* **98** (2018) 030001.
- [67] ATLAS Collaboration, *Search for resonances in diphoton events at $\sqrt{s} = 13$ TeV with the ATLAS detector*, *JHEP* **09** (2016) 001, arXiv: [1606.03833 \[hep-ex\]](#).
- [68] A. D. Martin, R. G. Roberts, W. J. Stirling and R. S. Thorne, *Parton distributions incorporating QED contributions*, *Eur. Phys. J. C* **39** (2005) 155, arXiv: [hep-ph/0411040](#).
- [69] J. Morlet, G. Arens, E. Fourgeau and D. Giard, *Wave propagation and sampling theory—Part I: Complex signal and scattering in multilayered media*, *Geophysics* **47** (1982) 203.
- [70] M. X. Cohen, *A better way to define and describe Morlet wavelets for time-frequency analysis*, *NeuroImage* **199** (2019) 81, ISSN: 1053-8119, URL: <https://www.sciencedirect.com/science/article/pii/S1053811919304409>.
- [71] F. Chollet et al., *Keras*, 2015, URL: <https://keras.io>.
- [72] M. Abadi et al., *TensorFlow: Large-Scale Machine Learning on Heterogeneous Distributed Systems*, (2016), arXiv: [1603.04467 \[cs.DC\]](#).
- [73] D. P. Kingma and J. Ba, *Adam: A Method for Stochastic Optimization*, (2014), arXiv: [1412.6980 \[cs.LG\]](#).
- [74] T. Cohen, M. Freytsis and B. Ostdiek, *(Machine) Learning to Do More with Less*, *JHEP* **02** (2018) 034, arXiv: [1706.09451 \[hep-ph\]](#).
- [75] A. L. Read, *Presentation of search results: the CL_S technique*, *J. Phys. G* **28** (2002) 2693.
- [76] T. Junk, *Confidence level computation for combining searches with small statistics*, *Nucl. Instrum. Meth. A* **434** (1999) 435, arXiv: [hep-ex/9902006](#).

- [77] Particle Data Group, P. Zyla et al., *Review of Particle Physics*, **PTEP** **2020** (2020) 083C01.
- [78] T. Heimel, G. Kasieczka, T. Plehn and J. M. Thompson, *QCD or What?*, **SciPost Phys.** **6** (2019) 030, arXiv: [1808.08979 \[hep-ph\]](https://arxiv.org/abs/1808.08979).
- [79] M. Farina, Y. Nakai and D. Shih, *Searching for New Physics with Deep Autoencoders*, **Phys. Rev. D** **101** (2020) 075021, arXiv: [1808.08992 \[hep-ph\]](https://arxiv.org/abs/1808.08992).
- [80] ATLAS Collaboration, *ATLAS Computing Acknowledgements*, ATL-SOFT-PUB-2021-003, 2021, URL: <https://cds.cern.ch/record/2776662>.

The ATLAS Collaboration

G. Aad [ID¹⁰³](#), B. Abbott [ID¹²¹](#), K. Abeling [ID⁵⁵](#), N.J. Abicht [ID⁴⁹](#), S.H. Abidi [ID²⁹](#), A. Aboulhorma [ID^{35e}](#), H. Abramowicz [ID¹⁵²](#), H. Abreu [ID¹⁵¹](#), Y. Abulaiti [ID¹¹⁸](#), A.C. Abusleme Hoffman [ID^{138a}](#), B.S. Acharya [ID^{69a,69b,o}](#), C. Adam Bourdarios [ID⁴](#), L. Adamczyk [ID^{86a}](#), L. Adamek [ID¹⁵⁶](#), S.V. Addepalli [ID²⁶](#), M.J. Addison [ID¹⁰²](#), J. Adelman [ID¹¹⁶](#), A. Adiguzel [ID^{21c}](#), T. Adye [ID¹³⁵](#), A.A. Affolder [ID¹³⁷](#), Y. Afik [ID³⁶](#), M.N. Agaras [ID¹³](#), J. Agarwala [ID^{73a,73b}](#), A. Aggarwal [ID¹⁰¹](#), C. Agheorghiesei [ID^{27c}](#), A. Ahmad [ID³⁶](#), F. Ahmadov [ID^{38,aa}](#), W.S. Ahmed [ID¹⁰⁵](#), S. Ahuja [ID⁹⁶](#), X. Ai [ID^{62a}](#), G. Aielli [ID^{76a,76b}](#), M. Ait Tamlihat [ID^{35e}](#), B. Aitbenchikh [ID^{35a}](#), I. Aizenberg [ID¹⁷⁰](#), M. Akbiyik [ID¹⁰¹](#), T.P.A. Åkesson [ID⁹⁹](#), A.V. Akimov [ID³⁷](#), D. Akiyama [ID¹⁶⁹](#), N.N. Akolkar [ID²⁴](#), K. Al Khoury [ID⁴¹](#), G.L. Alberghi [ID^{23b}](#), J. Albert [ID¹⁶⁶](#), P. Albicocco [ID⁵³](#), G.L. Albouy [ID⁶⁰](#), S. Alderweireldt [ID⁵²](#), M. Aleksa [ID³⁶](#), I.N. Aleksandrov [ID³⁸](#), C. Alexa [ID^{27b}](#), T. Alexopoulos [ID¹⁰](#), A. Alfonsi [ID¹¹⁵](#), F. Alfonsi [ID^{23b}](#), M. Algren [ID⁵⁶](#), M. Althroob [ID¹²¹](#), B. Ali [ID¹³³](#), H.M.J. Ali [ID⁹²](#), S. Ali [ID¹⁴⁹](#), S.W. Alibocus [ID⁹³](#), M. Aliev [ID³⁷](#), G. Alimonti [ID^{71a}](#), W. Alkakhi [ID⁵⁵](#), C. Allaire [ID⁶⁶](#), B.M.M. Allbrooke [ID¹⁴⁷](#), J.F. Allen [ID⁵²](#), C.A. Allendes Flores [ID^{138f}](#), P.P. Allport [ID²⁰](#), A. Aloisio [ID^{72a,72b}](#), F. Alonso [ID⁹¹](#), C. Alpigiani [ID¹³⁹](#), M. Alvarez Estevez [ID¹⁰⁰](#), A. Alvarez Fernandez [ID¹⁰¹](#), M.G. Alvaggi [ID^{72a,72b}](#), M. Aly [ID¹⁰²](#), Y. Amaral Coutinho [ID^{83b}](#), A. Ambler [ID¹⁰⁵](#), C. Amelung [ID³⁶](#), M. Amerl [ID¹⁰²](#), C.G. Ames [ID¹¹⁰](#), D. Amidei [ID¹⁰⁷](#), S.P. Amor Dos Santos [ID^{131a}](#), K.R. Amos [ID¹⁶⁴](#), V. Ananiev [ID¹²⁶](#), C. Anastopoulos [ID¹⁴⁰](#), T. Andeen [ID¹¹](#), J.K. Anders [ID³⁶](#), S.Y. Andrean [ID^{47a,47b}](#), A. Andreazza [ID^{71a,71b}](#), S. Angelidakis [ID⁹](#), A. Angerami [ID^{41,ad}](#), A.V. Anisenkov [ID³⁷](#), A. Annovi [ID^{74a}](#), C. Antel [ID⁵⁶](#), M.T. Anthony [ID¹⁴⁰](#), E. Antipov [ID¹⁴⁶](#), M. Antonelli [ID⁵³](#), D.J.A. Antrim [ID^{17a}](#), F. Anulli [ID^{75a}](#), M. Aoki [ID⁸⁴](#), T. Aoki [ID¹⁵⁴](#), J.A. Aparisi Pozo [ID¹⁶⁴](#), M.A. Aparo [ID¹⁴⁷](#), L. Aperio Bella [ID⁴⁸](#), C. Appelt [ID¹⁸](#), A. Apyan [ID²⁶](#), N. Aranzabal [ID³⁶](#), C. Arcangeletti [ID⁵³](#), A.T.H. Arce [ID⁵¹](#), E. Arena [ID⁹³](#), J-F. Arguin [ID¹⁰⁹](#), S. Argyropoulos [ID⁵⁴](#), J.-H. Arling [ID⁴⁸](#), A.J. Armbruster [ID³⁶](#), O. Arnaez [ID⁴](#), H. Arnold [ID¹¹⁵](#), Z.P. Arrubarrena Tame [ID¹¹⁰](#), G. Artoni [ID^{75a,75b}](#), H. Asada [ID¹¹²](#), K. Asai [ID¹¹⁹](#), S. Asai [ID¹⁵⁴](#), N.A. Asbah [ID⁶¹](#), J. Assahsah [ID^{35d}](#), K. Assamagan [ID²⁹](#), R. Astalos [ID^{28a}](#), S. Atashi [ID¹⁶¹](#), R.J. Atkin [ID^{33a}](#), M. Atkinson [ID¹⁶³](#), N.B. Atlay [ID¹⁸](#), H. Atmani [ID^{62b}](#), P.A. Atmasiddha [ID¹⁰⁷](#), K. Augsten [ID¹³³](#), S. Auricchio [ID^{72a,72b}](#), A.D. Auriol [ID²⁰](#), V.A. Astrup [ID¹⁰²](#), G. Avolio [ID³⁶](#), K. Axiotis [ID⁵⁶](#), G. Azuelos [ID^{109,ah}](#), D. Babal [ID^{28b}](#), H. Bachacou [ID¹³⁶](#), K. Bachas [ID^{153,r}](#), A. Bachiu [ID³⁴](#), F. Backman [ID^{47a,47b}](#), A. Badea [ID⁶¹](#), P. Bagnaia [ID^{75a,75b}](#), M. Bahmani [ID¹⁸](#), A.J. Bailey [ID¹⁶⁴](#), V.R. Bailey [ID¹⁶³](#), J.T. Baines [ID¹³⁵](#), L. Baines [ID⁹⁵](#), C. Bakalis [ID¹⁰](#), O.K. Baker [ID¹⁷³](#), E. Bakos [ID¹⁵](#), D. Bakshi Gupta [ID⁸](#), R. Balasubramanian [ID¹¹⁵](#), E.M. Baldin [ID³⁷](#), P. Balek [ID^{86a}](#), E. Ballabene [ID^{23b,23a}](#), F. Balli [ID¹³⁶](#), L.M. Baltes [ID^{63a}](#), W.K. Balunas [ID³²](#), J. Balz [ID¹⁰¹](#), E. Banas [ID⁸⁷](#), M. Bandieramonte [ID¹³⁰](#), A. Bandyopadhyay [ID²⁴](#), S. Bansal [ID²⁴](#), L. Barak [ID¹⁵²](#), M. Barakat [ID⁴⁸](#), E.L. Barberio [ID¹⁰⁶](#), D. Barberis [ID^{57b,57a}](#), M. Barbero [ID¹⁰³](#), G. Barbour [ID⁹⁷](#), K.N. Barends [ID^{33a}](#), T. Barillari [ID¹¹¹](#), M-S. Barisits [ID³⁶](#), T. Barklow [ID¹⁴⁴](#), P. Baron [ID¹²³](#), D.A. Baron Moreno [ID¹⁰²](#), A. Baroncelli [ID^{62a}](#), G. Barone [ID²⁹](#), A.J. Barr [ID¹²⁷](#), J.D. Barr [ID⁹⁷](#), L. Barranco Navarro [ID^{47a,47b}](#), F. Barreiro [ID¹⁰⁰](#), J. Barreiro Guimarães da Costa [ID^{14a}](#), U. Barron [ID¹⁵²](#), M.G. Barros Teixeira [ID^{131a}](#), S. Barsov [ID³⁷](#), F. Bartels [ID^{63a}](#), R. Bartoldus [ID¹⁴⁴](#), A.E. Barton [ID⁹²](#), P. Bartos [ID^{28a}](#), A. Basan [ID¹⁰¹](#), M. Baselga [ID⁴⁹](#), A. Bassalat [ID^{66,b}](#), M.J. Basso [ID^{157a}](#), C.R. Basson [ID¹⁰²](#), R.L. Bates [ID⁵⁹](#), S. Batlamous [ID^{35e}](#), J.R. Batley [ID³²](#), B. Batool [ID¹⁴²](#), M. Battaglia [ID¹³⁷](#), D. Battulga [ID¹⁸](#), M. Bauce [ID^{75a,75b}](#), M. Bauer [ID³⁶](#), P. Bauer [ID²⁴](#), L.T. Bazzano Hurrell [ID³⁰](#), J.B. Beacham [ID⁵¹](#), T. Beau [ID¹²⁸](#), P.H. Beauchemin [ID¹⁵⁹](#), H. Beauchesne [ID¹](#), F. Becherer [ID⁵⁴](#), P. Bechtle [ID²⁴](#), H.P. Beck [ID^{19,q}](#), K. Becker [ID¹⁶⁸](#), A.J. Beddall [ID⁸²](#), V.A. Bednyakov [ID³⁸](#), C.P. Bee [ID¹⁴⁶](#), L.J. Beemster [ID¹⁵](#), T.A. Beermann [ID³⁶](#), M. Begalli [ID^{83d}](#), M. Begel [ID²⁹](#), A. Behera [ID¹⁴⁶](#), J.K. Behr [ID⁴⁸](#), J.F. Beirer [ID⁵⁵](#), F. Beisiegel [ID²⁴](#), M. Belfkir [ID¹⁶⁰](#), G. Bella [ID¹⁵²](#), L. Bellagamba [ID^{23b}](#), A. Bellerive [ID³⁴](#), P. Bellos [ID²⁰](#), K. Beloborodov [ID³⁷](#), N.L. Belyaev [ID³⁷](#), D. Benchekroun [ID^{35a}](#),

F. Bendebba [ID^{35a}](#), Y. Benhammou [ID¹⁵²](#), M. Benoit [ID²⁹](#), J.R. Bensinger [ID²⁶](#), S. Bentvelsen [ID¹¹⁵](#),
 L. Beresford [ID⁴⁸](#), M. Beretta [ID⁵³](#), E. Bergeaas Kuutmann [ID¹⁶²](#), N. Berger [ID⁴](#), B. Bergmann [ID¹³³](#),
 J. Beringer [ID^{17a}](#), G. Bernardi [ID⁵](#), C. Bernius [ID¹⁴⁴](#), F.U. Bernlochner [ID²⁴](#), F. Bernon [ID^{36,103}](#), T. Berry [ID⁹⁶](#),
 P. Berta [ID¹³⁴](#), A. Berthold [ID⁵⁰](#), I.A. Bertram [ID⁹²](#), S. Bethke [ID¹¹¹](#), A. Betti [ID^{75a,75b}](#), A.J. Bevan [ID⁹⁵](#),
 M. Bhamjee [ID^{33c}](#), S. Bhatta [ID¹⁴⁶](#), D.S. Bhattacharya [ID¹⁶⁷](#), P. Bhattarai [ID²⁶](#), V.S. Bhopatkar [ID¹²²](#),
 R. Bi^{29,aj}, R.M. Bianchi [ID¹³⁰](#), G. Bianco [ID^{23b,23a}](#), O. Biebel [ID¹¹⁰](#), R. Bielski [ID¹²⁴](#), M. Biglietti [ID^{77a}](#),
 T.R.V. Billoud [ID¹³³](#), M. Bindi [ID⁵⁵](#), A. Bingul [ID^{21b}](#), C. Bini [ID^{75a,75b}](#), A. Biondini [ID⁹³](#),
 C.J. Birch-sykes [ID¹⁰²](#), G.A. Bird [ID^{20,135}](#), M. Birman [ID¹⁷⁰](#), M. Biros [ID¹³⁴](#), T. Bisanz [ID⁴⁹](#),
 E. Bisceglie [ID^{43b,43a}](#), D. Biswas [ID¹⁴²](#), A. Bitadze [ID¹⁰²](#), K. Bjørke [ID¹²⁶](#), I. Bloch [ID⁴⁸](#), C. Blocker [ID²⁶](#),
 A. Blue [ID⁵⁹](#), U. Blumenschein [ID⁹⁵](#), J. Blumenthal [ID¹⁰¹](#), G.J. Bobbink [ID¹¹⁵](#), V.S. Bobrovnikov [ID³⁷](#),
 M. Boehler [ID⁵⁴](#), B. Boehm [ID¹⁶⁷](#), D. Bogavac [ID³⁶](#), A.G. Bogdanchikov [ID³⁷](#), C. Bohm [ID^{47a}](#),
 V. Boisvert [ID⁹⁶](#), P. Bokan [ID⁴⁸](#), T. Bold [ID^{86a}](#), M. Bomben [ID⁵](#), M. Bona [ID⁹⁵](#), M. Boonekamp [ID¹³⁶](#),
 C.D. Booth [ID⁹⁶](#), A.G. Borbély [ID⁵⁹](#), I.S. Bordulev [ID³⁷](#), H.M. Borecka-Bielska [ID¹⁰⁹](#), L.S. Borgna [ID⁹⁷](#),
 G. Borissov [ID⁹²](#), D. Bortoletto [ID¹²⁷](#), D. Boscherini [ID^{23b}](#), M. Bosman [ID¹³](#), J.D. Bossio Sola [ID³⁶](#),
 K. Bouaouda [ID^{35a}](#), N. Bouchhar [ID¹⁶⁴](#), J. Boudreau [ID¹³⁰](#), E.V. Bouhova-Thacker [ID⁹²](#), D. Boumediene [ID⁴⁰](#),
 R. Bouquet [ID⁵](#), A. Boveia [ID¹²⁰](#), J. Boyd [ID³⁶](#), D. Boye [ID²⁹](#), I.R. Boyko [ID³⁸](#), J. Bracinik [ID²⁰](#),
 N. Brahimi [ID^{62d}](#), G. Brandt [ID¹⁷²](#), O. Brandt [ID³²](#), F. Braren [ID⁴⁸](#), B. Brau [ID¹⁰⁴](#), J.E. Brau [ID¹²⁴](#),
 R. Brener [ID¹⁷⁰](#), L. Brenner [ID¹¹⁵](#), R. Brenner [ID¹⁶²](#), S. Bressler [ID¹⁷⁰](#), D. Britton [ID⁵⁹](#), D. Britzger [ID¹¹¹](#),
 I. Brock [ID²⁴](#), G. Brooijmans [ID⁴¹](#), W.K. Brooks [ID^{138f}](#), E. Brost [ID²⁹](#), L.M. Brown [ID¹⁶⁶](#), L.E. Bruce [ID⁶¹](#),
 T.L. Bruckler [ID¹²⁷](#), P.A. Bruckman de Renstrom [ID⁸⁷](#), B. Briëters [ID⁴⁸](#), D. Bruncko [ID^{28b,*}](#), A. Bruni [ID^{23b}](#),
 G. Bruni [ID^{23b}](#), M. Bruschi [ID^{23b}](#), N. Bruscino [ID^{75a,75b}](#), T. Buanes [ID¹⁶](#), Q. Buat [ID¹³⁹](#), D. Buchin [ID¹¹¹](#),
 A.G. Buckley [ID⁵⁹](#), M.K. Bugge [ID¹²⁶](#), O. Bulekov [ID³⁷](#), B.A. Bullard [ID¹⁴⁴](#), S. Burdin [ID⁹³](#),
 C.D. Burgard [ID⁴⁹](#), A.M. Burger [ID⁴⁰](#), B. Burghgrave [ID⁸](#), O. Burlayenko [ID⁵⁴](#), J.T.P. Burr [ID³²](#),
 C.D. Burton [ID¹¹](#), J.C. Burzynski [ID¹⁴³](#), E.L. Busch [ID⁴¹](#), V. Büscher [ID¹⁰¹](#), P.J. Bussey [ID⁵⁹](#),
 J.M. Butler [ID²⁵](#), C.M. Buttar [ID⁵⁹](#), J.M. Butterworth [ID⁹⁷](#), W. Buttlinger [ID¹³⁵](#), C.J. Buxo Vazquez [ID¹⁰⁸](#),
 A.R. Buzykaev [ID³⁷](#), G. Cabras [ID^{23b}](#), S. Cabrera Urbán [ID¹⁶⁴](#), L. Cadamuro [ID⁶⁶](#), D. Caforio [ID⁵⁸](#),
 H. Cai [ID¹³⁰](#), Y. Cai [ID^{14a,14e}](#), V.M.M. Cairo [ID³⁶](#), O. Cakir [ID^{3a}](#), N. Calace [ID³⁶](#), P. Calafiura [ID^{17a}](#),
 G. Calderini [ID¹²⁸](#), P. Calfayan [ID⁶⁸](#), G. Callea [ID⁵⁹](#), L.P. Caloba^{83b}, D. Calvet [ID⁴⁰](#), S. Calvet [ID⁴⁰](#),
 T.P. Calvet [ID¹⁰³](#), M. Calvetti [ID^{74a,74b}](#), R. Camacho Toro [ID¹²⁸](#), S. Camarda [ID³⁶](#), D. Camarero Munoz [ID²⁶](#),
 P. Camarri [ID^{76a,76b}](#), M.T. Camerlingo [ID^{72a,72b}](#), D. Cameron [ID¹²⁶](#), C. Camincher [ID¹⁶⁶](#), M. Campanelli [ID⁹⁷](#),
 A. Camplani [ID⁴²](#), V. Canale [ID^{72a,72b}](#), A. Canesse [ID¹⁰⁵](#), M. Cano Bret [ID⁸⁰](#), J. Cantero [ID¹⁶⁴](#), Y. Cao [ID¹⁶³](#),
 F. Capocasa [ID²⁶](#), M. Capua [ID^{43b,43a}](#), A. Carbone [ID^{71a,71b}](#), R. Cardarelli [ID^{76a}](#), J.C.J. Cardenas [ID⁸](#),
 F. Cardillo [ID¹⁶⁴](#), T. Carli [ID³⁶](#), G. Carlino [ID^{72a}](#), J.I. Carlotto [ID¹³](#), B.T. Carlson [ID^{130,s}](#),
 E.M. Carlson [ID^{166,157a}](#), L. Carminati [ID^{71a,71b}](#), A. Carnelli [ID¹³⁶](#), M. Carnesale [ID^{75a,75b}](#), S. Caron [ID¹¹⁴](#),
 E. Carquin [ID^{138f}](#), S. Carrá [ID^{71a,71b}](#), G. Carratta [ID^{23b,23a}](#), F. Carrio Argos [ID^{33g}](#), J.W.S. Carter [ID¹⁵⁶](#),
 T.M. Carter [ID⁵²](#), M.P. Casado [ID^{13,i}](#), M. Caspar [ID⁴⁸](#), E.G. Castiglia [ID¹⁷³](#), F.L. Castillo [ID⁴](#),
 L. Castillo Garcia [ID¹³](#), V. Castillo Gimenez [ID¹⁶⁴](#), N.F. Castro [ID^{131a,131e}](#), A. Catinaccio [ID³⁶](#),
 J.R. Catmore [ID¹²⁶](#), V. Cavalieri [ID²⁹](#), N. Cavalli [ID^{23b,23a}](#), V. Cavasinni [ID^{74a,74b}](#), Y.C. Cekmecelioglu [ID⁴⁸](#),
 E. Celebi [ID^{21a}](#), F. Celli [ID¹²⁷](#), M.S. Centonze [ID^{70a,70b}](#), K. Cerny [ID¹²³](#), A.S. Cerqueira [ID^{83a}](#), A. Cerri [ID¹⁴⁷](#),
 L. Cerrito [ID^{76a,76b}](#), F. Cerutti [ID^{17a}](#), B. Cervato [ID¹⁴²](#), A. Cervelli [ID^{23b}](#), G. Cesarin [ID⁵³](#), S.A. Cetin [ID⁸²](#),
 Z. Chadi [ID^{35a}](#), D. Chakraborty [ID¹¹⁶](#), M. Chala [ID^{131f}](#), J. Chan [ID¹⁷¹](#), W.Y. Chan [ID¹⁵⁴](#), J.D. Chapman [ID³²](#),
 E. Chapon [ID¹³⁶](#), B. Chargeishvili [ID^{150b}](#), D.G. Charlton [ID²⁰](#), T.P. Charman [ID⁹⁵](#), M. Chatterjee [ID¹⁹](#),
 C. Chauhan [ID¹³⁴](#), S. Chekanov [ID⁶](#), S.V. Chekulaev [ID^{157a}](#), G.A. Chelkov [ID^{38,a}](#), A. Chen [ID¹⁰⁷](#),
 B. Chen [ID¹⁵²](#), B. Chen [ID¹⁶⁶](#), H. Chen [ID^{14c}](#), H. Chen [ID²⁹](#), J. Chen [ID^{62c}](#), J. Chen [ID¹⁴³](#), M. Chen [ID¹²⁷](#),
 S. Chen [ID¹⁵⁴](#), S.J. Chen [ID^{14c}](#), X. Chen [ID^{62c}](#), X. Chen [ID^{14b,ag}](#), Y. Chen [ID^{62a}](#), C.L. Cheng [ID¹⁷¹](#),
 H.C. Cheng [ID^{64a}](#), S. Cheong [ID¹⁴⁴](#), A. Cheplakov [ID³⁸](#), E. Cheremushkina [ID⁴⁸](#), E. Cherepanova [ID¹¹⁵](#),
 R. Cherkaoui El Moursli [ID^{35e}](#), E. Cheu [ID⁷](#), K. Cheung [ID⁶⁵](#), L. Chevalier [ID¹³⁶](#), V. Chiarella [ID⁵³](#),

G. Chiarelli [ID^{74a}](#), N. Chiedde [ID¹⁰³](#), G. Chiodini [ID^{70a}](#), A.S. Chisholm [ID²⁰](#), A. Chitan [ID^{27b}](#),
 M. Chitishvili [ID¹⁶⁴](#), M.V. Chizhov [ID³⁸](#), K. Choi [ID¹¹](#), A.R. Chomont [ID^{75a,75b}](#), Y. Chou [ID¹⁰⁴](#),
 E.Y.S. Chow [ID¹¹⁵](#), T. Chowdhury [ID^{33g}](#), K.L. Chu [ID¹⁷⁰](#), M.C. Chu [ID^{64a}](#), X. Chu [ID^{14a,14e}](#), J. Chudoba [ID¹³²](#),
 J.J. Chwastowski [ID⁸⁷](#), D. Cieri [ID¹¹¹](#), K.M. Ciesla [ID^{86a}](#), V. Cindro [ID⁹⁴](#), A. Ciocio [ID^{17a}](#), F. Cirotto [ID^{72a,72b}](#),
 Z.H. Citron [ID^{170,m}](#), M. Citterio [ID^{71a}](#), D.A. Ciubotaru [ID^{27b}](#), B.M. Ciungu [ID¹⁵⁶](#), A. Clark [ID⁵⁶](#), P.J. Clark [ID⁵²](#),
 J.M. Clavijo Columbie [ID⁴⁸](#), S.E. Clawson [ID⁴⁸](#), C. Clement [ID^{47a,47b}](#), J. Clercx [ID⁴⁸](#), L. Clissa [ID^{23b,23a}](#),
 Y. Coadou [ID¹⁰³](#), M. Cobal [ID^{69a,69c}](#), A. Coccaro [ID^{57b}](#), R.F. Coelho Barrue [ID^{131a}](#),
 R. Coelho Lopes De Sa [ID¹⁰⁴](#), S. Coelli [ID^{71a}](#), H. Cohen [ID¹⁵²](#), A.E.C. Coimbra [ID^{71a,71b}](#), B. Cole [ID⁴¹](#),
 J. Collot [ID⁶⁰](#), P. Conde Muiño [ID^{131a,131g}](#), M.P. Connell [ID^{33c}](#), S.H. Connell [ID^{33c}](#), I.A. Connelly [ID⁵⁹](#),
 E.I. Conroy [ID¹²⁷](#), F. Conventi [ID^{72a,ai}](#), H.G. Cooke [ID²⁰](#), A.M. Cooper-Sarkar [ID¹²⁷](#),
 A. Cordeiro Oudot Choi [ID¹²⁸](#), F. Cormier [ID¹⁶⁵](#), L.D. Corpé [ID⁴⁰](#), M. Corradi [ID^{75a,75b}](#), F. Corriveau [ID^{105,y}](#),
 A. Cortes-Gonzalez [ID¹⁸](#), M.J. Costa [ID¹⁶⁴](#), F. Costanza [ID⁴](#), D. Costanzo [ID¹⁴⁰](#), B.M. Cote [ID¹²⁰](#),
 G. Cowan [ID⁹⁶](#), K. Cranmer [ID¹⁷¹](#), D. Cremonini [ID^{23b,23a}](#), S. Crépé-Renaudin [ID⁶⁰](#), F. Crescioli [ID¹²⁸](#),
 M. Cristinziani [ID¹⁴²](#), M. Cristoforetti [ID^{78a,78b}](#), V. Croft [ID¹¹⁵](#), J.E. Crosby [ID¹²²](#), G. Crosetti [ID^{43b,43a}](#),
 A. Cueto [ID¹⁰⁰](#), T. Cuhadar Donszelmann [ID¹⁶¹](#), H. Cui [ID^{14a,14e}](#), Z. Cui [ID⁷](#), W.R. Cunningham [ID⁵⁹](#),
 F. Curcio [ID^{43b,43a}](#), P. Czodrowski [ID³⁶](#), M.M. Czurylo [ID^{63b}](#), M.J. Da Cunha Sargedas De Sousa [ID^{62a}](#),
 J.V. Da Fonseca Pinto [ID^{83b}](#), C. Da Via [ID¹⁰²](#), W. Dabrowski [ID^{86a}](#), T. Dado [ID⁴⁹](#), S. Dahbi [ID^{33g}](#),
 T. Dai [ID¹⁰⁷](#), C. Dallapiccola [ID¹⁰⁴](#), M. Dam [ID⁴²](#), G. D'amen [ID²⁹](#), V. D'Amico [ID¹¹⁰](#), J. Damp [ID¹⁰¹](#),
 J.R. Dandoy [ID¹²⁹](#), M.F. Daneri [ID³⁰](#), M. Danninger [ID¹⁴³](#), V. Dao [ID³⁶](#), G. Darbo [ID^{57b}](#), S. Darmora [ID⁶](#),
 S.J. Das [ID^{29,aj}](#), S. D'Auria [ID^{71a,71b}](#), C. David [ID^{157b}](#), T. Davidek [ID¹³⁴](#), B. Davis-Purcell [ID³⁴](#),
 I. Dawson [ID⁹⁵](#), H.A. Day-hall [ID¹³³](#), K. De [ID⁸](#), R. De Asmundis [ID^{72a}](#), N. De Biase [ID⁴⁸](#),
 S. De Castro [ID^{23b,23a}](#), N. De Groot [ID¹¹⁴](#), P. de Jong [ID¹¹⁵](#), H. De la Torre [ID¹⁰⁸](#), A. De Maria [ID^{14c}](#),
 A. De Salvo [ID^{75a}](#), U. De Sanctis [ID^{76a,76b}](#), A. De Santo [ID¹⁴⁷](#), J.B. De Vivie De Regie [ID⁶⁰](#),
 D.V. Dedovich³⁸, J. Degens [ID¹¹⁵](#), A.M. Deiana [ID⁴⁴](#), F. Del Corso [ID^{23b,23a}](#), J. Del Peso [ID¹⁰⁰](#),
 F. Del Rio [ID^{63a}](#), F. Deliot [ID¹³⁶](#), C.M. Delitzsch [ID⁴⁹](#), M. Della Pietra [ID^{72a,72b}](#), D. Della Volpe [ID⁵⁶](#),
 A. Dell'Acqua [ID³⁶](#), L. Dell'Asta [ID^{71a,71b}](#), M. Delmastro [ID⁴](#), P.A. Delsart [ID⁶⁰](#), S. Demers [ID¹⁷³](#),
 M. Demichev [ID³⁸](#), S.P. Denisov [ID³⁷](#), L. D'Eramo [ID⁴⁰](#), D. Derendarz [ID⁸⁷](#), F. Derue [ID¹²⁸](#), P. Dervan [ID⁹³](#),
 K. Desch [ID²⁴](#), C. Deutsch [ID²⁴](#), F.A. Di Bello [ID^{57b,57a}](#), A. Di Ciaccio [ID^{76a,76b}](#), L. Di Ciaccio [ID⁴](#),
 A. Di Domenico [ID^{75a,75b}](#), C. Di Donato [ID^{72a,72b}](#), A. Di Girolamo [ID³⁶](#), G. Di Gregorio [ID⁵](#),
 A. Di Luca [ID^{78a,78b}](#), B. Di Micco [ID^{77a,77b}](#), R. Di Nardo [ID^{77a,77b}](#), C. Diaconu [ID¹⁰³](#), F.A. Dias [ID¹¹⁵](#),
 T. Dias Do Vale [ID¹⁴³](#), M.A. Diaz [ID^{138a,138b}](#), F.G. Diaz Capriles [ID²⁴](#), M. Didenko [ID¹⁶⁴](#), E.B. Diehl [ID¹⁰⁷](#),
 L. Diehl [ID⁵⁴](#), S. Díez Cornell [ID⁴⁸](#), C. Diez Pardos [ID¹⁴²](#), C. Dimitriadi [ID^{24,162}](#), A. Dimitrievska [ID^{17a}](#),
 J. Dingfelder [ID²⁴](#), I-M. Dinu [ID^{27b}](#), S.J. Dittmeier [ID^{63b}](#), F. Dittus [ID³⁶](#), F. Djama [ID¹⁰³](#), T. Djobava [ID^{150b}](#),
 J.I. Djuvslund [ID¹⁶](#), C. Doglioni [ID^{102,99}](#), J. Dolejsi [ID¹³⁴](#), Z. Dolezal [ID¹³⁴](#), M. Donadelli [ID^{83c}](#),
 B. Dong [ID¹⁰⁸](#), J. Donini [ID⁴⁰](#), A. D'Onofrio [ID^{77a,77b}](#), M. D'Onofrio [ID⁹³](#), J. Dopke [ID¹³⁵](#), A. Doria [ID^{72a}](#),
 N. Dos Santos Fernandes [ID^{131a}](#), M.T. Dova [ID⁹¹](#), A.T. Doyle [ID⁵⁹](#), M.A. Draguet [ID¹²⁷](#), E. Dreyer [ID¹⁷⁰](#),
 I. Drivas-koulouris [ID¹⁰](#), A.S. Drobac [ID¹⁵⁹](#), M. Drozdova [ID⁵⁶](#), D. Du [ID^{62a}](#), T.A. du Pree [ID¹¹⁵](#),
 F. Dubinin [ID³⁷](#), M. Dubovsky [ID^{28a}](#), E. Duchovni [ID¹⁷⁰](#), G. Duckeck [ID¹¹⁰](#), O.A. Ducu [ID^{27b}](#), D. Duda [ID⁵²](#),
 A. Dudarev [ID³⁶](#), E.R. Duden [ID²⁶](#), M. D'uffizi [ID¹⁰²](#), L. Duflot [ID⁶⁶](#), M. Dührssen [ID³⁶](#), C. Dülsen [ID¹⁷²](#),
 A.E. Dumitriu [ID^{27b}](#), M. Dunford [ID^{63a}](#), S. Dungs [ID⁴⁹](#), K. Dunne [ID^{47a,47b}](#), A. Duperrin [ID¹⁰³](#),
 H. Duran Yildiz [ID^{3a}](#), M. Düren [ID⁵⁸](#), A. Durglishvili [ID^{150b}](#), B.L. Dwyer [ID¹¹⁶](#), G.I. Dyckes [ID^{17a}](#),
 M. Dyndal [ID^{86a}](#), S. Dysch [ID¹⁰²](#), B.S. Dziedzic [ID⁸⁷](#), Z.O. Earnshaw [ID¹⁴⁷](#), G.H. Eberwein [ID¹²⁷](#),
 B. Eckerova [ID^{28a}](#), S. Eggebrecht [ID⁵⁵](#), M.G. Eggleston⁵¹, E. Egidio Purcino De Souza [ID¹²⁸](#),
 L.F. Ehrke [ID⁵⁶](#), G. Eigen [ID¹⁶](#), K. Einsweiler [ID^{17a}](#), T. Ekelof [ID¹⁶²](#), P.A. Ekman [ID⁹⁹](#), S. El Farkh [ID^{35b}](#),
 Y. El Ghazali [ID^{35b}](#), H. El Jarrari [ID^{35e,149}](#), A. El Moussaoui [ID^{35a}](#), V. Ellajosyula [ID¹⁶²](#), M. Ellert [ID¹⁶²](#),
 F. Ellinghaus [ID¹⁷²](#), A.A. Elliot [ID⁹⁵](#), N. Ellis [ID³⁶](#), J. Elmsheuser [ID²⁹](#), M. Elsing [ID³⁶](#), D. Emeliyanov [ID¹³⁵](#),
 Y. Enari [ID¹⁵⁴](#), I. Ene [ID^{17a}](#), S. Epari [ID¹³](#), J. Erdmann [ID⁴⁹](#), P.A. Erland [ID⁸⁷](#), M. Errenst [ID¹⁷²](#),

M. Escalier [ID⁶⁶](#), C. Escobar [ID¹⁶⁴](#), E. Etzion [ID¹⁵²](#), G. Evans [ID^{131a}](#), H. Evans [ID⁶⁸](#), L.S. Evans [ID⁹⁶](#),
 M.O. Evans [ID¹⁴⁷](#), A. Ezhilov [ID³⁷](#), S. Ezzarqtouni [ID^{35a}](#), F. Fabbri [ID⁵⁹](#), L. Fabbri [ID^{23b,23a}](#), G. Facini [ID⁹⁷](#),
 V. Fadeyev [ID¹³⁷](#), R.M. Fakhrutdinov [ID³⁷](#), S. Falciano [ID^{75a}](#), L.F. Falda Ulhoa Coelho [ID³⁶](#), P.J. Falke [ID²⁴](#),
 J. Faltova [ID¹³⁴](#), C. Fan [ID¹⁶³](#), Y. Fan [ID^{14a}](#), Y. Fang [ID^{14a,14e}](#), M. Fanti [ID^{71a,71b}](#), M. Faraj [ID^{69a,69b}](#),
 Z. Farazpay [ID⁹⁸](#), A. Farbin [ID⁸](#), A. Farilla [ID^{77a}](#), T. Farooque [ID¹⁰⁸](#), S.M. Farrington [ID⁵²](#), F. Fassi [ID^{35e}](#),
 D. Fassouliotis [ID⁹](#), M. Faucci Giannelli [ID^{76a,76b}](#), W.J. Fawcett [ID³²](#), L. Fayard [ID⁶⁶](#), P. Federic [ID¹³⁴](#),
 P. Federicova [ID¹³²](#), O.L. Fedin [ID^{37,a}](#), G. Fedotov [ID³⁷](#), M. Feickert [ID¹⁷¹](#), L. Feligioni [ID¹⁰³](#),
 D.E. Fellers [ID¹²⁴](#), C. Feng [ID^{62b}](#), M. Feng [ID^{14b}](#), Z. Feng [ID¹¹⁵](#), M.J. Fenton [ID¹⁶¹](#), A.B. Fenyuk [ID³⁷](#),
 L. Ferencz [ID⁴⁸](#), R.A.M. Ferguson [ID⁹²](#), S.I. Fernandez Luengo [ID^{138f}](#), M.J.V. Fernoux [ID¹⁰³](#),
 J. Ferrando [ID⁴⁸](#), A. Ferrari [ID¹⁶²](#), P. Ferrari [ID^{115,114}](#), R. Ferrari [ID^{73a}](#), D. Ferrere [ID⁵⁶](#), C. Ferretti [ID¹⁰⁷](#),
 F. Fiedler [ID¹⁰¹](#), A. Filipčič [ID⁹⁴](#), E.K. Filmer [ID¹](#), F. Filthaut [ID¹¹⁴](#), M.C.N. Fiolhais [ID^{131a,131c,c}](#),
 L. Fiorini [ID¹⁶⁴](#), W.C. Fisher [ID¹⁰⁸](#), T. Fitschen [ID¹⁰²](#), P.M. Fitzhugh [ID¹³⁶](#), I. Fleck [ID¹⁴²](#), P. Fleischmann [ID¹⁰⁷](#),
 T. Flick [ID¹⁷²](#), L. Flores [ID¹²⁹](#), M. Flores [ID^{33d,ae}](#), L.R. Flores Castillo [ID^{64a}](#), L. Flores Sanz De Aedo [ID³⁶](#),
 F.M. Follega [ID^{78a,78b}](#), N. Fomin [ID¹⁶](#), J.H. Foo [ID¹⁵⁶](#), B.C. Forland [ID⁶⁸](#), A. Formica [ID¹³⁶](#), A.C. Forti [ID¹⁰²](#),
 E. Fortin [ID³⁶](#), A.W. Fortman [ID⁶¹](#), M.G. Foti [ID^{17a}](#), L. Fountas [ID^{9j}](#), D. Fournier [ID⁶⁶](#), H. Fox [ID⁹²](#),
 P. Francavilla [ID^{74a,74b}](#), S. Francescato [ID⁶¹](#), S. Franchellucci [ID⁵⁶](#), M. Franchini [ID^{23b,23a}](#),
 S. Franchino [ID^{63a}](#), D. Francis [ID³⁶](#), L. Franco [ID¹¹⁴](#), L. Franconi [ID⁴⁸](#), M. Franklin [ID⁶¹](#), G. Frattari [ID²⁶](#),
 A.C. Freegard [ID⁹⁵](#), W.S. Freund [ID^{83b}](#), Y.Y. Frid [ID¹⁵²](#), N. Fritzsche [ID⁵⁰](#), A. Froch [ID⁵⁴](#), D. Froidevaux [ID³⁶](#),
 J.A. Frost [ID¹²⁷](#), Y. Fu [ID^{62a}](#), M. Fujimoto [ID¹¹⁹](#), E. Fullana Torregrosa [ID^{164,*}](#), K.Y. Fung [ID^{64a}](#),
 E. Furtado De Simas Filho [ID^{83b}](#), M. Furukawa [ID¹⁵⁴](#), J. Fuster [ID¹⁶⁴](#), A. Gabrielli [ID^{23b,23a}](#),
 A. Gabrielli [ID¹⁵⁶](#), P. Gadow [ID⁴⁸](#), G. Gagliardi [ID^{57b,57a}](#), L.G. Gagnon [ID^{17a}](#), E.J. Gallas [ID¹²⁷](#),
 B.J. Gallop [ID¹³⁵](#), K.K. Gan [ID¹²⁰](#), S. Ganguly [ID¹⁵⁴](#), J. Gao [ID^{62a}](#), Y. Gao [ID⁵²](#), F.M. Garay Walls [ID^{138a,138b}](#),
 B. Garcia ^{29,aj}, C. García [ID¹⁶⁴](#), A. Garcia Alonso [ID¹¹⁵](#), A.G. Garcia Caffaro [ID¹⁷³](#),
 J.E. García Navarro [ID¹⁶⁴](#), M. Garcia-Sciveres [ID^{17a}](#), G.L. Gardner [ID¹²⁹](#), R.W. Gardner [ID³⁹](#),
 N. Garelli [ID¹⁵⁹](#), D. Garg [ID⁸⁰](#), R.B. Garg [ID^{144,p}](#), J.M. Gargan ⁵², C.A. Garner ¹⁵⁶, S.J. Gasiorowski [ID¹³⁹](#),
 P. Gaspar [ID^{83b}](#), G. Gaudio [ID^{73a}](#), V. Gautam ¹³, P. Gauzzi [ID^{75a,75b}](#), I.L. Gavrilenko [ID³⁷](#), A. Gavrilyuk [ID³⁷](#),
 C. Gay [ID¹⁶⁵](#), G. Gaycken [ID⁴⁸](#), E.N. Gazis [ID¹⁰](#), A.A. Geanta [ID^{27b}](#), C.M. Gee [ID¹³⁷](#), C. Gemme [ID^{57b}](#),
 M.H. Genest [ID⁶⁰](#), S. Gentile [ID^{75a,75b}](#), S. George [ID⁹⁶](#), W.F. George [ID²⁰](#), T. Geralis [ID⁴⁶](#),
 P. Gessinger-Befurt [ID³⁶](#), M.E. Geyik [ID¹⁷²](#), M. Ghneimat [ID¹⁴²](#), K. Ghorbanian [ID⁹⁵](#), A. Ghosal [ID¹⁴²](#),
 A. Ghosh [ID¹⁶¹](#), A. Ghosh [ID⁷](#), B. Giacobbe [ID^{23b}](#), S. Giagu [ID^{75a,75b}](#), P. Giannetti [ID^{74a}](#), A. Giannini [ID^{62a}](#),
 S.M. Gibson [ID⁹⁶](#), M. Gignac [ID¹³⁷](#), D.T. Gil [ID^{86b}](#), A.K. Gilbert [ID^{86a}](#), B.J. Gilbert [ID⁴¹](#), D. Gillberg [ID³⁴](#),
 G. Gilles [ID¹¹⁵](#), N.E.K. Gillwald [ID⁴⁸](#), L. Ginabat [ID¹²⁸](#), D.M. Gingrich [ID^{2,ah}](#), M.P. Giordani [ID^{69a,69c}](#),
 P.F. Giraud [ID¹³⁶](#), G. Giugliarelli [ID^{69a,69c}](#), D. Giugni [ID^{71a}](#), F. Giuli [ID³⁶](#), I. Gkialas [ID^{9j}](#), L.K. Gladilin [ID³⁷](#),
 C. Glasman [ID¹⁰⁰](#), G.R. Gledhill [ID¹²⁴](#), M. Glisic ¹²⁴, I. Gnesi [ID^{43b,f}](#), Y. Go ^{29,aj}, M. Goblirsch-Kolb [ID³⁶](#),
 B. Gocke [ID⁴⁹](#), D. Godin ¹⁰⁹, B. Gokturk [ID^{21a}](#), S. Goldfarb [ID¹⁰⁶](#), T. Golling [ID⁵⁶](#), M.G.D. Gololo ^{33g},
 D. Golubkov [ID³⁷](#), J.P. Gombas [ID¹⁰⁸](#), A. Gomes [ID^{131a,131b}](#), G. Gomes Da Silva [ID¹⁴²](#),
 A.J. Gomez Delegido [ID¹⁶⁴](#), R. Gonçalo [ID^{131a,131c}](#), G. Gonella [ID¹²⁴](#), L. Gonella [ID²⁰](#), A. Gongadze [ID³⁸](#),
 F. Gonnella [ID²⁰](#), J.L. Gonski [ID⁴¹](#), R.Y. González Andana [ID⁵²](#), S. González de la Hoz [ID¹⁶⁴](#),
 S. Gonzalez Fernandez [ID¹³](#), R. Gonzalez Lopez [ID⁹³](#), C. Gonzalez Renteria [ID^{17a}](#),
 R. Gonzalez Suarez [ID¹⁶²](#), S. Gonzalez-Sevilla [ID⁵⁶](#), G.R. Gonzalvo Rodriguez [ID¹⁶⁴](#), L. Goossens [ID³⁶](#),
 P.A. Gorbounov [ID³⁷](#), B. Gorini [ID³⁶](#), E. Gorini [ID^{70a,70b}](#), A. Gorišek [ID⁹⁴](#), T.C. Gosart [ID¹²⁹](#),
 A.T. Goshaw [ID⁵¹](#), M.I. Gostkin [ID³⁸](#), S. Goswami [ID¹²²](#), C.A. Gottardo [ID³⁶](#), M. Gouighri [ID^{35b}](#),
 V. Goumarre [ID⁴⁸](#), A.G. Goussiou [ID¹³⁹](#), N. Govender [ID^{33c}](#), I. Grabowska-Bold [ID^{86a}](#), K. Graham [ID³⁴](#),
 E. Gramstad [ID¹²⁶](#), S. Grancagnolo [ID^{70a,70b}](#), M. Grandi [ID¹⁴⁷](#), V. Gratchev ^{37,*}, P.M. Gravila [ID^{27f}](#),
 F.G. Gravili [ID^{70a,70b}](#), H.M. Gray [ID^{17a}](#), M. Greco [ID^{70a,70b}](#), C. Grefe [ID²⁴](#), I.M. Gregor [ID⁴⁸](#), P. Grenier [ID¹⁴⁴](#),
 C. Grieco [ID¹³](#), A.A. Grillo [ID¹³⁷](#), K. Grimm [ID³¹](#), S. Grinstein [ID^{13,u}](#), J.-F. Grivaz [ID⁶⁶](#), E. Gross [ID¹⁷⁰](#),
 J. Grosse-Knetter [ID⁵⁵](#), C. Grud [ID¹⁰⁷](#), J.C. Grundy [ID¹²⁷](#), L. Guan [ID¹⁰⁷](#), W. Guan [ID²⁹](#), C. Gubbels [ID¹⁶⁵](#),

J.G.R. Guerrero Rojas ID^{164} , G. Guerrieri $\text{ID}^{69a,69b}$, F. Guescini ID^{111} , R. Gugel ID^{101} , J.A.M. Guhit ID^{107} , A. Guida ID^{18} , T. Guillemin ID^4 , E. Guilloton $\text{ID}^{168,135}$, S. Guindon ID^{36} , F. Guo $\text{ID}^{14a,14e}$, J. Guo ID^{62c} , L. Guo ID^{48} , Y. Guo ID^{107} , R. Gupta ID^{48} , S. Gurbuz ID^{24} , S.S. Gurdasani ID^{54} , G. Gustavino ID^{36} , M. Guth ID^{56} , P. Gutierrez ID^{121} , L.F. Gutierrez Zagazeta ID^{129} , C. Gutschow ID^{97} , C. Gwenlan ID^{127} , C.B. Gwilliam ID^{93} , E.S. Haaland ID^{126} , A. Haas ID^{118} , M. Habedank ID^{48} , C. Haber ID^{17a} , H.K. Hadavand ID^8 , A. Hadef ID^{101} , S. Hadzic ID^{111} , J.J. Hahn ID^{142} , E.H. Haines ID^{97} , M. Haleem ID^{167} , J. Haley ID^{122} , J.J. Hall ID^{140} , G.D. Hallewell ID^{103} , L. Halser ID^{19} , K. Hamano ID^{166} , H. Hamdaoui ID^{35e} , M. Hamer ID^{24} , G.N. Hamity ID^{52} , E.J. Hampshire ID^{96} , J. Han ID^{62b} , K. Han ID^{62a} , L. Han ID^{14c} , L. Han ID^{62a} , S. Han ID^{17a} , Y.F. Han ID^{156} , K. Hanagaki ID^{84} , M. Hance ID^{137} , D.A. Hangal $\text{ID}^{41,ad}$, H. Hanif ID^{143} , M.D. Hank ID^{129} , R. Hankache ID^{102} , J.B. Hansen ID^{42} , J.D. Hansen ID^{42} , P.H. Hansen ID^{42} , K. Hara ID^{158} , D. Harada ID^{56} , T. Harenberg ID^{172} , S. Harkusha ID^{37} , M.L. Harris ID^{104} , Y.T. Harris ID^{127} , J. Harrison ID^{13} , N.M. Harrison ID^{120} , P.F. Harrison 168 , N.M. Hartman ID^{111} , N.M. Hartmann ID^{110} , Y. Hasegawa ID^{141} , A. Hasib ID^{52} , S. Haug ID^{19} , R. Hauser ID^{108} , C.M. Hawkes ID^{20} , R.J. Hawkings ID^{36} , Y. Hayashi ID^{154} , S. Hayashida ID^{112} , D. Hayden ID^{108} , C. Hayes ID^{107} , R.L. Hayes ID^{115} , C.P. Hays ID^{127} , J.M. Hays ID^{95} , H.S. Hayward ID^{93} , F. He ID^{62a} , M. He $\text{ID}^{14a,14e}$, Y. He ID^{155} , Y. He ID^{128} , N.B. Heatley ID^{95} , V. Hedberg ID^{99} , A.L. Heggelund ID^{126} , N.D. Hehir ID^{95} , C. Heidegger ID^{54} , K.K. Heidegger ID^{54} , W.D. Heidorn ID^{81} , J. Heilman ID^{34} , S. Heim ID^{48} , T. Heim ID^{17a} , J.G. Heinlein ID^{129} , J.J. Heinrich ID^{124} , L. Heinrich $\text{ID}^{111,af}$, J. Hejbal ID^{132} , L. Helary ID^{48} , A. Held ID^{171} , S. Hellesund ID^{16} , C.M. Helling ID^{165} , S. Hellman $\text{ID}^{47a,47b}$, C. Helsens ID^{36} , R.C.W. Henderson 92 , L. Henkelmann ID^{32} , A.M. Henriques Correia 36 , H. Herde ID^{99} , Y. Hernández Jiménez ID^{146} , L.M. Herrmann ID^{24} , T. Herrmann ID^{50} , G. Herten ID^{54} , R. Hertenberger ID^{110} , L. Hervas ID^{36} , M.E. Hesping ID^{101} , N.P. Hessey ID^{157a} , H. Hibi ID^{85} , S.J. Hillier ID^{20} , J.R. Hinds ID^{108} , F. Hinterkeuser ID^{24} , M. Hirose ID^{125} , S. Hirose ID^{158} , D. Hirschbuehl ID^{172} , T.G. Hitchings ID^{102} , B. Hiti ID^{94} , J. Hobbs ID^{146} , R. Hobincu ID^{27e} , N. Hod ID^{170} , M.C. Hodgkinson ID^{140} , B.H. Hodkinson ID^{32} , A. Hoecker ID^{36} , J. Hofer ID^{48} , T. Holm ID^{24} , M. Holzbock ID^{111} , L.B.A.H. Hommels ID^{32} , B.P. Honan ID^{102} , J. Hong ID^{62c} , T.M. Hong ID^{130} , B.H. Hooberman ID^{163} , W.H. Hopkins ID^6 , Y. Horii ID^{112} , S. Hou ID^{149} , A.S. Howard ID^{94} , J. Howarth ID^{59} , J. Hoya ID^6 , M. Hrabovsky ID^{123} , A. Hrynevich ID^{48} , T. Hrynevich ID^4 , P.J. Hsu ID^{65} , S.-C. Hsu ID^{139} , Q. Hu ID^{41} , Y.F. Hu $\text{ID}^{14a,14e}$, S. Huang ID^{64b} , X. Huang ID^{14c} , Y. Huang ID^{62a} , Y. Huang ID^{14a} , Z. Huang ID^{102} , Z. Hubacek ID^{133} , M. Huebner ID^{24} , F. Huegging ID^{24} , T.B. Huffman ID^{127} , C.A. Hugli ID^{48} , M. Huhtinen ID^{36} , S.K. Huiberts ID^{16} , R. Hulskens ID^{105} , N. Huseynov $\text{ID}^{12,a}$, J. Huston ID^{108} , J. Huth ID^{61} , R. Hyneman ID^{144} , G. Iacobucci ID^{56} , G. Iakovidis ID^{29} , I. Ibragimov ID^{142} , L. Iconomidou-Fayard ID^{66} , P. Iengo $\text{ID}^{72a,72b}$, R. Iguchi ID^{154} , T. Iizawa ID^{84} , Y. Ikegami ID^{84} , N. Ilic ID^{156} , H. Imam ID^{35a} , M. Ince Lezki ID^{56} , T. Ingebretsen Carlson $\text{ID}^{47a,47b}$, G. Introzzi $\text{ID}^{73a,73b}$, M. Iodice ID^{77a} , V. Ippolito $\text{ID}^{75a,75b}$, R.K. Irwin ID^{93} , M. Ishino ID^{154} , W. Islam ID^{171} , C. Issever $\text{ID}^{18,48}$, S. Istin $\text{ID}^{21a,al}$, H. Ito ID^{169} , J.M. Iturbe Ponce ID^{64a} , R. Iuppa $\text{ID}^{78a,78b}$, A. Ivina ID^{170} , J.M. Izen ID^{45} , V. Izzo ID^{72a} , P. Jacka $\text{ID}^{132,133}$, P. Jackson ID^1 , R.M. Jacobs ID^{48} , B.P. Jaeger ID^{143} , C.S. Jagfeld ID^{110} , P. Jain ID^{54} , G. Jäkel ID^{172} , K. Jakobs ID^{54} , T. Jakoubek ID^{170} , J. Jamieson ID^{59} , K.W. Janas ID^{86a} , A.E. Jaspan ID^{93} , M. Javurkova ID^{104} , F. Jeanneau ID^{136} , L. Jeanty ID^{124} , J. Jejelava $\text{ID}^{150a,ab}$, P. Jenni $\text{ID}^{54,g}$, C.E. Jessiman ID^{34} , S. Jézéquel ID^4 , C. Jia ID^{62b} , J. Jia ID^{146} , X. Jia ID^{61} , X. Jia $\text{ID}^{14a,14e}$, Z. Jia ID^{14c} , Y. Jiang ID^{62a} , S. Jiggins ID^{48} , J. Jimenez Pena ID^{13} , S. Jin ID^{14c} , A. Jinaru ID^{27b} , O. Jinnouchi ID^{155} , P. Johansson ID^{140} , K.A. Johns ID^7 , J.W. Johnson ID^{137} , D.M. Jones ID^{32} , E. Jones ID^{48} , P. Jones ID^{32} , R.W.L. Jones ID^{92} , T.J. Jones ID^{93} , R. Joshi ID^{120} , J. Jovicevic ID^{15} , X. Ju ID^{17a} , J.J. Junggeburth ID^{36} , T. Junkermann ID^{63a} , A. Juste Rozas $\text{ID}^{13,u}$, M.K. Juzek ID^{87} , S. Kabana ID^{138e} , A. Kaczmarska ID^{87} , M. Kado ID^{111} , H. Kagan ID^{120} , M. Kagan ID^{144} , A. Kahn 41 , A. Kahn ID^{129} , C. Kahra ID^{101} , T. Kaji ID^{169} , E. Kajomovitz ID^{151} , N. Kakati ID^{170} , I. Kalaitzidou ID^{54} , C.W. Kalderon ID^{29} , A. Kamenshchikov ID^{156} , S. Kanayama ID^{155} , N.J. Kang ID^{137} , D. Kar ID^{33g} , K. Karava ID^{127} , M.J. Kareem ID^{157b} , E. Karentzos ID^{54} , I. Karkanias ID^{153} , O. Karkout ID^{115} , S.N. Karpov ID^{38} , Z.M. Karpova ID^{38} , V. Kartvelishvili ID^{92} ,

A.N. Karyukhin [ID³⁷](#), E. Kasimi [ID¹⁵³](#), Y. Kats¹, J. Katzy [ID⁴⁸](#), S. Kaur [ID³⁴](#), K. Kawade [ID¹⁴¹](#),
 T. Kawamoto [ID¹³⁶](#), E.F. Kay [ID³⁶](#), F.I. Kaya [ID¹⁵⁹](#), S. Kazakos [ID¹⁰⁸](#), V.F. Kazanin [ID³⁷](#), Y. Ke [ID¹⁴⁶](#),
 J.M. Keaveney [ID^{33a}](#), R. Keeler [ID¹⁶⁶](#), G.V. Kehris [ID⁶¹](#), J.S. Keller [ID³⁴](#), A.S. Kelly⁹⁷, J.J. Kempster [ID¹⁴⁷](#),
 K.E. Kennedy [ID⁴¹](#), P.D. Kennedy [ID¹⁰¹](#), O. Kepka [ID¹³²](#), B.P. Kerridge [ID¹⁶⁸](#), S. Kersten [ID¹⁷²](#),
 B.P. Kerševan [ID⁹⁴](#), S. Keshri [ID⁶⁶](#), L. Keszeghova [ID^{28a}](#), S. Ketabchi Haghighat [ID¹⁵⁶](#), M. Khandoga [ID¹²⁸](#),
 A. Khanov [ID¹²²](#), A.G. Kharlamov [ID³⁷](#), T. Kharlamova [ID³⁷](#), E.E. Khoda [ID¹³⁹](#), T.J. Khoo [ID¹⁸](#),
 G. Khoriauli [ID¹⁶⁷](#), J. Khubua [ID^{150b}](#), Y.A.R. Khwaira [ID⁶⁶](#), M. Kiehn [ID³⁶](#), A. Kilgallon [ID¹²⁴](#),
 D.W. Kim [ID^{47a,47b}](#), Y.K. Kim [ID³⁹](#), N. Kimura [ID⁹⁷](#), A. Kirchhoff [ID⁵⁵](#), C. Kirfel [ID²⁴](#), F. Kirfel [ID²⁴](#),
 J. Kirk [ID¹³⁵](#), A.E. Kiryunin [ID¹¹¹](#), C. Kitsaki [ID¹⁰](#), O. Kivernyk [ID²⁴](#), M. Klassen [ID^{63a}](#), C. Klein [ID³⁴](#),
 L. Klein [ID¹⁶⁷](#), M.H. Klein [ID¹⁰⁷](#), M. Klein [ID⁹³](#), S.B. Klein [ID⁵⁶](#), U. Klein [ID⁹³](#), P. Klimek [ID³⁶](#),
 A. Klimentov [ID²⁹](#), T. Klioutchnikova [ID³⁶](#), P. Kluit [ID¹¹⁵](#), S. Kluth [ID¹¹¹](#), E. Knerner [ID⁷⁹](#),
 T.M. Knight [ID¹⁵⁶](#), A. Knue [ID⁵⁴](#), R. Kobayashi [ID⁸⁸](#), S.F. Koch [ID¹²⁷](#), M. Kocian [ID¹⁴⁴](#), P. Kodyš [ID¹³⁴](#),
 D.M. Koeck [ID¹²⁴](#), P.T. Koenig [ID²⁴](#), T. Koffas [ID³⁴](#), M. Kolb [ID¹³⁶](#), I. Koletsou [ID⁴](#), T. Komarek [ID¹²³](#),
 K. Köneke [ID⁵⁴](#), A.X.Y. Kong [ID¹](#), T. Kono [ID¹¹⁹](#), N. Konstantinidis [ID⁹⁷](#), B. Konya [ID⁹⁹](#),
 R. Kopeliansky [ID⁶⁸](#), S. Koperny [ID^{86a}](#), K. Korcyl [ID⁸⁷](#), K. Kordas [ID^{153,e}](#), G. Koren [ID¹⁵²](#), A. Korn [ID⁹⁷](#),
 S. Korn [ID⁵⁵](#), I. Korolkov [ID¹³](#), N. Korotkova [ID³⁷](#), B. Kortman [ID¹¹⁵](#), O. Kortner [ID¹¹¹](#), S. Kortner [ID¹¹¹](#),
 W.H. Kostecka [ID¹¹⁶](#), V.V. Kostyukhin [ID¹⁴²](#), A. Kotsokechagia [ID¹³⁶](#), A. Kotwal [ID⁵¹](#), A. Koulouris [ID³⁶](#),
 A. Kourkoumeli-Charalampidi [ID^{73a,73b}](#), C. Kourkoumelis [ID⁹](#), E. Kourlitis [ID⁶](#), O. Kovanda [ID¹⁴⁷](#),
 R. Kowalewski [ID¹⁶⁶](#), W. Kozanecki [ID¹³⁶](#), A.S. Kozhin [ID³⁷](#), V.A. Kramarenko [ID³⁷](#), G. Kramberger [ID⁹⁴](#),
 P. Kramer [ID¹⁰¹](#), M.W. Krasny [ID¹²⁸](#), A. Krasznahorkay [ID³⁶](#), J.W. Kraus [ID¹⁷²](#), J.A. Kremer [ID¹⁰¹](#),
 T. Kresse [ID⁵⁰](#), J. Kretzschmar [ID⁹³](#), K. Kreul [ID¹⁸](#), P. Krieger [ID¹⁵⁶](#), S. Krishnamurthy [ID¹⁰⁴](#),
 M. Krivos [ID¹³⁴](#), K. Krizka [ID²⁰](#), K. Kroeninger [ID⁴⁹](#), H. Kroha [ID¹¹¹](#), J. Kroll [ID¹³²](#), J. Kroll [ID¹²⁹](#),
 K.S. Krowppman [ID¹⁰⁸](#), U. Kruchonak [ID³⁸](#), H. Krüger [ID²⁴](#), N. Krumnack⁸¹, M.C. Kruse [ID⁵¹](#),
 J.A. Krzysiak [ID⁸⁷](#), O. Kuchinskaia [ID³⁷](#), S. Kuday [ID^{3a}](#), S. Kuehn [ID³⁶](#), R. Kuesters [ID⁵⁴](#), T. Kuhl [ID⁴⁸](#),
 V. Kukhtin [ID³⁸](#), Y. Kulchitsky [ID^{37,a}](#), S. Kuleshov [ID^{138d,138b}](#), M. Kumar [ID^{33g}](#), N. Kumari [ID¹⁰³](#),
 A. Kupco [ID¹³²](#), T. Kupfer⁴⁹, A. Kupich [ID³⁷](#), O. Kuprash [ID⁵⁴](#), H. Kurashige [ID⁸⁵](#), L.L. Kurchaninov [ID^{157a}](#),
 O. Kurdysh [ID⁶⁶](#), Y.A. Kurochkin [ID³⁷](#), A. Kurova [ID³⁷](#), M. Kuze [ID¹⁵⁵](#), A.K. Kvam [ID¹⁰⁴](#), J. Kvita [ID¹²³](#),
 T. Kwan [ID¹⁰⁵](#), N.G. Kyriacou [ID¹⁰⁷](#), L.A.O. Laatu [ID¹⁰³](#), C. Lacasta [ID¹⁶⁴](#), F. Lacava [ID^{75a,75b}](#),
 H. Lacker [ID¹⁸](#), D. Lacour [ID¹²⁸](#), N.N. Lad [ID⁹⁷](#), E. Ladygin [ID³⁸](#), B. Laforge [ID¹²⁸](#), T. Lagouri [ID^{138e}](#),
 S. Lai [ID⁵⁵](#), I.K. Lakomiec [ID^{86a}](#), N. Lalloue [ID⁶⁰](#), J.E. Lambert [ID¹⁶⁶](#), S. Lammers [ID⁶⁸](#), W. Lampl [ID⁷](#),
 C. Lampoudis [ID^{153,e}](#), A.N. Lancaster [ID¹¹⁶](#), E. Lançon [ID²⁹](#), U. Landgraf [ID⁵⁴](#), M.P.J. Landon [ID⁹⁵](#),
 V.S. Lang [ID⁵⁴](#), R.J. Langenberg [ID¹⁰⁴](#), O.K.B. Langrekken [ID¹²⁶](#), A.J. Lankford [ID¹⁶¹](#), F. Lanni [ID³⁶](#),
 K. Lantzsch [ID²⁴](#), A. Lanza [ID^{73a}](#), A. Lapertosa [ID^{57b,57a}](#), J.F. Laporte [ID¹³⁶](#), T. Lari [ID^{71a}](#),
 F. Lasagni Manghi [ID^{23b}](#), M. Lassnig [ID³⁶](#), V. Latonova [ID¹³²](#), A. Laudrain [ID¹⁰¹](#), A. Laurier [ID¹⁵¹](#),
 S.D. Lawlor [ID⁹⁶](#), Z. Lawrence [ID¹⁰²](#), M. Lazzaroni [ID^{71a,71b}](#), B. Le¹⁰², E.M. Le Boulicaut [ID⁵¹](#),
 B. Leban [ID⁹⁴](#), A. Lebedev [ID⁸¹](#), M. LeBlanc [ID³⁶](#), F. Ledroit-Guillon [ID⁶⁰](#), A.C.A. Lee⁹⁷, S.C. Lee [ID¹⁴⁹](#),
 S. Lee [ID^{47a,47b}](#), T.F. Lee [ID⁹³](#), L.L. Leeuw [ID^{33c}](#), H.P. Lefebvre [ID⁹⁶](#), M. Lefebvre [ID¹⁶⁶](#), C. Leggett [ID^{17a}](#),
 G. Lehmann Miotto [ID³⁶](#), M. Leigh [ID⁵⁶](#), W.A. Leight [ID¹⁰⁴](#), W. Leinonen [ID¹¹⁴](#), A. Leisos [ID^{153,t}](#),
 M.A.L. Leite [ID^{83c}](#), C.E. Leitgeb [ID⁴⁸](#), R. Leitner [ID¹³⁴](#), K.J.C. Leney [ID⁴⁴](#), T. Lenz [ID²⁴](#), S. Leone [ID^{74a}](#),
 C. Leonidopoulos [ID⁵²](#), A. Leopold [ID¹⁴⁵](#), C. Leroy [ID¹⁰⁹](#), R. Les [ID¹⁰⁸](#), C.G. Lester [ID³²](#),
 M. Levchenko [ID³⁷](#), J. Levêque [ID⁴](#), D. Levin [ID¹⁰⁷](#), L.J. Levinson [ID¹⁷⁰](#), M.P. Lewicki [ID⁸⁷](#), D.J. Lewis [ID⁴](#),
 A. Li [ID⁵](#), B. Li [ID^{62b}](#), C. Li^{62a}, C.-Q. Li [ID^{62c}](#), H. Li [ID^{62a}](#), H. Li [ID^{62b}](#), H. Li [ID^{14c}](#), H. Li [ID^{62b}](#), K. Li [ID¹³⁹](#),
 L. Li [ID^{62c}](#), M. Li [ID^{14a,14e}](#), Q.Y. Li [ID^{62a}](#), S. Li [ID^{14a,14e}](#), S. Li [ID^{62d,62c,d}](#), T. Li [ID⁵](#), X. Li [ID¹⁰⁵](#), Z. Li [ID¹²⁷](#),
 Z. Li [ID¹⁰⁵](#), Z. Li [ID⁹³](#), Z. Li [ID^{14a,14e}](#), Z. Liang [ID^{14a}](#), M. Liberatore [ID⁴⁸](#), B. Liberti [ID^{76a}](#), K. Lie [ID^{64c}](#),
 J. Lieber Marin [ID^{83b}](#), H. Lien [ID⁶⁸](#), K. Lin [ID¹⁰⁸](#), R.E. Lindley [ID⁷](#), J.H. Lindon [ID²](#), A. Linss [ID⁴⁸](#),
 E. Lipeles [ID¹²⁹](#), A. Lipniacka [ID¹⁶](#), A. Lister [ID¹⁶⁵](#), J.D. Little [ID⁴](#), B. Liu [ID^{14a}](#), B.X. Liu [ID¹⁴³](#),
 D. Liu [ID^{62d,62c}](#), J.B. Liu [ID^{62a}](#), J.K.K. Liu [ID³²](#), K. Liu [ID^{62d,62c}](#), M. Liu [ID^{62a}](#), M.Y. Liu [ID^{62a}](#), P. Liu [ID^{14a}](#),

Q. Liu [ID^{62d,139,62c}](#), X. Liu [ID^{62a}](#), Y. Liu [ID^{14d,14e}](#), Y.L. Liu [ID¹⁰⁷](#), Y.W. Liu [ID^{62a}](#), J. Llorente Merino [ID¹⁴³](#), S.L. Lloyd [ID⁹⁵](#), E.M. Lobodzinska [ID⁴⁸](#), P. Loch [ID⁷](#), S. Loffredo [ID^{76a,76b}](#), T. Lohse [ID¹⁸](#), K. Lohwasser [ID¹⁴⁰](#), E. Loiacono [ID⁴⁸](#), M. Lokajicek [ID^{132,*}](#), J.D. Lomas [ID²⁰](#), J.D. Long [ID¹⁶³](#), I. Longarini [ID¹⁶¹](#), L. Longo [ID^{70a,70b}](#), R. Longo [ID¹⁶³](#), I. Lopez Paz [ID⁶⁷](#), A. Lopez Solis [ID⁴⁸](#), J. Lorenz [ID¹¹⁰](#), N. Lorenzo Martinez [ID⁴](#), A.M. Lory [ID¹¹⁰](#), G. Löscheke Centeno [ID¹⁴⁷](#), O. Loseva [ID³⁷](#), X. Lou [ID^{47a,47b}](#), X. Lou [ID^{14a,14e}](#), A. Lounis [ID⁶⁶](#), J. Love [ID⁶](#), P.A. Love [ID⁹²](#), G. Lu [ID^{14a,14e}](#), M. Lu [ID⁸⁰](#), S. Lu [ID¹²⁹](#), Y.J. Lu [ID⁶⁵](#), H.J. Lubatti [ID¹³⁹](#), C. Luci [ID^{75a,75b}](#), F.L. Lucio Alves [ID^{14c}](#), A. Lucotte [ID⁶⁰](#), F. Luehring [ID⁶⁸](#), I. Luise [ID¹⁴⁶](#), O. Lukianchuk [ID⁶⁶](#), O. Lundberg [ID¹⁴⁵](#), B. Lund-Jensen [ID¹⁴⁵](#), N.A. Luongo [ID¹²⁴](#), M.S. Lutz [ID¹⁵²](#), D. Lynn [ID²⁹](#), H. Lyons [ID⁹³](#), R. Lysak [ID¹³²](#), E. Lytken [ID⁹⁹](#), V. Lyubushkin [ID³⁸](#), T. Lyubushkina [ID³⁸](#), M.M. Lyukova [ID¹⁴⁶](#), H. Ma [ID²⁹](#), K. Ma [ID^{62a}](#), L.L. Ma [ID^{62b}](#), Y. Ma [ID¹²²](#), D.M. Mac Donell [ID¹⁶⁶](#), G. Maccarrone [ID⁵³](#), J.C. MacDonald [ID¹⁰¹](#), R. Madar [ID⁴⁰](#), W.F. Mader [ID⁵⁰](#), J. Maeda [ID⁸⁵](#), T. Maeno [ID²⁹](#), M. Maerker [ID⁵⁰](#), H. Maguire [ID¹⁴⁰](#), V. Maiboroda [ID¹³⁶](#), A. Maio [ID^{131a,131b,131d}](#), K. Maj [ID^{86a}](#), O. Majersky [ID⁴⁸](#), S. Majewski [ID¹²⁴](#), N. Makovec [ID⁶⁶](#), V. Maksimovic [ID¹⁵](#), B. Malaescu [ID¹²⁸](#), Pa. Malecki [ID⁸⁷](#), V.P. Maleev [ID³⁷](#), F. Malek [ID⁶⁰](#), M. Mali [ID⁹⁴](#), D. Malito [ID⁹⁶](#), U. Mallik [ID⁸⁰](#), S. Maltezos [ID¹⁰](#), S. Malyukov [ID³⁸](#), J. Mamuzic [ID¹³](#), G. Mancini [ID⁵³](#), G. Manco [ID^{73a,73b}](#), J.P. Mandalia [ID⁹⁵](#), I. Mandić [ID⁹⁴](#), L. Manhaes de Andrade Filho [ID^{83a}](#), I.M. Maniatis [ID¹⁷⁰](#), J. Manjarres Ramos [ID^{103,ac}](#), D.C. Mankad [ID¹⁷⁰](#), A. Mann [ID¹¹⁰](#), B. Mansoulie [ID¹³⁶](#), S. Manzoni [ID³⁶](#), A. Marantis [ID^{153,t}](#), G. Marchiori [ID⁵](#), M. Marcisovsky [ID¹³²](#), C. Marcon [ID^{71a,71b}](#), M. Marinescu [ID²⁰](#), M. Marjanovic [ID¹²¹](#), E.J. Marshall [ID⁹²](#), Z. Marshall [ID^{17a}](#), S. Marti-Garcia [ID¹⁶⁴](#), T.A. Martin [ID¹⁶⁸](#), V.J. Martin [ID⁵²](#), B. Martin dit Latour [ID¹⁶](#), L. Martinelli [ID^{75a,75b}](#), M. Martinez [ID^{13,u}](#), P. Martinez Agullo [ID¹⁶⁴](#), V.I. Martinez Outschoorn [ID¹⁰⁴](#), P. Martinez Suarez [ID¹³](#), S. Martin-Haugh [ID¹³⁵](#), V.S. Martoiu [ID^{27b}](#), A.C. Martyniuk [ID⁹⁷](#), A. Marzin [ID³⁶](#), D. Mascione [ID^{78a,78b}](#), L. Masetti [ID¹⁰¹](#), T. Mashimo [ID¹⁵⁴](#), J. Masik [ID¹⁰²](#), A.L. Maslennikov [ID³⁷](#), L. Massa [ID^{23b}](#), P. Massarotti [ID^{72a,72b}](#), P. Mastrandrea [ID^{74a,74b}](#), A. Mastroberardino [ID^{43b,43a}](#), T. Masubuchi [ID¹⁵⁴](#), T. Mathisen [ID¹⁶²](#), J. Matousek [ID¹³⁴](#), N. Matsuzawa [ID¹⁵⁴](#), J. Maurer [ID^{27b}](#), B. Maček [ID⁹⁴](#), D.A. Maximov [ID³⁷](#), R. Mazini [ID¹⁴⁹](#), I. Maznas [ID¹⁵³](#), M. Mazza [ID¹⁰⁸](#), S.M. Mazza [ID¹³⁷](#), E. Mazzeo [ID^{71a,71b}](#), C. Mc Ginn [ID²⁹](#), J.P. Mc Gowan [ID¹⁰⁵](#), S.P. Mc Kee [ID¹⁰⁷](#), E.F. McDonald [ID¹⁰⁶](#), A.E. McDougall [ID¹¹⁵](#), J.A. Mcfayden [ID¹⁴⁷](#), R.P. McGovern [ID¹²⁹](#), G. Mchedlidze [ID^{150b}](#), R.P. Mckenzie [ID^{33g}](#), T.C. Mclachlan [ID⁴⁸](#), D.J. McLaughlin [ID⁹⁷](#), K.D. McLean [ID¹⁶⁶](#), S.J. McMahon [ID¹³⁵](#), P.C. McNamara [ID¹⁰⁶](#), C.M. Mcpartland [ID⁹³](#), R.A. McPherson [ID^{166,y}](#), S. Mehlhase [ID¹¹⁰](#), A. Mehta [ID⁹³](#), D. Melini [ID¹⁵¹](#), B.R. Mellado Garcia [ID^{33g}](#), A.H. Melo [ID⁵⁵](#), F. Meloni [ID⁴⁸](#), A.M. Mendes Jacques Da Costa [ID¹⁰²](#), H.Y. Meng [ID¹⁵⁶](#), L. Meng [ID⁹²](#), S. Menke [ID¹¹¹](#), M. Mentink [ID³⁶](#), E. Meoni [ID^{43b,43a}](#), C. Merlassino [ID¹²⁷](#), L. Merola [ID^{72a,72b}](#), C. Meroni [ID^{71a,71b}](#), G. Merz [ID¹⁰⁷](#), O. Meshkov [ID³⁷](#), J. Metcalfe [ID⁶](#), A.S. Mete [ID⁶](#), C. Meyer [ID⁶⁸](#), J-P. Meyer [ID¹³⁶](#), R.P. Middleton [ID¹³⁵](#), L. Mijović [ID⁵²](#), G. Mikenberg [ID¹⁷⁰](#), M. Mikestikova [ID¹³²](#), M. Mikuž [ID⁹⁴](#), H. Mildner [ID¹⁰¹](#), A. Milic [ID³⁶](#), C.D. Milke [ID⁴⁴](#), D.W. Miller [ID³⁹](#), L.S. Miller [ID³⁴](#), A. Milov [ID¹⁷⁰](#), D.A. Milstead [ID^{47a,47b}](#), T. Min [ID^{14c}](#), A.A. Minaenko [ID³⁷](#), I.A. Minashvili [ID^{150b}](#), L. Mince [ID⁵⁹](#), A.I. Mincer [ID¹¹⁸](#), B. Mindur [ID^{86a}](#), M. Mineev [ID³⁸](#), Y. Mino [ID⁸⁸](#), L.M. Mir [ID¹³](#), M. Miralles Lopez [ID¹⁶⁴](#), M. Mironova [ID^{17a}](#), A. Mishima [ID¹⁵⁴](#), M.C. Missio [ID¹¹⁴](#), T. Mitani [ID¹⁶⁹](#), A. Mitra [ID¹⁶⁸](#), V.A. Mitsou [ID¹⁶⁴](#), O. Miu [ID¹⁵⁶](#), P.S. Miyagawa [ID⁹⁵](#), Y. Miyazaki [ID⁹⁰](#), A. Mizukami [ID⁸⁴](#), T. Mkrtchyan [ID^{63a}](#), M. Mlinarevic [ID⁹⁷](#), T. Mlinarevic [ID⁹⁷](#), M. Mlynarikova [ID³⁶](#), S. Mobius [ID¹⁹](#), K. Mochizuki [ID¹⁰⁹](#), P. Moder [ID⁴⁸](#), P. Mogg [ID¹¹⁰](#), A.F. Mohammed [ID^{14a,14e}](#), S. Mohapatra [ID⁴¹](#), G. Mokgatitswana [ID^{33g}](#), L. Moleri [ID¹⁷⁰](#), B. Mondal [ID¹⁴²](#), S. Mondal [ID¹³³](#), K. Mönig [ID⁴⁸](#), E. Monnier [ID¹⁰³](#), L. Monsonis Romero [ID¹⁶⁴](#), J. Montejano Berlingen [ID^{13,84}](#), M. Montella [ID¹²⁰](#), F. Montereali [ID^{77a,77b}](#), F. Monticelli [ID⁹¹](#), S. Monzani [ID^{69a,69c}](#), N. Morange [ID⁶⁶](#), A.L. Moreira De Carvalho [ID^{131a}](#), M. Moreno Llácer [ID¹⁶⁴](#), C. Moreno Martinez [ID⁵⁶](#), P. Morettini [ID^{57b}](#), S. Morgenstern [ID³⁶](#), M. Morii [ID⁶¹](#), M. Morinaga [ID¹⁵⁴](#), A.K. Morley [ID³⁶](#), F. Morodei [ID^{75a,75b}](#), L. Morvaj [ID³⁶](#), P. Moschovakos [ID³⁶](#), B. Moser [ID³⁶](#), M. Mosidze [ID^{150b}](#), T. Moskalets [ID⁵⁴](#),

P. Moskvitina [ID¹¹⁴](#), J. Moss [ID^{31,n}](#), E.J.W. Moyse [ID¹⁰⁴](#), O. Mtintsilana [ID^{33g}](#), S. Muanza [ID¹⁰³](#),
 J. Mueller [ID¹³⁰](#), D. Muenstermann [ID⁹²](#), R. Müller [ID¹⁹](#), G.A. Mullier [ID¹⁶²](#), A.J. Mullin³², J.J. Mullin¹²⁹,
 D.P. Mungo [ID¹⁵⁶](#), D. Munoz Perez [ID¹⁶⁴](#), F.J. Munoz Sanchez [ID¹⁰²](#), M. Murin [ID¹⁰²](#), W.J. Murray [ID^{168,135}](#),
 A. Murrone [ID^{71a,71b}](#), J.M. Muse [ID¹²¹](#), M. Muškinja [ID^{17a}](#), C. Mwewa [ID²⁹](#), A.G. Myagkov [ID^{37,a}](#),
 A.J. Myers [ID⁸](#), A.A. Myers¹³⁰, G. Myers [ID⁶⁸](#), M. Myska [ID¹³³](#), B.P. Nachman [ID^{17a}](#), O. Nackenhorst [ID⁴⁹](#),
 A. Nag [ID⁵⁰](#), K. Nagai [ID¹²⁷](#), K. Nagano [ID⁸⁴](#), J.L. Nagle [ID^{29,aj}](#), E. Nagy [ID¹⁰³](#), A.M. Nairz [ID³⁶](#),
 Y. Nakahama [ID⁸⁴](#), K. Nakamura [ID⁸⁴](#), K. Nakkalil [ID⁵](#), H. Nanjo [ID¹²⁵](#), R. Narayan [ID⁴⁴](#),
 E.A. Narayanan [ID¹¹³](#), I. Naryshkin [ID³⁷](#), M. Naseri [ID³⁴](#), S. Nasri [ID¹⁶⁰](#), C. Nass [ID²⁴](#), G. Navarro [ID^{22a}](#),
 J. Navarro-Gonzalez [ID¹⁶⁴](#), R. Nayak [ID¹⁵²](#), A. Nayaz [ID¹⁸](#), P.Y. Nechaeva [ID³⁷](#), F. Nechansky [ID⁴⁸](#),
 L. Nedic [ID¹²⁷](#), T.J. Neep [ID²⁰](#), A. Negri [ID^{73a,73b}](#), M. Negrini [ID^{23b}](#), C. Nellist [ID¹¹⁵](#), C. Nelson [ID¹⁰⁵](#),
 K. Nelson [ID¹⁰⁷](#), S. Nemecek [ID¹³²](#), M. Nessi [ID^{36,h}](#), M.S. Neubauer [ID¹⁶³](#), F. Neuhaus [ID¹⁰¹](#),
 J. Neundorf [ID⁴⁸](#), R. Newhouse [ID¹⁶⁵](#), P.R. Newman [ID²⁰](#), C.W. Ng [ID¹³⁰](#), Y.W.Y. Ng [ID⁴⁸](#), B. Ngair [ID^{35e}](#),
 H.D.N. Nguyen [ID¹⁰⁹](#), R.B. Nickerson [ID¹²⁷](#), R. Nicolaïdou [ID¹³⁶](#), J. Nielsen [ID¹³⁷](#), M. Niemeyer [ID⁵⁵](#),
 J. Niermann [ID^{55,36}](#), N. Nikiforou [ID³⁶](#), V. Nikolaenko [ID^{37,a}](#), I. Nikolic-Audit [ID¹²⁸](#), K. Nikolopoulos [ID²⁰](#),
 P. Nilsson [ID²⁹](#), I. Ninca [ID⁴⁸](#), H.R. Nindhito [ID⁵⁶](#), G. Ninio [ID¹⁵²](#), A. Nisati [ID^{75a}](#), N. Nishu [ID²](#),
 R. Nisius [ID¹¹¹](#), J-E. Nitschke [ID⁵⁰](#), E.K. Nkademeng [ID^{33g}](#), S.J. Noacco Rosende [ID⁹¹](#), T. Nobe [ID¹⁵⁴](#),
 D.L. Noel [ID³²](#), T. Nommensen [ID¹⁴⁸](#), M.B. Norfolk [ID¹⁴⁰](#), R.R.B. Norisam [ID⁹⁷](#), B.J. Norman [ID³⁴](#),
 J. Novak [ID⁹⁴](#), T. Novak [ID⁴⁸](#), L. Novotny [ID¹³³](#), R. Novotny [ID¹¹³](#), L. Nozka [ID¹²³](#), K. Ntekas [ID¹⁶¹](#),
 N.M.J. Nunes De Moura Junior [ID^{83b}](#), E. Nurse⁹⁷, J. Ocariz [ID¹²⁸](#), A. Ochi [ID⁸⁵](#), I. Ochoa [ID^{131a}](#),
 S. Oerdekk [ID¹⁶²](#), J.T. Offermann [ID³⁹](#), A. Ogorodnik [ID¹³⁴](#), A. Oh [ID¹⁰²](#), C.C. Ohm [ID¹⁴⁵](#), H. Oide [ID⁸⁴](#),
 R. Oishi [ID¹⁵⁴](#), M.L. Ojeda [ID⁴⁸](#), Y. Okazaki [ID⁸⁸](#), M.W. O'Keefe⁹³, Y. Okumura [ID¹⁵⁴](#),
 L.F. Oleiro Seabra [ID^{131a}](#), S.A. Olivares Pino [ID^{138d}](#), D. Oliveira Damazio [ID²⁹](#), D. Oliveira Goncalves [ID^{83a}](#),
 J.L. Oliver [ID¹⁶¹](#), A. Olszewski [ID⁸⁷](#), Ö.O. Öncel [ID⁵⁴](#), D.C. O'Neil [ID¹⁴³](#), A.P. O'Neill [ID¹⁹](#),
 A. Onofre [ID^{131a,131e}](#), P.U.E. Onyisi [ID¹¹](#), M.J. Oreglia [ID³⁹](#), G.E. Orellana [ID⁹¹](#), D. Orestano [ID^{77a,77b}](#),
 N. Orlando [ID¹³](#), R.S. Orr [ID¹⁵⁶](#), V. O'Shea [ID⁵⁹](#), L.M. Osojnak [ID¹²⁹](#), R. Ospanov [ID^{62a}](#),
 G. Otero y Garzon [ID³⁰](#), H. Otono [ID⁹⁰](#), P.S. Ott [ID^{63a}](#), G.J. Ottino [ID^{17a}](#), M. Ouchrif [ID^{35d}](#), J. Ouellette [ID²⁹](#),
 F. Ould-Saada [ID¹²⁶](#), M. Owen [ID⁵⁹](#), R.E. Owen [ID¹³⁵](#), K.Y. Oyulmaz [ID^{21a}](#), V.E. Ozcan [ID^{21a}](#), N. Ozturk [ID⁸](#),
 S. Ozturk [ID⁸²](#), H.A. Pacey [ID³²](#), A. Pacheco Pages [ID¹³](#), C. Padilla Aranda [ID¹³](#), G. Padovano [ID^{75a,75b}](#),
 S. Pagan Griso [ID^{17a}](#), G. Palacino [ID⁶⁸](#), A. Palazzo [ID^{70a,70b}](#), S. Palestini [ID³⁶](#), J. Pan [ID¹⁷³](#), T. Pan [ID^{64a}](#),
 D.K. Panchal [ID¹¹](#), C.E. Pandini [ID¹¹⁵](#), J.G. Panduro Vazquez [ID⁹⁶](#), H. Pang [ID^{14b}](#), P. Pani [ID⁴⁸](#),
 G. Panizzo [ID^{69a,69c}](#), L. Paolozzi [ID⁵⁶](#), C. Papadatos [ID¹⁰⁹](#), S. Parajuli [ID⁴⁴](#), A. Paramonov [ID⁶](#),
 C. Paraskevopoulos [ID¹⁰](#), D. Paredes Hernandez [ID^{64b}](#), T.H. Park [ID¹⁵⁶](#), M.A. Parker [ID³²](#), F. Parodi [ID^{57b,57a}](#),
 E.W. Parrish [ID¹¹⁶](#), V.A. Parrish [ID⁵²](#), J.A. Parsons [ID⁴¹](#), U. Parzefall [ID⁵⁴](#), B. Pascual Dias [ID¹⁰⁹](#),
 L. Pascual Dominguez [ID¹⁵²](#), F. Pasquali [ID¹¹⁵](#), E. Pasqualucci [ID^{75a}](#), S. Passaggio [ID^{57b}](#), F. Pastore [ID⁹⁶](#),
 P. Pasuwan [ID^{47a,47b}](#), P. Patel [ID⁸⁷](#), U.M. Patel [ID⁵¹](#), J.R. Pater [ID¹⁰²](#), T. Pauly [ID³⁶](#), J. Pearkes [ID¹⁴⁴](#),
 M. Pedersen [ID¹²⁶](#), R. Pedro [ID^{131a}](#), S.V. Peleganchuk [ID³⁷](#), O. Penc [ID³⁶](#), E.A. Pender [ID⁵²](#), H. Peng [ID^{62a}](#),
 K.E. Penski [ID¹¹⁰](#), M. Penzin [ID³⁷](#), B.S. Peralva [ID^{83d}](#), A.P. Pereira Peixoto [ID⁶⁰](#), L. Pereira Sanchez [ID^{47a,47b}](#),
 D.V. Perepelitsa [ID^{29,aj}](#), E. Perez Codina [ID^{157a}](#), M. Perganti [ID¹⁰](#), L. Perini [ID^{71a,71b,*}](#), H. Pernegger [ID³⁶](#),
 A. Perrevoort [ID¹¹⁴](#), O. Perrin [ID⁴⁰](#), K. Peters [ID⁴⁸](#), R.F.Y. Peters [ID¹⁰²](#), B.A. Petersen [ID³⁶](#),
 T.C. Petersen [ID⁴²](#), E. Petit [ID¹⁰³](#), V. Petousis [ID¹³³](#), C. Petridou [ID^{153,e}](#), A. Petrukhin [ID¹⁴²](#), M. Pettee [ID^{17a}](#),
 N.E. Pettersson [ID³⁶](#), A. Petukhov [ID³⁷](#), K. Petukhova [ID¹³⁴](#), A. Peyaud [ID¹³⁶](#), R. Pezoa [ID^{138f}](#),
 L. Pezzotti [ID³⁶](#), G. Pezzullo [ID¹⁷³](#), T.M. Pham [ID¹⁷¹](#), T. Pham [ID¹⁰⁶](#), P.W. Phillips [ID¹³⁵](#), G. Piacquadio [ID¹⁴⁶](#),
 E. Pianori [ID^{17a}](#), F. Piazza [ID^{71a,71b}](#), R. Piegala [ID³⁰](#), D. Pietreanu [ID^{27b}](#), A.D. Pilkington [ID¹⁰²](#),
 M. Pinamonti [ID^{69a,69c}](#), J.L. Pinfold [ID²](#), B.C. Pinheiro Pereira [ID^{131a}](#), A.E. Pinto Pinoargote [ID¹³⁶](#),
 K.M. Piper [ID¹⁴⁷](#), A. Pirttikoski [ID⁵⁶](#), C. Pitman Donaldson⁹⁷, D.A. Pizzi [ID³⁴](#), L. Pizzimento [ID^{76a,76b}](#),
 A. Pizzini [ID¹¹⁵](#), M.-A. Pleier [ID²⁹](#), V. Plesanovs⁵⁴, V. Pleskot [ID¹³⁴](#), E. Plotnikova³⁸, G. Poddar [ID⁴](#),
 R. Poettgen [ID⁹⁹](#), L. Poggioli [ID¹²⁸](#), I. Pokharel [ID⁵⁵](#), S. Polacek [ID¹³⁴](#), G. Polesello [ID^{73a}](#), A. Poley [ID^{143,157a}](#),

R. Polifka [ID¹³³](#), A. Polini [ID^{23b}](#), C.S. Pollard [ID¹⁶⁸](#), Z.B. Pollock [ID¹²⁰](#), V. Polychronakos [ID²⁹](#),
 E. Pompa Pacchi [ID^{75a,75b}](#), D. Ponomarenko [ID¹¹⁴](#), L. Pontecorvo [ID³⁶](#), S. Popa [ID^{27a}](#), G.A. Popeneciu [ID^{27d}](#),
 A. Poreba [ID³⁶](#), D.M. Portillo Quintero [ID^{157a}](#), S. Pospisil [ID¹³³](#), M.A. Postill [ID¹⁴⁰](#), P. Postolache [ID^{27c}](#),
 K. Potamianos [ID¹⁶⁸](#), P.A. Potepe [ID^{86a}](#), I.N. Potrap [ID³⁸](#), C.J. Potter [ID³²](#), H. Potti [ID¹](#), T. Poulsen [ID⁴⁸](#),
 J. Poveda [ID¹⁶⁴](#), M.E. Pozo Astigarraga [ID³⁶](#), A. Prades Ibanez [ID¹⁶⁴](#), J. Pretel [ID⁵⁴](#), D. Price [ID¹⁰²](#),
 M. Primavera [ID^{70a}](#), M.A. Principe Martin [ID¹⁰⁰](#), R. Privara [ID¹²³](#), T. Procter [ID⁵⁹](#), M.L. Proffitt [ID¹³⁹](#),
 N. Proklova [ID¹²⁹](#), K. Prokofiev [ID^{64c}](#), G. Proto [ID¹¹¹](#), S. Protopopescu [ID²⁹](#), J. Proudfoot [ID⁶](#),
 M. Przybycien [ID^{86a}](#), W.W. Przygoda [ID^{86b}](#), J.E. Puddefoot [ID¹⁴⁰](#), D. Pudzha [ID³⁷](#), D. Pyatiizbyantseva [ID³⁷](#),
 J. Qian [ID¹⁰⁷](#), D. Qichen [ID¹⁰²](#), Y. Qin [ID¹⁰²](#), T. Qiu [ID⁵²](#), A. Quadt [ID⁵⁵](#), M. Queitsch-Maitland [ID¹⁰²](#),
 G. Quetant [ID⁵⁶](#), G. Rabanal Bolanos [ID⁶¹](#), D. Rafanoharana [ID⁵⁴](#), F. Ragusa [ID^{71a,71b}](#), J.L. Rainbolt [ID³⁹](#),
 J.A. Raine [ID⁵⁶](#), S. Rajagopalan [ID²⁹](#), E. Ramakoti [ID³⁷](#), K. Ran [ID^{48,14e}](#), N.P. Rapheeha [ID^{33g}](#),
 H. Rasheed [ID^{27b}](#), V. Raskina [ID¹²⁸](#), D.F. Rassloff [ID^{63a}](#), S. Rave [ID¹⁰¹](#), B. Ravina [ID⁵⁵](#), I. Ravinovich [ID¹⁷⁰](#),
 M. Raymond [ID³⁶](#), A.L. Read [ID¹²⁶](#), N.P. Readioff [ID¹⁴⁰](#), D.M. Rebuzzi [ID^{73a,73b}](#), G. Redlinger [ID²⁹](#),
 A.S. Reed [ID¹¹¹](#), K. Reeves [ID²⁶](#), J.A. Reidelsturz [ID¹⁷²](#), D. Reikher [ID¹⁵²](#), A. Rej [ID¹⁴²](#), C. Rembser [ID³⁶](#),
 A. Renardi [ID⁴⁸](#), M. Renda [ID^{27b}](#), M.B. Rendel [ID¹¹¹](#), F. Renner [ID⁴⁸](#), A.G. Rennie [ID⁵⁹](#), S. Resconi [ID^{71a}](#),
 M. Ressegotti [ID^{57b,57a}](#), S. Rettie [ID³⁶](#), J.G. Reyes Rivera [ID¹⁰⁸](#), B. Reynolds [ID¹²⁰](#), E. Reynolds [ID^{17a}](#),
 O.L. Rezanova [ID³⁷](#), P. Reznicek [ID¹³⁴](#), N. Ribaric [ID⁹²](#), E. Ricci [ID^{78a,78b}](#), R. Richter [ID¹¹¹](#),
 S. Richter [ID^{47a,47b}](#), E. Richter-Was [ID^{86b}](#), M. Ridel [ID¹²⁸](#), S. Ridouani [ID^{35d}](#), P. Rieck [ID¹¹⁸](#), P. Riedler [ID³⁶](#),
 M. Rijssenbeek [ID¹⁴⁶](#), A. Rimoldi [ID^{73a,73b}](#), M. Rimoldi [ID⁴⁸](#), L. Rinaldi [ID^{23b,23a}](#), T.T. Rinn [ID²⁹](#),
 M.P. Rinnagel [ID¹¹⁰](#), G. Ripellino [ID¹⁶²](#), I. Riu [ID¹³](#), P. Rivadeneira [ID⁴⁸](#), J.C. Rivera Vergara [ID¹⁶⁶](#),
 F. Rizatdinova [ID¹²²](#), E. Rizvi [ID⁹⁵](#), B.A. Roberts [ID¹⁶⁸](#), B.R. Roberts [ID^{17a}](#), S.H. Robertson [ID^{105,y}](#),
 M. Robin [ID⁴⁸](#), D. Robinson [ID³²](#), C.M. Robles Gajardo [ID^{138f}](#), M. Robles Manzano [ID¹⁰¹](#), A. Robson [ID⁵⁹](#),
 A. Rocchi [ID^{76a,76b}](#), C. Roda [ID^{74a,74b}](#), S. Rodriguez Bosca [ID^{63a}](#), Y. Rodriguez Garcia [ID^{22a}](#),
 A. Rodriguez Rodriguez [ID⁵⁴](#), A.M. Rodríguez Vera [ID^{157b}](#), S. Roe [ID³⁶](#), J.T. Roemer [ID¹⁶¹](#),
 A.R. Roepe-Gier [ID¹³⁷](#), J. Roggel [ID¹⁷²](#), O. Røhne [ID¹²⁶](#), R.A. Rojas [ID¹⁰⁴](#), C.P.A. Roland [ID⁶⁸](#), J. Roloff [ID²⁹](#),
 A. Romaniouk [ID³⁷](#), E. Romano [ID^{73a,73b}](#), M. Romano [ID^{23b}](#), A.C. Romero Hernandez [ID¹⁶³](#),
 N. Rompotis [ID⁹³](#), L. Roos [ID¹²⁸](#), S. Rosati [ID^{75a}](#), B.J. Rosser [ID³⁹](#), E. Rossi [ID¹²⁷](#), E. Rossi [ID^{72a,72b}](#),
 L.P. Rossi [ID^{57b}](#), L. Rossini [ID⁴⁸](#), R. Rosten [ID¹²⁰](#), M. Rotaru [ID^{27b}](#), B. Rottler [ID⁵⁴](#), C. Rougier [ID^{103,ac}](#),
 D. Rousseau [ID⁶⁶](#), D. Rousso [ID³²](#), A. Roy [ID¹⁶³](#), S. Roy-Garand [ID¹⁵⁶](#), A. Rozanov [ID¹⁰³](#), Y. Rozen [ID¹⁵¹](#),
 X. Ruan [ID^{33g}](#), A. Rubio Jimenez [ID¹⁶⁴](#), A.J. Ruby [ID⁹³](#), V.H. Ruelas Rivera [ID¹⁸](#), T.A. Ruggeri [ID¹](#),
 A. Ruggiero [ID¹²⁷](#), A. Ruiz-Martinez [ID¹⁶⁴](#), A. Rummler [ID³⁶](#), Z. Rurikova [ID⁵⁴](#), N.A. Rusakovich [ID³⁸](#),
 H.L. Russell [ID¹⁶⁶](#), G. Russo [ID^{75a,75b}](#), J.P. Rutherford [ID⁷](#), S. Rutherford Colmenares [ID³²](#), K. Rybacki [ID⁹²](#),
 M. Rybar [ID¹³⁴](#), E.B. Rye [ID¹²⁶](#), A. Ryzhov [ID⁴⁴](#), J.A. Sabater Iglesias [ID⁵⁶](#), P. Sabatini [ID¹⁶⁴](#),
 L. Sabetta [ID^{75a,75b}](#), H.F-W. Sadrozinski [ID¹³⁷](#), F. Safai Tehrani [ID^{75a}](#), B. Safarzadeh Samani [ID¹⁴⁷](#),
 M. Safdari [ID¹⁴⁴](#), S. Saha [ID¹⁶⁶](#), M. Sahinsoy [ID¹¹¹](#), M. Saimpert [ID¹³⁶](#), M. Saito [ID¹⁵⁴](#), T. Saito [ID¹⁵⁴](#),
 D. Salamani [ID³⁶](#), A. Salnikov [ID¹⁴⁴](#), J. Salt [ID¹⁶⁴](#), A. Salvador Salas [ID¹³](#), D. Salvatore [ID^{43b,43a}](#),
 F. Salvatore [ID¹⁴⁷](#), A. Salzburger [ID³⁶](#), D. Sammel [ID⁵⁴](#), D. Sampsonidis [ID^{153,e}](#), D. Sampsonidou [ID¹²⁴](#),
 J. Sánchez [ID¹⁶⁴](#), A. Sanchez Pineda [ID⁴](#), V. Sanchez Sebastian [ID¹⁶⁴](#), H. Sandaker [ID¹²⁶](#), C.O. Sander [ID⁴⁸](#),
 J.A. Sandesara [ID¹⁰⁴](#), M. Sandhoff [ID¹⁷²](#), C. Sandoval [ID^{22b}](#), D.P.C. Sankey [ID¹³⁵](#), T. Sano [ID⁸⁸](#),
 A. Sansoni [ID⁵³](#), L. Santi [ID^{75a,75b}](#), C. Santoni [ID⁴⁰](#), H. Santos [ID^{131a,131b}](#), S.N. Santpur [ID^{17a}](#), A. Santra [ID¹⁷⁰](#),
 K.A. Saoucha [ID¹⁴⁰](#), J.G. Saraiva [ID^{131a,131d}](#), J. Sardain [ID⁷](#), O. Sasaki [ID⁸⁴](#), K. Sato [ID¹⁵⁸](#), C. Sauer [ID^{63b}](#),
 F. Sauerburger [ID⁵⁴](#), E. Sauvan [ID⁴](#), P. Savard [ID^{156,ah}](#), R. Sawada [ID¹⁵⁴](#), C. Sawyer [ID¹³⁵](#), L. Sawyer [ID⁹⁸](#),
 I. Sayago Galvan [ID¹⁶⁴](#), C. Sbarra [ID^{23b}](#), A. Sbrizzi [ID^{23b,23a}](#), T. Scanlon [ID⁹⁷](#), J. Schaarschmidt [ID¹³⁹](#),
 P. Schacht [ID¹¹¹](#), D. Schaefer [ID³⁹](#), U. Schäfer [ID¹⁰¹](#), A.C. Schaffer [ID^{66,44}](#), D. Schaile [ID¹¹⁰](#),
 R.D. Schamberger [ID¹⁴⁶](#), C. Scharf [ID¹⁸](#), M.M. Schefer [ID¹⁹](#), V.A. Schegelsky [ID³⁷](#), D. Scheirich [ID¹³⁴](#),
 F. Schenck [ID¹⁸](#), M. Schernau [ID¹⁶¹](#), C. Scheulen [ID⁵⁵](#), C. Schiavi [ID^{57b,57a}](#), E.J. Schioppa [ID^{70a,70b}](#),
 M. Schioppa [ID^{43b,43a}](#), B. Schlag [ID^{144,p}](#), K.E. Schleicher [ID⁵⁴](#), S. Schlenker [ID³⁶](#), J. Schmeing [ID¹⁷²](#),

M.A. Schmidt [ID¹⁷²](#), K. Schmieden [ID¹⁰¹](#), C. Schmitt [ID¹⁰¹](#), S. Schmitt [ID⁴⁸](#), L. Schoeffel [ID¹³⁶](#),
 A. Schoening [ID^{63b}](#), P.G. Scholer [ID⁵⁴](#), E. Schopf [ID¹²⁷](#), M. Schott [ID¹⁰¹](#), J. Schovancova [ID³⁶](#),
 S. Schramm [ID⁵⁶](#), F. Schroeder [ID¹⁷²](#), T. Schroer [ID⁵⁶](#), H-C. Schultz-Coulon [ID^{63a}](#), M. Schumacher [ID⁵⁴](#),
 B.A. Schumm [ID¹³⁷](#), Ph. Schune [ID¹³⁶](#), A.J. Schuy [ID¹³⁹](#), H.R. Schwartz [ID¹³⁷](#), A. Schwartzman [ID¹⁴⁴](#),
 T.A. Schwarz [ID¹⁰⁷](#), Ph. Schwemling [ID¹³⁶](#), R. Schwienhorst [ID¹⁰⁸](#), A. Sciandra [ID¹³⁷](#), G. Sciolla [ID²⁶](#),
 F. Scuri [ID^{74a}](#), C.D. Sebastiani [ID⁹³](#), K. Sedlaczek [ID¹¹⁶](#), P. Seema [ID¹⁸](#), S.C. Seidel [ID¹¹³](#), A. Seiden [ID¹³⁷](#),
 B.D. Seidlitz [ID⁴¹](#), C. Seitz [ID⁴⁸](#), J.M. Seixas [ID^{83b}](#), G. Sekhniaidze [ID^{72a}](#), S.J. Sekula [ID⁴⁴](#), L. Selem [ID⁶⁰](#),
 N. Semprini-Cesari [ID^{23b,23a}](#), D. Sengupta [ID⁵⁶](#), V. Senthilkumar [ID¹⁶⁴](#), L. Serin [ID⁶⁶](#), L. Serkin [ID^{69a,69b}](#),
 M. Sessa [ID^{76a,76b}](#), H. Severini [ID¹²¹](#), F. Sforza [ID^{57b,57a}](#), A. Sfyrla [ID⁵⁶](#), E. Shabalina [ID⁵⁵](#), R. Shaheen [ID¹⁴⁵](#),
 J.D. Shahinian [ID¹²⁹](#), D. Shaked Renous [ID¹⁷⁰](#), L.Y. Shan [ID^{14a}](#), M. Shapiro [ID^{17a}](#), A. Sharma [ID³⁶](#),
 A.S. Sharma [ID¹⁶⁵](#), P. Sharma [ID⁸⁰](#), S. Sharma [ID⁴⁸](#), P.B. Shatalov [ID³⁷](#), K. Shaw [ID¹⁴⁷](#), S.M. Shaw [ID¹⁰²](#),
 A. Shcherbakova [ID³⁷](#), Q. Shen [ID^{62c,5}](#), P. Sherwood [ID⁹⁷](#), L. Shi [ID⁹⁷](#), X. Shi [ID^{14a}](#), C.O. Shimmin [ID¹⁷³](#),
 Y. Shimogama [ID¹⁶⁹](#), J.D. Shinner [ID⁹⁶](#), I.P.J. Shipsey [ID¹²⁷](#), S. Shirabe [ID^{56,h}](#), M. Shiyakova [ID^{38,w}](#),
 J. Shlomi [ID¹⁷⁰](#), M.J. Shochet [ID³⁹](#), J. Shojaii [ID¹⁰⁶](#), D.R. Shope [ID¹²⁶](#), B. Shrestha [ID¹²¹](#), S. Shrestha [ID^{120,ak}](#),
 E.M. Shrif [ID^{33g}](#), M.J. Shroff [ID¹⁶⁶](#), P. Sicho [ID¹³²](#), A.M. Sickles [ID¹⁶³](#), E. Sideras Haddad [ID^{33g}](#),
 A. Sidoti [ID^{23b}](#), F. Siegert [ID⁵⁰](#), Dj. Sijacki [ID¹⁵](#), R. Sikora [ID^{86a}](#), F. Sili [ID⁹¹](#), J.M. Silva [ID²⁰](#),
 M.V. Silva Oliveira [ID²⁹](#), S.B. Silverstein [ID^{47a}](#), S. Simion [ID⁶⁶](#), R. Simonello [ID³⁶](#), E.L. Simpson [ID⁵⁹](#),
 H. Simpson [ID¹⁴⁷](#), L.R. Simpson [ID¹⁰⁷](#), N.D. Simpson [ID⁹⁹](#), S. Simsek [ID⁸²](#), S. Sindhu [ID⁵⁵](#), P. Sinervo [ID¹⁵⁶](#),
 S. Singh [ID¹⁵⁶](#), S. Sinha [ID⁴⁸](#), S. Sinha [ID¹⁰²](#), M. Sioli [ID^{23b,23a}](#), I. Siral [ID³⁶](#), E. Sitnikova [ID⁴⁸](#),
 S.Yu. Sivoklokov [ID^{37,*}](#), J. Sjölin [ID^{47a,47b}](#), A. Skaf [ID⁵⁵](#), E. Skorda [ID⁹⁹](#), P. Skubic [ID¹²¹](#), M. Slawinska [ID⁸⁷](#),
 V. Smakhtin [ID¹⁷⁰](#), B.H. Smart [ID¹³⁵](#), J. Smiesko [ID³⁶](#), S.Yu. Smirnov [ID³⁷](#), Y. Smirnov [ID³⁷](#),
 L.N. Smirnova [ID^{37,a}](#), O. Smirnova [ID⁹⁹](#), A.C. Smith [ID⁴¹](#), E.A. Smith [ID³⁹](#), H.A. Smith [ID¹²⁷](#),
 J.L. Smith [ID⁹³](#), R. Smith [ID¹⁴⁴](#), M. Smizanska [ID⁹²](#), K. Smolek [ID¹³³](#), A.A. Snesarev [ID³⁷](#), S.R. Snider [ID¹⁵⁶](#),
 H.L. Snoek [ID¹¹⁵](#), S. Snyder [ID²⁹](#), R. Sobie [ID^{166,y}](#), A. Soffer [ID¹⁵²](#), C.A. Solans Sanchez [ID³⁶](#),
 E.Yu. Soldatov [ID³⁷](#), U. Soldevila [ID¹⁶⁴](#), A.A. Solodkov [ID³⁷](#), S. Solomon [ID²⁶](#), A. Soloshenko [ID³⁸](#),
 K. Solovieva [ID⁵⁴](#), O.V. Solovyanov [ID⁴⁰](#), V. Solovyev [ID³⁷](#), P. Sommer [ID³⁶](#), A. Sonay [ID¹³](#),
 W.Y. Song [ID^{157b}](#), J.M. Sonneveld [ID¹¹⁵](#), A. Sopczak [ID¹³³](#), A.L. Sopio [ID⁹⁷](#), F. Sopkova [ID^{28b}](#),
 V. Sothilingam [ID^{63a}](#), S. Sottocornola [ID⁶⁸](#), R. Soualah [ID^{117b}](#), Z. Soumaimi [ID^{35e}](#), D. South [ID⁴⁸](#),
 S. Spagnolo [ID^{70a,70b}](#), M. Spalla [ID¹¹¹](#), D. Sperlich [ID⁵⁴](#), G. Spigo [ID³⁶](#), M. Spina [ID¹⁴⁷](#), S. Spinali [ID⁹²](#),
 D.P. Spiteri [ID⁵⁹](#), M. Spousta [ID¹³⁴](#), E.J. Staats [ID³⁴](#), A. Stabile [ID^{71a,71b}](#), R. Stamen [ID^{63a}](#),
 M. Stamenkovic [ID¹¹⁵](#), A. Stampekitis [ID²⁰](#), M. Standke [ID²⁴](#), E. Stanecka [ID⁸⁷](#), M.V. Stange [ID⁵⁰](#),
 B. Stanislaus [ID^{17a}](#), M.M. Stanitzki [ID⁴⁸](#), B. Stapf [ID⁴⁸](#), E.A. Starchenko [ID³⁷](#), G.H. Stark [ID¹³⁷](#),
 J. Stark [ID^{103,ac}](#), D.M. Starko [ID^{157b}](#), P. Staroba [ID¹³²](#), P. Starovoitov [ID^{63a}](#), S. Stärz [ID¹⁰⁵](#), R. Staszewski [ID⁸⁷](#),
 G. Stavropoulos [ID⁴⁶](#), J. Steentoft [ID¹⁶²](#), P. Steinberg [ID²⁹](#), B. Stelzer [ID^{143,157a}](#), H.J. Stelzer [ID¹³⁰](#),
 O. Stelzer-Chilton [ID^{157a}](#), H. Stenzel [ID⁵⁸](#), T.J. Stevenson [ID¹⁴⁷](#), G.A. Stewart [ID³⁶](#), J.R. Stewart [ID¹²²](#),
 M.C. Stockton [ID³⁶](#), G. Stoica [ID^{27b}](#), M. Stolarski [ID^{131a}](#), S. Stonjek [ID¹¹¹](#), A. Straessner [ID⁵⁰](#),
 J. Strandberg [ID¹⁴⁵](#), S. Strandberg [ID^{47a,47b}](#), M. Strauss [ID¹²¹](#), T. Strebler [ID¹⁰³](#), P. Strizenec [ID^{28b}](#),
 R. Ströhmer [ID¹⁶⁷](#), D.M. Strom [ID¹²⁴](#), L.R. Strom [ID⁴⁸](#), R. Stroynowski [ID⁴⁴](#), A. Strubig [ID^{47a,47b}](#),
 S.A. Stucci [ID²⁹](#), B. Stugu [ID¹⁶](#), J. Stupak [ID¹²¹](#), N.A. Styles [ID⁴⁸](#), D. Su [ID¹⁴⁴](#), S. Su [ID^{62a}](#), W. Su [ID^{62d}](#),
 X. Su [ID^{62a,66}](#), K. Sugizaki [ID¹⁵⁴](#), V.V. Sulin [ID³⁷](#), M.J. Sullivan [ID⁹³](#), D.M.S. Sultan [ID^{78a,78b}](#),
 L. Sultanaliyeva [ID³⁷](#), S. Sultansoy [ID^{3b}](#), T. Sumida [ID⁸⁸](#), S. Sun [ID¹⁰⁷](#), S. Sun [ID¹⁷¹](#),
 O. Sunneborn Gudnadottir [ID¹⁶²](#), N. Sur [ID¹⁰³](#), M.R. Sutton [ID¹⁴⁷](#), H. Suzuki [ID¹⁵⁸](#), M. Svatos [ID¹³²](#),
 M. Swiatlowski [ID^{157a}](#), T. Swirski [ID¹⁶⁷](#), I. Sykora [ID^{28a}](#), M. Sykora [ID¹³⁴](#), T. Sykora [ID¹³⁴](#), D. Ta [ID¹⁰¹](#),
 K. Tackmann [ID^{48,v}](#), A. Taffard [ID¹⁶¹](#), R. Tafirout [ID^{157a}](#), J.S. Tafoya Vargas [ID⁶⁶](#), R. Takashima [ID⁸⁹](#),
 E.P. Takeva [ID⁵²](#), Y. Takubo [ID⁸⁴](#), M. Talby [ID¹⁰³](#), A.A. Talyshев [ID³⁷](#), K.C. Tam [ID^{64b}](#), N.M. Tamir [ID¹⁵²](#),
 A. Tanaka [ID¹⁵⁴](#), J. Tanaka [ID¹⁵⁴](#), R. Tanaka [ID⁶⁶](#), M. Tanasini [ID^{57b,57a}](#), Z. Tao [ID¹⁶⁵](#), S. Tapia Araya [ID^{138f}](#),
 S. Tapprogge [ID¹⁰¹](#), A. Tarek Abouelfadl Mohamed [ID¹⁰⁸](#), S. Tarem [ID¹⁵¹](#), K. Tariq [ID^{14a}](#), G. Tarna [ID^{103,27b}](#)

G.F. Tartarelli [ID^{71a}](#), P. Tas [ID¹³⁴](#), M. Tasevsky [ID¹³²](#), E. Tassi [ID^{43b,43a}](#), A.C. Tate [ID¹⁶³](#), G. Tateno [ID¹⁵⁴](#), Y. Tayalati [ID^{35e,x}](#), G.N. Taylor [ID¹⁰⁶](#), W. Taylor [ID^{157b}](#), H. Teagle⁹³, A.S. Tee [ID¹⁷¹](#), R. Teixeira De Lima [ID¹⁴⁴](#), P. Teixeira-Dias [ID⁹⁶](#), J.J. Teoh [ID¹⁵⁶](#), K. Terashi [ID¹⁵⁴](#), J. Terron [ID¹⁰⁰](#), S. Terzo [ID¹³](#), M. Testa [ID⁵³](#), R.J. Teuscher [ID^{156,y}](#), A. Thaler [ID⁷⁹](#), O. Theiner [ID⁵⁶](#), N. Themistokleous [ID⁵²](#), T. Theveneaux-Pelzer [ID¹⁰³](#), O. Thielmann [ID¹⁷²](#), D.W. Thomas⁹⁶, J.P. Thomas [ID²⁰](#), E.A. Thompson [ID^{17a}](#), P.D. Thompson [ID²⁰](#), E. Thomson [ID¹²⁹](#), Y. Tian [ID⁵⁵](#), V. Tikhomirov [ID^{37,a}](#), Yu.A. Tikhonov [ID³⁷](#), S. Timoshenko³⁷, D. Timoshyn [ID¹³⁴](#), E.X.L. Ting [ID¹](#), P. Tipton [ID¹⁷³](#), S.H. Tlou [ID^{33g}](#), A. Tnourji [ID⁴⁰](#), K. Todome [ID^{23b,23a}](#), S. Todorova-Nova [ID¹³⁴](#), S. Todt⁵⁰, M. Togawa [ID⁸⁴](#), J. Tojo [ID⁹⁰](#), S. Tokár [ID^{28a}](#), K. Tokushuku [ID⁸⁴](#), O. Toldaiev [ID⁶⁸](#), R. Tombs [ID³²](#), M. Tomoto [ID^{84,112}](#), L. Tompkins [ID^{144,p}](#), K.W. Topolnicki [ID^{86b}](#), E. Torrence [ID¹²⁴](#), H. Torres [ID^{103,ac}](#), E. Torró Pastor [ID¹⁶⁴](#), M. Toscani [ID³⁰](#), C. Tosciri [ID³⁹](#), M. Tost [ID¹¹](#), D.R. Tovey [ID¹⁴⁰](#), A. Traeet¹⁶, I.S. Trandafir [ID^{27b}](#), T. Trefzger [ID¹⁶⁷](#), A. Tricoli [ID²⁹](#), I.M. Trigger [ID^{157a}](#), S. Trincaz-Duvold [ID¹²⁸](#), D.A. Trischuk [ID²⁶](#), B. Trocmé [ID⁶⁰](#), C. Troncon [ID^{71a}](#), L. Truong [ID^{33c}](#), M. Trzebinski [ID⁸⁷](#), A. Trzupek [ID⁸⁷](#), F. Tsai [ID¹⁴⁶](#), M. Tsai [ID¹⁰⁷](#), A. Tsiamis [ID^{153,e}](#), P.V. Tsiareshka³⁷, S. Tsigaridas [ID^{157a}](#), A. Tsirigotis [ID^{153,t}](#), V. Tsiskaridze [ID¹⁵⁶](#), E.G. Tskhadadze [ID^{150a}](#), M. Tsopoulou [ID^{153,e}](#), Y. Tsujikawa [ID⁸⁸](#), I.I. Tsukerman [ID³⁷](#), V. Tsulaia [ID^{17a}](#), S. Tsuno [ID⁸⁴](#), O. Tsur¹⁵¹, K. Tsuri [ID¹¹⁹](#), D. Tsybychev [ID¹⁴⁶](#), Y. Tu [ID^{64b}](#), A. Tudorache [ID^{27b}](#), V. Tudorache [ID^{27b}](#), A.N. Tuna [ID³⁶](#), S. Turchikhin [ID³⁸](#), I. Turk Cakir [ID^{3a}](#), R. Turra [ID^{71a}](#), T. Turtuvshin [ID^{38,z}](#), P.M. Tuts [ID⁴¹](#), S. Tzamarias [ID^{153,e}](#), P. Tzanis [ID¹⁰](#), E. Tzovara [ID¹⁰¹](#), K. Uchida¹⁵⁴, F. Ukegawa [ID¹⁵⁸](#), P.A. Ulloa Poblete [ID^{138c,138b}](#), E.N. Umaka [ID²⁹](#), G. Unal [ID³⁶](#), M. Unal [ID¹¹](#), A. Undrus [ID²⁹](#), G. Unel [ID¹⁶¹](#), J. Urban [ID^{28b}](#), P. Urquijo [ID¹⁰⁶](#), G. Usai [ID⁸](#), R. Ushioda [ID¹⁵⁵](#), M. Usman [ID¹⁰⁹](#), Z. Uysal [ID^{21b}](#), L. Vacavant [ID¹⁰³](#), V. Vacek [ID¹³³](#), B. Vachon [ID¹⁰⁵](#), K.O.H. Vadla [ID¹²⁶](#), T. Vafeiadis [ID³⁶](#), A. Vaitkus [ID⁹⁷](#), C. Valderanis [ID¹¹⁰](#), E. Valdes Santurio [ID^{47a,47b}](#), M. Valente [ID^{157a}](#), S. Valentinetti [ID^{23b,23a}](#), A. Valero [ID¹⁶⁴](#), E. Valiente Moreno [ID¹⁶⁴](#), A. Vallier [ID^{103,ac}](#), J.A. Valls Ferrer [ID¹⁶⁴](#), D.R. Van Arneman [ID¹¹⁵](#), T.R. Van Daalen [ID¹³⁹](#), A. Van Der Graaf [ID⁴⁹](#), P. Van Gemmeren [ID⁶](#), M. Van Rijnbach [ID^{126,36}](#), S. Van Stroud [ID⁹⁷](#), I. Van Vulpen [ID¹¹⁵](#), M. Vanadia [ID^{76a,76b}](#), W. Vandelli [ID³⁶](#), M. Vandenbroucke [ID¹³⁶](#), E.R. Vandewall [ID¹²²](#), D. Vannicola [ID¹⁵²](#), L. Vannoli [ID^{57b,57a}](#), R. Vari [ID^{75a}](#), E.W. Varnes [ID⁷](#), C. Varni [ID^{17a}](#), T. Varol [ID¹⁴⁹](#), D. Varouchas [ID⁶⁶](#), L. Varriale [ID¹⁶⁴](#), K.E. Varvell [ID¹⁴⁸](#), M.E. Vasile [ID^{27b}](#), L. Vaslin⁴⁰, G.A. Vasquez [ID¹⁶⁶](#), F. Vazeille [ID⁴⁰](#), T. Vazquez Schroeder [ID³⁶](#), J. Veatch [ID³¹](#), V. Vecchio [ID¹⁰²](#), M.J. Veen [ID¹⁰⁴](#), I. Velisek [ID¹²⁷](#), L.M. Veloce [ID¹⁵⁶](#), F. Veloso [ID^{131a,131c}](#), S. Veneziano [ID^{75a}](#), A. Ventura [ID^{70a,70b}](#), A. Verbytskyi [ID¹¹¹](#), M. Verducci [ID^{74a,74b}](#), C. Vergis [ID²⁴](#), M. Verissimo De Araujo [ID^{83b}](#), W. Verkerke [ID¹¹⁵](#), J.C. Vermeulen [ID¹¹⁵](#), C. Vernieri [ID¹⁴⁴](#), P.J. Verschuuren [ID⁹⁶](#), M. Vessella [ID¹⁰⁴](#), M.C. Vetterli [ID^{143,ah}](#), A. Vgenopoulos [ID^{153,e}](#), N. Viaux Maira [ID^{138f}](#), T. Vickey [ID¹⁴⁰](#), O.E. Vickey Boeriu [ID¹⁴⁰](#), G.H.A. Viehhauser [ID¹²⁷](#), L. Vigani [ID^{63b}](#), M. Villa [ID^{23b,23a}](#), M. Villaplana Perez [ID¹⁶⁴](#), E.M. Villhauer⁵², E. Vilucchi [ID⁵³](#), M.G. Vincter [ID³⁴](#), G.S. Virdee [ID²⁰](#), A. Vishwakarma [ID⁵²](#), A. Visibile¹¹⁵, C. Vittori [ID³⁶](#), I. Vivarelli [ID¹⁴⁷](#), V. Vladimirov¹⁶⁸, E. Voevodina [ID¹¹¹](#), F. Vogel [ID¹¹⁰](#), P. Vokac [ID¹³³](#), J. Von Ahnen [ID⁴⁸](#), E. Von Toerne [ID²⁴](#), B. Vormwald [ID³⁶](#), V. Vorobel [ID¹³⁴](#), K. Vorobev [ID³⁷](#), M. Vos [ID¹⁶⁴](#), K. Voss [ID¹⁴²](#), J.H. Vossebeld [ID⁹³](#), M. Vozak [ID¹¹⁵](#), L. Vozdecky [ID⁹⁵](#), N. Vranjes [ID¹⁵](#), M. Vranjes Milosavljevic [ID¹⁵](#), M. Vreeswijk [ID¹¹⁵](#), R. Vuillermet [ID³⁶](#), O. Vujinovic [ID¹⁰¹](#), I. Vukotic [ID³⁹](#), S. Wada [ID¹⁵⁸](#), C. Wagner¹⁰⁴, J.M. Wagner [ID^{17a}](#), W. Wagner [ID¹⁷²](#), S. Wahdan [ID¹⁷²](#), H. Wahlberg [ID⁹¹](#), R. Wakasa [ID¹⁵⁸](#), M. Wakida [ID¹¹²](#), J. Walder [ID¹³⁵](#), R. Walker [ID¹¹⁰](#), W. Walkowiak [ID¹⁴²](#), A. Wall [ID¹²⁹](#), T. Wamorkar [ID⁶](#), A.Z. Wang [ID¹⁷¹](#), C. Wang [ID¹⁰¹](#), C. Wang [ID^{62c}](#), H. Wang [ID^{17a}](#), J. Wang [ID^{64a}](#), R.-J. Wang [ID¹⁰¹](#), R. Wang [ID⁶¹](#), R. Wang [ID⁶](#), S.M. Wang [ID¹⁴⁹](#), S. Wang [ID^{62b}](#), T. Wang [ID^{62a}](#), W.T. Wang [ID⁸⁰](#), W. Wang [ID^{14a}](#), X. Wang [ID^{14c}](#), X. Wang [ID¹⁶³](#), X. Wang [ID^{62c}](#), Y. Wang [ID^{62d}](#), Y. Wang [ID^{14c}](#), Z. Wang [ID¹⁰⁷](#), Z. Wang [ID^{62d,51,62c}](#), Z. Wang [ID¹⁰⁷](#), A. Warburton [ID¹⁰⁵](#), R.J. Ward [ID²⁰](#), N. Warrack [ID⁵⁹](#), A.T. Watson [ID²⁰](#), H. Watson [ID⁵⁹](#), M.F. Watson [ID²⁰](#), E. Watton [ID^{59,135}](#), G. Watts [ID¹³⁹](#), B.M. Waugh [ID⁹⁷](#), C. Weber [ID²⁹](#), H.A. Weber [ID¹⁸](#), M.S. Weber [ID¹⁹](#), S.M. Weber [ID^{63a}](#), C. Wei [ID^{62a}](#), Y. Wei [ID¹²⁷](#), A.R. Weidberg [ID¹²⁷](#), E.J. Weik [ID¹¹⁸](#),

J. Weingarten [id⁴⁹](#), M. Weirich [id¹⁰¹](#), C. Weiser [id⁵⁴](#), C.J. Wells [id⁴⁸](#), T. Wenaus [id²⁹](#), B. Wendland [id⁴⁹](#), T. Wengler [id³⁶](#), N.S. Wenke¹¹¹, N. Wermes [id²⁴](#), M. Wessels [id^{63a}](#), K. Whalen [id¹²⁴](#), A.M. Wharton [id⁹²](#), A.S. White [id⁶¹](#), A. White [id⁸](#), M.J. White [id¹](#), D. Whiteson [id¹⁶¹](#), L. Wickremasinghe [id¹²⁵](#), W. Wiedenmann [id¹⁷¹](#), C. Wiel [id⁵⁰](#), M. Wielers [id¹³⁵](#), C. Wiglesworth [id⁴²](#), D.J. Wilbern¹²¹, H.G. Wilkens [id³⁶](#), D.M. Williams [id⁴¹](#), H.H. Williams¹²⁹, S. Williams [id³²](#), S. Willocq [id¹⁰⁴](#), B.J. Wilson [id¹⁰²](#), P.J. Windischhofer [id³⁹](#), F.I. Winkel [id³⁰](#), F. Winklmeier [id¹²⁴](#), B.T. Winter [id⁵⁴](#), J.K. Winter [id¹⁰²](#), M. Wittgen¹⁴⁴, M. Wobisch [id⁹⁸](#), Z. Wolffs [id¹¹⁵](#), R. Wölker [id¹²⁷](#), J. Wollrath¹⁶¹, M.W. Wolter [id⁸⁷](#), H. Wolters [id^{131a,131c}](#), A.F. Wongel [id⁴⁸](#), S.D. Worm [id⁴⁸](#), B.K. Wosiek [id⁸⁷](#), K.W. Woźniak [id⁸⁷](#), S. Wozniewski [id⁵⁵](#), K. Wraight [id⁵⁹](#), C. Wu [id²⁰](#), J. Wu [id^{14a,14e}](#), M. Wu [id^{64a}](#), M. Wu [id¹¹⁴](#), S.L. Wu [id¹⁷¹](#), X. Wu [id⁵⁶](#), Y. Wu [id^{62a}](#), Z. Wu [id¹³⁶](#), J. Wuerzinger [id¹¹¹](#), T.R. Wyatt [id¹⁰²](#), B.M. Wynne [id⁵²](#), S. Xella [id⁴²](#), L. Xia [id^{14c}](#), M. Xia [id^{14b}](#), J. Xiang [id^{64c}](#), X. Xiao [id¹⁰⁷](#), M. Xie [id^{62a}](#), X. Xie [id^{62a}](#), S. Xin [id^{14a,14e}](#), J. Xiong [id^{17a}](#), D. Xu [id^{14a}](#), H. Xu [id^{62a}](#), L. Xu [id^{62a}](#), R. Xu [id¹²⁹](#), T. Xu [id¹⁰⁷](#), Y. Xu [id^{14b}](#), Z. Xu [id⁵²](#), Z. Xu [id^{14a}](#), B. Yabsley [id¹⁴⁸](#), S. Yacoob [id^{33a}](#), N. Yamaguchi [id⁹⁰](#), Y. Yamaguchi [id¹⁵⁵](#), E. Yamashita [id¹⁵⁴](#), H. Yamauchi [id¹⁵⁸](#), T. Yamazaki [id^{17a}](#), Y. Yamazaki [id⁸⁵](#), J. Yan^{62c}, S. Yan [id¹²⁷](#), Z. Yan [id²⁵](#), H.J. Yang [id^{62c,62d}](#), H.T. Yang [id^{62a}](#), S. Yang [id^{62a}](#), T. Yang [id^{64c}](#), X. Yang [id^{62a}](#), X. Yang [id^{14a}](#), Y. Yang [id⁴⁴](#), Y. Yang^{62a}, Z. Yang [id^{62a}](#), W-M. Yao [id^{17a}](#), Y.C. Yap [id⁴⁸](#), H. Ye [id^{14c}](#), H. Ye [id⁵⁵](#), J. Ye [id⁴⁴](#), S. Ye [id²⁹](#), X. Ye [id^{62a}](#), Y. Yeh [id⁹⁷](#), I. Yeletskikh [id³⁸](#), B.K. Yeo [id^{17a}](#), M.R. Yexley [id⁹⁷](#), P. Yin [id⁴¹](#), K. Yorita [id¹⁶⁹](#), S. Younas [id^{27b}](#), C.J.S. Young [id⁵⁴](#), C. Young [id¹⁴⁴](#), Y. Yu [id^{62a}](#), M. Yuan [id¹⁰⁷](#), R. Yuan [id^{62b,k}](#), L. Yue [id⁹⁷](#), M. Zaazoua [id^{62a}](#), B. Zabinski [id⁸⁷](#), E. Zaid⁵², T. Zakareishvili [id^{150b}](#), N. Zakharchuk [id³⁴](#), S. Zambito [id⁵⁶](#), J.A. Zamora Saa [id^{138d,138b}](#), J. Zang [id¹⁵⁴](#), D. Zanzi [id⁵⁴](#), O. Zaplatilek [id¹³³](#), C. Zeitnitz [id¹⁷²](#), H. Zeng [id^{14a}](#), J.C. Zeng [id¹⁶³](#), D.T. Zenger Jr [id²⁶](#), O. Zenin [id³⁷](#), T. Ženiš [id^{28a}](#), S. Zenz [id⁹⁵](#), S. Zerradi [id^{35a}](#), D. Zerwas [id⁶⁶](#), M. Zhai [id^{14a,14e}](#), B. Zhang [id^{14c}](#), D.F. Zhang [id¹⁴⁰](#), J. Zhang [id^{62b}](#), J. Zhang [id⁶](#), K. Zhang [id^{14a,14e}](#), L. Zhang [id^{14c}](#), P. Zhang^{14a,14e}, R. Zhang [id¹⁷¹](#), S. Zhang [id¹⁰⁷](#), T. Zhang [id¹⁵⁴](#), X. Zhang [id^{62c}](#), X. Zhang [id^{62b}](#), Y. Zhang [id^{62c,5}](#), Y. Zhang [id⁹⁷](#), Z. Zhang [id^{17a}](#), Z. Zhang [id⁶⁶](#), H. Zhao [id¹³⁹](#), P. Zhao [id⁵¹](#), T. Zhao [id^{62b}](#), Y. Zhao [id¹³⁷](#), Z. Zhao [id^{62a}](#), A. Zhemchugov [id³⁸](#), K. Zheng [id¹⁶³](#), X. Zheng [id^{62a}](#), Z. Zheng [id¹⁴⁴](#), D. Zhong [id¹⁶³](#), B. Zhou¹⁰⁷, H. Zhou [id⁷](#), N. Zhou [id^{62c}](#), Y. Zhou⁷, C.G. Zhu [id^{62b}](#), J. Zhu [id¹⁰⁷](#), Y. Zhu [id^{62c}](#), Y. Zhu [id^{62a}](#), X. Zhuang [id^{14a}](#), K. Zhukov [id³⁷](#), V. Zhulanov [id³⁷](#), N.I. Zimine [id³⁸](#), J. Zinsser [id^{63b}](#), M. Ziolkowski [id¹⁴²](#), L. Živković [id¹⁵](#), A. Zoccoli [id^{23b,23a}](#), K. Zoch [id⁵⁶](#), T.G. Zorbas [id¹⁴⁰](#), O. Zormpa [id⁴⁶](#), W. Zou [id⁴¹](#), L. Zwalski [id³⁶](#).

¹Department of Physics, University of Adelaide, Adelaide; Australia.

²Department of Physics, University of Alberta, Edmonton AB; Canada.

^{3(a)}Department of Physics, Ankara University, Ankara; ^(b)Division of Physics, TOBB University of Economics and Technology, Ankara; Türkiye.

⁴LAPP, Université Savoie Mont Blanc, CNRS/IN2P3, Annecy; France.

⁵APC, Université Paris Cité, CNRS/IN2P3, Paris; France.

⁶High Energy Physics Division, Argonne National Laboratory, Argonne IL; United States of America.

⁷Department of Physics, University of Arizona, Tucson AZ; United States of America.

⁸Department of Physics, University of Texas at Arlington, Arlington TX; United States of America.

⁹Physics Department, National and Kapodistrian University of Athens, Athens; Greece.

¹⁰Physics Department, National Technical University of Athens, Zografou; Greece.

¹¹Department of Physics, University of Texas at Austin, Austin TX; United States of America.

¹²Institute of Physics, Azerbaijan Academy of Sciences, Baku; Azerbaijan.

¹³Institut de Física d'Altes Energies (IFAE), Barcelona Institute of Science and Technology, Barcelona; Spain.

^{14(a)}Institute of High Energy Physics, Chinese Academy of Sciences, Beijing; ^(b)Physics Department,

Tsinghua University, Beijing;^(c)Department of Physics, Nanjing University, Nanjing;^(d)School of Science, Shenzhen Campus of Sun Yat-sen University;^(e)University of Chinese Academy of Science (UCAS), Beijing; China.

¹⁵Institute of Physics, University of Belgrade, Belgrade; Serbia.

¹⁶Department for Physics and Technology, University of Bergen, Bergen; Norway.

^{17(a)}Physics Division, Lawrence Berkeley National Laboratory, Berkeley CA;^(b)University of California, Berkeley CA; United States of America.

¹⁸Institut für Physik, Humboldt Universität zu Berlin, Berlin; Germany.

¹⁹Albert Einstein Center for Fundamental Physics and Laboratory for High Energy Physics, University of Bern, Bern; Switzerland.

²⁰School of Physics and Astronomy, University of Birmingham, Birmingham; United Kingdom.

^{21(a)}Department of Physics, Bogazici University, Istanbul;^(b)Department of Physics Engineering, Gaziantep University, Gaziantep;^(c)Department of Physics, Istanbul University, Istanbul; Türkiye.

^{22(a)}Facultad de Ciencias y Centro de Investigaciones, Universidad Antonio Nariño, Bogotá;^(b)Departamento de Física, Universidad Nacional de Colombia, Bogotá; Colombia.

^{23(a)}Dipartimento di Fisica e Astronomia A. Righi, Università di Bologna, Bologna;^(b)INFN Sezione di Bologna; Italy.

²⁴Physikalischs Institut, Universität Bonn, Bonn; Germany.

²⁵Department of Physics, Boston University, Boston MA; United States of America.

²⁶Department of Physics, Brandeis University, Waltham MA; United States of America.

^{27(a)}Transilvania University of Brasov, Brasov;^(b)Horia Hulubei National Institute of Physics and Nuclear Engineering, Bucharest;^(c)Department of Physics, Alexandru Ioan Cuza University of Iasi, Iasi;^(d)National Institute for Research and Development of Isotopic and Molecular Technologies, Physics Department, Cluj-Napoca;^(e)University Politehnica Bucharest, Bucharest;^(f)West University in Timisoara, Timisoara;^(g)Faculty of Physics, University of Bucharest, Bucharest; Romania.

^{28(a)}Faculty of Mathematics, Physics and Informatics, Comenius University, Bratislava;^(b)Department of Subnuclear Physics, Institute of Experimental Physics of the Slovak Academy of Sciences, Kosice; Slovak Republic.

²⁹Physics Department, Brookhaven National Laboratory, Upton NY; United States of America.

³⁰Universidad de Buenos Aires, Facultad de Ciencias Exactas y Naturales, Departamento de Física, y CONICET, Instituto de Física de Buenos Aires (IFIBA), Buenos Aires; Argentina.

³¹California State University, CA; United States of America.

³²Cavendish Laboratory, University of Cambridge, Cambridge; United Kingdom.

^{33(a)}Department of Physics, University of Cape Town, Cape Town;^(b)iThemba Labs, Western Cape;^(c)Department of Mechanical Engineering Science, University of Johannesburg, Johannesburg;^(d)National Institute of Physics, University of the Philippines Diliman (Philippines);^(e)University of South Africa, Department of Physics, Pretoria;^(f)University of Zululand, KwaDlangezwa;^(g)School of Physics, University of the Witwatersrand, Johannesburg; South Africa.

³⁴Department of Physics, Carleton University, Ottawa ON; Canada.

^{35(a)}Faculté des Sciences Ain Chock, Réseau Universitaire de Physique des Hautes Energies - Université Hassan II, Casablanca;^(b)Faculté des Sciences, Université Ibn-Tofail, Kénitra;^(c)Faculté des Sciences Semlalia, Université Cadi Ayyad, LPHEA-Marrakech;^(d)LPMR, Faculté des Sciences, Université Mohamed Premier, Oujda;^(e)Faculté des sciences, Université Mohammed V, Rabat;^(f)Institute of Applied Physics, Mohammed VI Polytechnic University, Ben Guerir; Morocco.

³⁶CERN, Geneva; Switzerland.

³⁷Affiliated with an institute covered by a cooperation agreement with CERN.

³⁸Affiliated with an international laboratory covered by a cooperation agreement with CERN.

- ³⁹Enrico Fermi Institute, University of Chicago, Chicago IL; United States of America.
- ⁴⁰LPC, Université Clermont Auvergne, CNRS/IN2P3, Clermont-Ferrand; France.
- ⁴¹Nevis Laboratory, Columbia University, Irvington NY; United States of America.
- ⁴²Niels Bohr Institute, University of Copenhagen, Copenhagen; Denmark.
- ⁴³^(a)Dipartimento di Fisica, Università della Calabria, Rende;^(b)INFN Gruppo Collegato di Cosenza, Laboratori Nazionali di Frascati; Italy.
- ⁴⁴Physics Department, Southern Methodist University, Dallas TX; United States of America.
- ⁴⁵Physics Department, University of Texas at Dallas, Richardson TX; United States of America.
- ⁴⁶National Centre for Scientific Research "Demokritos", Agia Paraskevi; Greece.
- ⁴⁷^(a)Department of Physics, Stockholm University;^(b)Oskar Klein Centre, Stockholm; Sweden.
- ⁴⁸Deutsches Elektronen-Synchrotron DESY, Hamburg and Zeuthen; Germany.
- ⁴⁹Fakultät Physik , Technische Universität Dortmund, Dortmund; Germany.
- ⁵⁰Institut für Kern- und Teilchenphysik, Technische Universität Dresden, Dresden; Germany.
- ⁵¹Department of Physics, Duke University, Durham NC; United States of America.
- ⁵²SUPA - School of Physics and Astronomy, University of Edinburgh, Edinburgh; United Kingdom.
- ⁵³INFN e Laboratori Nazionali di Frascati, Frascati; Italy.
- ⁵⁴Physikalisches Institut, Albert-Ludwigs-Universität Freiburg, Freiburg; Germany.
- ⁵⁵II. Physikalisches Institut, Georg-August-Universität Göttingen, Göttingen; Germany.
- ⁵⁶Département de Physique Nucléaire et Corpusculaire, Université de Genève, Genève; Switzerland.
- ⁵⁷^(a)Dipartimento di Fisica, Università di Genova, Genova;^(b)INFN Sezione di Genova; Italy.
- ⁵⁸II. Physikalisches Institut, Justus-Liebig-Universität Giessen, Giessen; Germany.
- ⁵⁹SUPA - School of Physics and Astronomy, University of Glasgow, Glasgow; United Kingdom.
- ⁶⁰LPSC, Université Grenoble Alpes, CNRS/IN2P3, Grenoble INP, Grenoble; France.
- ⁶¹Laboratory for Particle Physics and Cosmology, Harvard University, Cambridge MA; United States of America.
- ⁶²^(a)Department of Modern Physics and State Key Laboratory of Particle Detection and Electronics, University of Science and Technology of China, Hefei;^(b)Institute of Frontier and Interdisciplinary Science and Key Laboratory of Particle Physics and Particle Irradiation (MOE), Shandong University, Qingdao;^(c)School of Physics and Astronomy, Shanghai Jiao Tong University, Key Laboratory for Particle Astrophysics and Cosmology (MOE), SKLPPC, Shanghai;^(d)Tsung-Dao Lee Institute, Shanghai; China.
- ⁶³^(a)Kirchhoff-Institut für Physik, Ruprecht-Karls-Universität Heidelberg, Heidelberg;^(b)Physikalisches Institut, Ruprecht-Karls-Universität Heidelberg, Heidelberg; Germany.
- ⁶⁴^(a)Department of Physics, Chinese University of Hong Kong, Shatin, N.T., Hong Kong;^(b)Department of Physics, University of Hong Kong, Hong Kong;^(c)Department of Physics and Institute for Advanced Study, Hong Kong University of Science and Technology, Clear Water Bay, Kowloon, Hong Kong; China.
- ⁶⁵Department of Physics, National Tsing Hua University, Hsinchu; Taiwan.
- ⁶⁶IJCLab, Université Paris-Saclay, CNRS/IN2P3, 91405, Orsay; France.
- ⁶⁷Centro Nacional de Microelectrónica (IMB-CNM-CSIC), Barcelona; Spain.
- ⁶⁸Department of Physics, Indiana University, Bloomington IN; United States of America.
- ⁶⁹^(a)INFN Gruppo Collegato di Udine, Sezione di Trieste, Udine;^(b)ICTP, Trieste;^(c)Dipartimento Politecnico di Ingegneria e Architettura, Università di Udine, Udine; Italy.
- ⁷⁰^(a)INFN Sezione di Lecce;^(b)Dipartimento di Matematica e Fisica, Università del Salento, Lecce; Italy.
- ⁷¹^(a)INFN Sezione di Milano;^(b)Dipartimento di Fisica, Università di Milano, Milano; Italy.
- ⁷²^(a)INFN Sezione di Napoli;^(b)Dipartimento di Fisica, Università di Napoli, Napoli; Italy.
- ⁷³^(a)INFN Sezione di Pavia;^(b)Dipartimento di Fisica, Università di Pavia, Pavia; Italy.
- ⁷⁴^(a)INFN Sezione di Pisa;^(b)Dipartimento di Fisica E. Fermi, Università di Pisa, Pisa; Italy.
- ⁷⁵^(a)INFN Sezione di Roma;^(b)Dipartimento di Fisica, Sapienza Università di Roma, Roma; Italy.

^{76(a)}INFN Sezione di Roma Tor Vergata; ^(b)Dipartimento di Fisica, Università di Roma Tor Vergata, Roma; Italy.

^{77(a)}INFN Sezione di Roma Tre; ^(b)Dipartimento di Matematica e Fisica, Università Roma Tre, Roma; Italy.

^{78(a)}INFN-TIFPA; ^(b)Università degli Studi di Trento, Trento; Italy.

⁷⁹Universität Innsbruck, Department of Astro and Particle Physics, Innsbruck; Austria.

⁸⁰University of Iowa, Iowa City IA; United States of America.

⁸¹Department of Physics and Astronomy, Iowa State University, Ames IA; United States of America.

⁸²Istinye University, Sarıyer, İstanbul; Türkiye.

^{83(a)}Departamento de Engenharia Elétrica, Universidade Federal de Juiz de Fora (UFJF), Juiz de Fora; ^(b)Universidade Federal do Rio De Janeiro COPPE/EE/IF, Rio de Janeiro; ^(c)Instituto de Física, Universidade de São Paulo, São Paulo; ^(d)Rio de Janeiro State University, Rio de Janeiro; Brazil.

⁸⁴KEK, High Energy Accelerator Research Organization, Tsukuba; Japan.

⁸⁵Graduate School of Science, Kobe University, Kobe; Japan.

^{86(a)}AGH University of Krakow, Faculty of Physics and Applied Computer Science, Krakow; ^(b)Marian Smoluchowski Institute of Physics, Jagiellonian University, Krakow; Poland.

⁸⁷Institute of Nuclear Physics Polish Academy of Sciences, Krakow; Poland.

⁸⁸Faculty of Science, Kyoto University, Kyoto; Japan.

⁸⁹Kyoto University of Education, Kyoto; Japan.

⁹⁰Research Center for Advanced Particle Physics and Department of Physics, Kyushu University, Fukuoka ; Japan.

⁹¹Instituto de Física La Plata, Universidad Nacional de La Plata and CONICET, La Plata; Argentina.

⁹²Physics Department, Lancaster University, Lancaster; United Kingdom.

⁹³Oliver Lodge Laboratory, University of Liverpool, Liverpool; United Kingdom.

⁹⁴Department of Experimental Particle Physics, Jožef Stefan Institute and Department of Physics, University of Ljubljana, Ljubljana; Slovenia.

⁹⁵School of Physics and Astronomy, Queen Mary University of London, London; United Kingdom.

⁹⁶Department of Physics, Royal Holloway University of London, Egham; United Kingdom.

⁹⁷Department of Physics and Astronomy, University College London, London; United Kingdom.

⁹⁸Louisiana Tech University, Ruston LA; United States of America.

⁹⁹Fysiska institutionen, Lunds universitet, Lund; Sweden.

¹⁰⁰Departamento de Física Teórica C-15 and CIAFF, Universidad Autónoma de Madrid, Madrid; Spain.

¹⁰¹Institut für Physik, Universität Mainz, Mainz; Germany.

¹⁰²School of Physics and Astronomy, University of Manchester, Manchester; United Kingdom.

¹⁰³CPPM, Aix-Marseille Université, CNRS/IN2P3, Marseille; France.

¹⁰⁴Department of Physics, University of Massachusetts, Amherst MA; United States of America.

¹⁰⁵Department of Physics, McGill University, Montreal QC; Canada.

¹⁰⁶School of Physics, University of Melbourne, Victoria; Australia.

¹⁰⁷Department of Physics, University of Michigan, Ann Arbor MI; United States of America.

¹⁰⁸Department of Physics and Astronomy, Michigan State University, East Lansing MI; United States of America.

¹⁰⁹Group of Particle Physics, University of Montreal, Montreal QC; Canada.

¹¹⁰Fakultät für Physik, Ludwig-Maximilians-Universität München, München; Germany.

¹¹¹Max-Planck-Institut für Physik (Werner-Heisenberg-Institut), München; Germany.

¹¹²Graduate School of Science and Kobayashi-Maskawa Institute, Nagoya University, Nagoya; Japan.

¹¹³Department of Physics and Astronomy, University of New Mexico, Albuquerque NM; United States of America.

- ¹¹⁴Institute for Mathematics, Astrophysics and Particle Physics, Radboud University/Nikhef, Nijmegen; Netherlands.
- ¹¹⁵Nikhef National Institute for Subatomic Physics and University of Amsterdam, Amsterdam; Netherlands.
- ¹¹⁶Department of Physics, Northern Illinois University, DeKalb IL; United States of America.
- ^{117(a)}New York University Abu Dhabi, Abu Dhabi;^(b)University of Sharjah, Sharjah; United Arab Emirates.
- ¹¹⁸Department of Physics, New York University, New York NY; United States of America.
- ¹¹⁹Ochanomizu University, Otsuka, Bunkyo-ku, Tokyo; Japan.
- ¹²⁰Ohio State University, Columbus OH; United States of America.
- ¹²¹Homer L. Dodge Department of Physics and Astronomy, University of Oklahoma, Norman OK; United States of America.
- ¹²²Department of Physics, Oklahoma State University, Stillwater OK; United States of America.
- ¹²³Palacký University, Joint Laboratory of Optics, Olomouc; Czech Republic.
- ¹²⁴Institute for Fundamental Science, University of Oregon, Eugene, OR; United States of America.
- ¹²⁵Graduate School of Science, Osaka University, Osaka; Japan.
- ¹²⁶Department of Physics, University of Oslo, Oslo; Norway.
- ¹²⁷Department of Physics, Oxford University, Oxford; United Kingdom.
- ¹²⁸LPNHE, Sorbonne Université, Université Paris Cité, CNRS/IN2P3, Paris; France.
- ¹²⁹Department of Physics, University of Pennsylvania, Philadelphia PA; United States of America.
- ¹³⁰Department of Physics and Astronomy, University of Pittsburgh, Pittsburgh PA; United States of America.
- ^{131(a)}Laboratório de Instrumentação e Física Experimental de Partículas - LIP, Lisboa;^(b)Departamento de Física, Faculdade de Ciências, Universidade de Lisboa, Lisboa;^(c)Departamento de Física, Universidade de Coimbra, Coimbra;^(d)Centro de Física Nuclear da Universidade de Lisboa, Lisboa;^(e)Departamento de Física, Universidade do Minho, Braga;^(f)Departamento de Física Teórica y del Cosmos, Universidad de Granada, Granada (Spain);^(g)Departamento de Física, Instituto Superior Técnico, Universidade de Lisboa, Lisboa; Portugal.
- ¹³²Institute of Physics of the Czech Academy of Sciences, Prague; Czech Republic.
- ¹³³Czech Technical University in Prague, Prague; Czech Republic.
- ¹³⁴Charles University, Faculty of Mathematics and Physics, Prague; Czech Republic.
- ¹³⁵Particle Physics Department, Rutherford Appleton Laboratory, Didcot; United Kingdom.
- ¹³⁶IRFU, CEA, Université Paris-Saclay, Gif-sur-Yvette; France.
- ¹³⁷Santa Cruz Institute for Particle Physics, University of California Santa Cruz, Santa Cruz CA; United States of America.
- ^{138(a)}Departamento de Física, Pontificia Universidad Católica de Chile, Santiago;^(b)Millennium Institute for Subatomic physics at high energy frontier (SAPHIR), Santiago;^(c)Instituto de Investigación Multidisciplinario en Ciencia y Tecnología, y Departamento de Física, Universidad de La Serena;^(d)Universidad Andres Bello, Department of Physics, Santiago;^(e)Instituto de Alta Investigación, Universidad de Tarapacá, Arica;^(f)Departamento de Física, Universidad Técnica Federico Santa María, Valparaíso; Chile.
- ¹³⁹Department of Physics, University of Washington, Seattle WA; United States of America.
- ¹⁴⁰Department of Physics and Astronomy, University of Sheffield, Sheffield; United Kingdom.
- ¹⁴¹Department of Physics, Shinshu University, Nagano; Japan.
- ¹⁴²Department Physik, Universität Siegen, Siegen; Germany.
- ¹⁴³Department of Physics, Simon Fraser University, Burnaby BC; Canada.
- ¹⁴⁴SLAC National Accelerator Laboratory, Stanford CA; United States of America.

- ¹⁴⁵Department of Physics, Royal Institute of Technology, Stockholm; Sweden.
- ¹⁴⁶Departments of Physics and Astronomy, Stony Brook University, Stony Brook NY; United States of America.
- ¹⁴⁷Department of Physics and Astronomy, University of Sussex, Brighton; United Kingdom.
- ¹⁴⁸School of Physics, University of Sydney, Sydney; Australia.
- ¹⁴⁹Institute of Physics, Academia Sinica, Taipei; Taiwan.
- ¹⁵⁰^(a)E. Andronikashvili Institute of Physics, Iv. Javakhishvili Tbilisi State University, Tbilisi; ^(b)High Energy Physics Institute, Tbilisi State University, Tbilisi; ^(c)University of Georgia, Tbilisi; Georgia.
- ¹⁵¹Department of Physics, Technion, Israel Institute of Technology, Haifa; Israel.
- ¹⁵²Raymond and Beverly Sackler School of Physics and Astronomy, Tel Aviv University, Tel Aviv; Israel.
- ¹⁵³Department of Physics, Aristotle University of Thessaloniki, Thessaloniki; Greece.
- ¹⁵⁴International Center for Elementary Particle Physics and Department of Physics, University of Tokyo, Tokyo; Japan.
- ¹⁵⁵Department of Physics, Tokyo Institute of Technology, Tokyo; Japan.
- ¹⁵⁶Department of Physics, University of Toronto, Toronto ON; Canada.
- ¹⁵⁷^(a)TRIUMF, Vancouver BC; ^(b)Department of Physics and Astronomy, York University, Toronto ON; Canada.
- ¹⁵⁸Division of Physics and Tomonaga Center for the History of the Universe, Faculty of Pure and Applied Sciences, University of Tsukuba, Tsukuba; Japan.
- ¹⁵⁹Department of Physics and Astronomy, Tufts University, Medford MA; United States of America.
- ¹⁶⁰United Arab Emirates University, Al Ain; United Arab Emirates.
- ¹⁶¹Department of Physics and Astronomy, University of California Irvine, Irvine CA; United States of America.
- ¹⁶²Department of Physics and Astronomy, University of Uppsala, Uppsala; Sweden.
- ¹⁶³Department of Physics, University of Illinois, Urbana IL; United States of America.
- ¹⁶⁴Instituto de Física Corpuscular (IFIC), Centro Mixto Universidad de Valencia - CSIC, Valencia; Spain.
- ¹⁶⁵Department of Physics, University of British Columbia, Vancouver BC; Canada.
- ¹⁶⁶Department of Physics and Astronomy, University of Victoria, Victoria BC; Canada.
- ¹⁶⁷Fakultät für Physik und Astronomie, Julius-Maximilians-Universität Würzburg, Würzburg; Germany.
- ¹⁶⁸Department of Physics, University of Warwick, Coventry; United Kingdom.
- ¹⁶⁹Waseda University, Tokyo; Japan.
- ¹⁷⁰Department of Particle Physics and Astrophysics, Weizmann Institute of Science, Rehovot; Israel.
- ¹⁷¹Department of Physics, University of Wisconsin, Madison WI; United States of America.
- ¹⁷²Fakultät für Mathematik und Naturwissenschaften, Fachgruppe Physik, Bergische Universität Wuppertal, Wuppertal; Germany.
- ¹⁷³Department of Physics, Yale University, New Haven CT; United States of America.
- ^a Also Affiliated with an institute covered by a cooperation agreement with CERN.
- ^b Also at An-Najah National University, Nablus; Palestine.
- ^c Also at Borough of Manhattan Community College, City University of New York, New York NY; United States of America.
- ^d Also at Center for High Energy Physics, Peking University; China.
- ^e Also at Center for Interdisciplinary Research and Innovation (CIRI-AUTH), Thessaloniki; Greece.
- ^f Also at Centro Studi e Ricerche Enrico Fermi; Italy.
- ^g Also at CERN, Geneva; Switzerland.
- ^h Also at Département de Physique Nucléaire et Corpusculaire, Université de Genève, Genève; Switzerland.
- ⁱ Also at Departament de Fisica de la Universitat Autonoma de Barcelona, Barcelona; Spain.

- ^j Also at Department of Financial and Management Engineering, University of the Aegean, Chios; Greece.
- ^k Also at Department of Physics and Astronomy, Michigan State University, East Lansing MI; United States of America.
- ^l Associated at Department of Physics, Ben Gurion University of the Negev, Beer Sheva; Israel.
- ^m Also at Department of Physics, Ben Gurion University of the Negev, Beer Sheva; Israel.
- ⁿ Also at Department of Physics, California State University, Sacramento; United States of America.
- ^o Also at Department of Physics, King's College London, London; United Kingdom.
- ^p Also at Department of Physics, Stanford University, Stanford CA; United States of America.
- ^q Also at Department of Physics, University of Fribourg, Fribourg; Switzerland.
- ^r Also at Department of Physics, University of Thessaly; Greece.
- ^s Also at Department of Physics, Westmont College, Santa Barbara; United States of America.
- ^t Also at Hellenic Open University, Patras; Greece.
- ^u Also at Institutio Catalana de Recerca i Estudis Avancats, ICREA, Barcelona; Spain.
- ^v Also at Institut für Experimentalphysik, Universität Hamburg, Hamburg; Germany.
- ^w Also at Institute for Nuclear Research and Nuclear Energy (INRNE) of the Bulgarian Academy of Sciences, Sofia; Bulgaria.
- ^x Also at Institute of Applied Physics, Mohammed VI Polytechnic University, Ben Guerir; Morocco.
- ^y Also at Institute of Particle Physics (IPP); Canada.
- ^z Also at Institute of Physics and Technology, Ulaanbaatar; Mongolia.
- ^{aa} Also at Institute of Physics, Azerbaijan Academy of Sciences, Baku; Azerbaijan.
- ^{ab} Also at Institute of Theoretical Physics, Ilia State University, Tbilisi; Georgia.
- ^{ac} Also at L2IT, Université de Toulouse, CNRS/IN2P3, UPS, Toulouse; France.
- ^{ad} Also at Lawrence Livermore National Laboratory, Livermore; United States of America.
- ^{ae} Also at National Institute of Physics, University of the Philippines Diliman (Philippines); Philippines.
- ^{af} Also at Technical University of Munich, Munich; Germany.
- ^{ag} Also at The Collaborative Innovation Center of Quantum Matter (CICQM), Beijing; China.
- ^{ah} Also at TRIUMF, Vancouver BC; Canada.
- ^{ai} Also at Università di Napoli Parthenope, Napoli; Italy.
- ^{aj} Also at University of Colorado Boulder, Department of Physics, Colorado; United States of America.
- ^{ak} Also at Washington College, Chestertown, MD; United States of America.
- ^{al} Also at Yeditepe University, Physics Department, Istanbul; Türkiye.
- * Deceased